



KAPITAŁ LUDZKI
NARODOWA STRATEGIA SPÓJNOŚCI



Politechnika Wroclawska

UNIA EUROPEJSKA
EUROPEJSKI
FUNDUSZ SPOŁECZNY



ROZWÓJ POTENCJAŁU I OFERTY DYDAKTYCZNEJ POLITECHNIKI WROCŁAWSKIEJ

Wrocław University of Technology

Control in Electrical Power Engineering

Krzystian Leonard Chrzan

HIGH VOLTAGE LABORATORY TRAINING

Wrocław 2011

Projekt współfinansowany ze środków Unii Europejskiej w ramach
Europejskiego Funduszu Społecznego

Wrocław University of Technology

Control in Electrical Power Engineering

Krzysztof Leonard Chrzan

HIGH VOLTAGE LABORATORY TRAINING

Wrocław 2011

Copyright © by Wrocław University of Technology
Wrocław 2011

Reviewer: Ryszard Kacprzyk

ISBN 978-83-62098-60-6

Published by PRINTPAP Łódź, www.printpap.pl

MEMORY

In the memory of the *M. Sc. Jerzy Lisiecki,*

Head of The High Voltage Laboratory

Wroclaw University of Technology

1954 – 1995.

He has built the set ups presented here and also has written the student instructions. The greater part of this script shows his original work.



M. Sc. Jerzy Lisiecki, 1925-2008

Born on 06.01.1925 in Rogow. The soldier of Armia Krajowa during the world war II. He studied at Wroclaw University of Technology, Faculty of Electrical Engineering from 1946 and worked as tutor since 1949. He was also, a co-designer of High Voltage Laboratory and the author of High Voltage Department modernisation between 1975-1978. He has designed the high voltage equipments. Among others, we cite the 160 kV, 300 kVA transformer for polluted insulator testing, the 200 kV transformer for surge arrester testing and the 2 MV DC voltage source. He achieved 11 patents and wrote 5 scripts for High Voltage Engineering and Measurements.

CONTENTS

Preface

Theory for practical 3 : Surface discharges and surface flashover

Theory for practical 8 : Voltage distribution along the cap and pin insulators : string
and along the post insulator model

Theory for Practical 10 : Leakage current on polluted overhead insulators

Theory for practical 11 : The reverse polarity phenomenon of insulation arrangements with
weakly non- uniform field

Practical 1. AC High Voltage Measurement -

Practical 2. Air breakdown in uniform or non-uniform field

Practical 3. Surface discharges and surface flashover

Practical 4. Measurement of dielectric losses and partial discharges -

Practical 5. Generation of impulse voltages, impulse flashovers

Practical 6. Travelling waves based on a long line model -

Practical 7. Generation and measurement of DC voltage

Practical 8. Voltage distribution along the cap and pin insulators string and along the
post insulator model -

Practical 9. Diagnostics of surge arresters -

Practical 10. Leakage current on polluted overhead insulators -

Practical 11. The reverse polarity phenomenon of insulation arrangements with weakly non-
uniform field

Appendix A. Special experiments in HV Laboratory

Appendix B. Safety in HV Laboratory

Appendix C. The label – description of report folder

Appendix D. Template of the laboratory report

Appendix E. History of HV Laboratory

Appendix F. English-Polish terminology

PREFACE

This script should help students to prepare them for the training in High Voltage Laboratory at home and to write well organised notes of measuring data. It contains 11 different tutorials which can be carried out by the student team in any sequence. The last section shows some High Voltage experiments. Some of these experiments are demonstrated to the students and to our visitors in a well established frame such as the show of *“sparks and electrical discharges”*. Similar demonstrations are also established in other High Voltage Laboratories around the world.

There is a lot of good reading books in English describing the theory and applications of High Voltage Engineering. They can be read to extend the knowledge of engineers and are good base material for students. However, there is probably only one English book by Dieter Kind available in Europe [1] which was written especially for tutorial in High Voltage Laboratory. There are a few similar books in German [2-4] or in Russian [5]. The offer in Polish is surprisingly large [6-15]. There are relatively many High Voltage Laboratories at the Universities in Poland located in Warsaw, Krakow, **Wroclaw**, Opole, Gliwice, Rzeszow, Lublin, Częstochowa, Poznań, Szczecin, Gdańsk and Białystok. The program of tutorials offered in Polish Laboratories is generally similar and therefore the contents of the scripts do not differ very much.

Only theories of certain practicals have been included since the other practical theories are very well documented in most of the references. The reader will, also, find only 2 new tutorials in this book which are originally worked out by the author: *“Leakage current on polluted overhead insulators”* and *“The reverse polarity phenomenon of insulation arrangements with weakly non-uniform field”*. The English-Polish terminology attached at the end, containing about 200 words, can help polish students to know the Technical High Voltage terms.

Author would like to express his many thanks to **Prof. Salah Leulmi** from from **Skikda University in Algeria** who during his second stay in Wroclaw kindly corrected the English text. His 8 year-long experience at the American Universities greatly improved the book quality.

REFERENCES

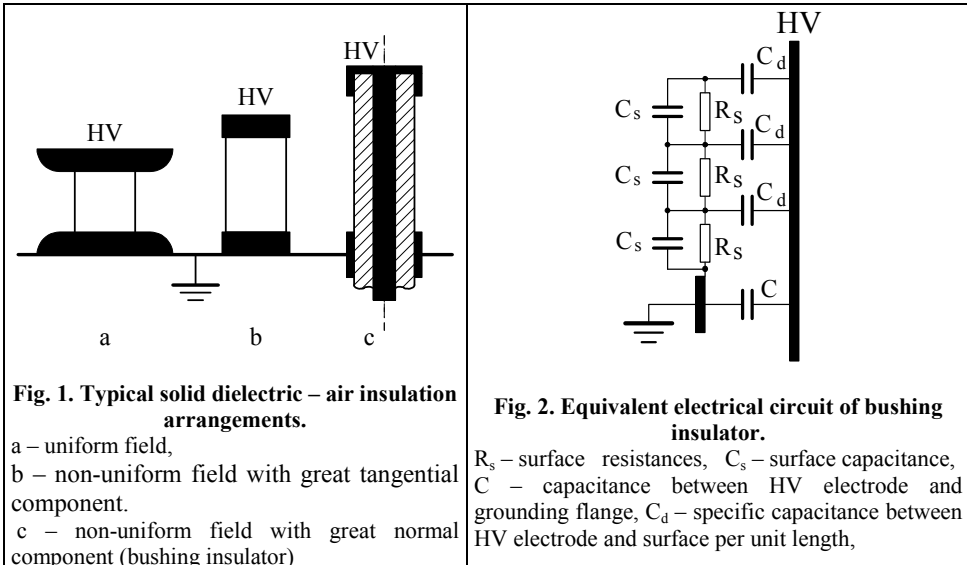
- [1] Kind D., An introduction to high-voltage experimental technique. Vieweg, Braunschweig 1978.
- [2] Kind D., (Feser K.), Hochspannungs-Versuchstechnik. Vieweg, Braunschweig 1972, 1978, 1982, 1985, 1995.
- [3] Marx E., Hochspannungs-praktikum. Springer, Berlin 1941, 1952.
- [4] Obenaus F., Hochspannungstechnik, Praktikum I. 3. Ausgabe, VEB Verlag Technik, Berlin 1960'
- [5] Aronov M.A., Bazutkin W.W. et al., Laboratornyje raboty po technike vysokich napriazenij. Energia, Moscou 1974.
- [6] Krawczyński R., Lidmanowski W., Roguski Z., Stańczak B, Laboratorium wysokich napięć, wyd. 2., Zakład Graficzny Politechniki Warszawskiej 1968.
- [7] Wira A., Zybert R., Laboratorium techniki wysokich napięć. Politechnika Łódzka 1973, 2003.
- [8] Stępniewski T. i inni, Laboratorium techniki wysokich napięć i materiałoznawstwa. elektrycznego. Politechnika Śląska, Gliwice 1979.
- [9] Brzostek E., Juzwa B., Kędzia J., Komorowski W., Skubis J., Laboratorium wysokich napięć. wyd. 2, Wyższa Szkoła Inżynierska w Opolu 1981.
- [10] Mościcka-Grzesiak H. (red.) „Ćwiczenia laboratoryjne z materiałoznawstwa elektrotechnicznego i techniki wysokich napięć”. Wyd. Politechniki Poznańskiej, 2002..
- [11] Gacek. Z., Kiś W., Laboratorium wysokich napięć. Zarys techniki probierczej i pomiarowej. Politechnika Śląska, Gliwice 2002.
- [12] Flisowski Z. (red.)Laboratorium techniki wysokich napięć. Oficyna wydawnicza Politechniki Warszawskiej 2006.
- [13] Boryń H., Olesz M., Rynkowski A., Wojtas S., Laboratorium Techniki wysokich napięć. Politechnika Gdańska 2007.
- [14] Boczar T. (red.), Laboratorium techniki wysokich napięć. Oficyna Wydawnicza Politechniki Opolskiej 2008 .
- [15] Kacejko L., Karwat C., Wójcik H., Laboratorium techniki wysokich napięć, Wydawnictwo Politechniki Lubelskiej .

THEORY FOR PRACTICAL 3

SURFACE DISCHARGES AND SURFACE FLASHOVER

1. Preamble

The mechanism of electrical discharges burning in air on solid surface depends on the electrical field. The solid insulation – air arrangements can be divided into 3 main cases (fig. 1).



The surface discharge mechanism in uniform field (fig. 1a) and in non-uniform field (fig. 1b) is similar to the case without solid dielectric between electrodes. However, the surface flashover voltage is considerably lower than the breakdown voltage through the air (the insulation arrangement without solid dielectric). The solid dielectric causes the additional field deformation which depends on dielectric permittivity, surface resistances (contamination), surface charge and contact quality between solid dielectrics and metal electrodes.

Discharges on bushing arrangement burns in different manners due to the high normal component of electrical field. These discharges called “creeping discharges” can be explained based on the electrical model of the bushing insulator shown in figure 2. In the case of clean surface (great surface resistances), the highest electrical field occur adjacent to the grounded flange. The non-uniform field depends on the dielectric permittivity ratio of solid dielectrics and air, dielectric thickness and on the electrodes shape. The air ionisation begins at the smaller electrode under the voltage U_0 . The blue light emission (glow discharge) increases with the applied voltage. The brighter yellow sparks are observed together with a characteristic click under the voltage called onset voltage of the creeping discharges..

The creeping sparks are high ionised, their current is higher than that of glow. It flows to the opposite electrode through the capacitance C_d (fig. 2). The creepage discharge are well conducting and the voltage drop along them is small. Therefore, the potential of these spark tips is high . This will promote further the elongation. Great capacitances C_d increase the current and allow the flashover under the voltage gradient smaller than that of post insulator.

The spark current flowing at the grounding electrode is given by the following formula :

$$i_s = C_s \cdot \frac{dU_s}{dt} + U_s \cdot \frac{dC_s}{dt} \quad (1)$$

where:

C_s - the total capacitance below the spark which increases with the spark length,

U_s - the medium voltage at the capacitance C_s .

This latter voltage is smaller than the total voltage between the HV electrode and grounded electrode due to the voltage drop along the spark. Under high frequency or under the impulse voltage, the discharge grow is easier than under 50 Hz voltage.

2. Qualitative analysis of creeping discharges

Max Toepler studied the creeping discharges in 1920s using the set up model shown in figure 3. Here the HV electrode is separated from a grounded plate by a dielectric material.

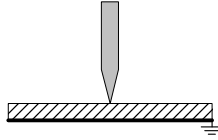


Fig. 3. Needle - plate arrangement for study of creeping discharges used by Toepler [1]

The perpendicular component of electrical field vector E_p (perpendicular to the surface) is greater than the tangential component of electrical field E_t . The creeping discharges are pressed to the dielectric surface by the perpendicular component of electrical field.

The thinner the dielectrics and the greater the dielectric constant ϵ_r , the greater is the electrical field non-uniformity. When the field in the air access the value of $30 \text{ kV}_{\text{peak}}/\text{cm}$ then the gas ionisation, de-ionisation and light emission takes places. The onset voltage of light emission U_0 is inversely proportional to the specific capacitance C_d . Note that the onset voltage depends not only on the capacitance C but on the dimensions and the edge sharpness of the grounded flange. There, only, are few equations (Kappeler, Haefely, Pappen) that estimate the value of the onset voltage U_0 . U_0 value has to be measured with a great precision. An example of such equation is given below. It is valid for a specific capacitance greater than $0,25 \text{ pF}/\text{cm}^2$ [2].

$$U_o = \frac{1,06 \cdot 10^{-4}}{C^{0,44}} \text{ [kV]} \quad (2)$$

where: C is the specific capacitance greater than $0,25 \text{ pF}/\text{cm}^2$.

If the grounded flange does not have sharp edges, then the beginning of light emission have a form of blue glow discharges which burn directly at the flange – dielectric border. At higher voltage, the discharges convert to the blue threads. Next, to the higher voltage, at the onset voltage of creeping discharges U_c , the brighter, yellow sparks appear. The creeping discharges are associated with loud clics.

$$U_c = \frac{1,36 \cdot 10^{-4}}{C^{0,44}} \text{ [kV]} \quad (3)$$

It is interesting that the value of the creeping voltage does not depend on the grounded flange geometry. The maximum length of creeping discharges is given by the Toepler equation [1]:

$$l = k \cdot C^2 \cdot U^5 \cdot \sqrt[4]{\frac{du}{dt}} \text{ [cm]} \quad (4)$$

where: k is a constant, C is the capacitance in [F /cm²], U is the voltage in [kV] and du/dt characterizes the voltage rise in [kV/μs]

The flashover voltage can be calculate from equation (4) after replacing the discharge length l by the electrode distance L.

$$U_F = \sqrt[5]{\frac{L}{k \cdot C^2}} \cdot \frac{1}{\sqrt[20]{\frac{du}{dt}}} \text{ [kV]} \quad (5)$$

The root value $\sqrt[20]{\frac{du}{dt}}$ changes relatively slow for wide voltage rise changes: e.g. from 0,7 to 1,26 for

the rise changes from 0,001 to 100 kV/μs. Assuming that $\sqrt[20]{\frac{du}{dt}} \cong 1$ and using the following equation (6) for specific capacitance between HV bus and grounded flange,

$$C = \frac{\epsilon_0 \cdot \epsilon_r}{R \cdot \ln \frac{R}{r}} \quad (6)$$

the equation (5) can be written, in a general form, as follows [3]:

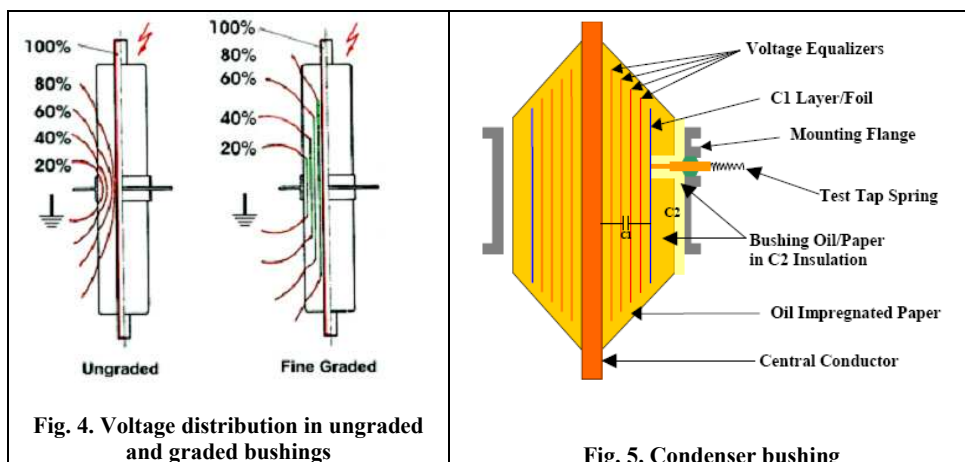
$$U_F = K \cdot L^{0,2} \cdot \left(\frac{R \cdot \ln \frac{R}{r}}{\epsilon_r} \right)^{0,4} \quad (7)$$

where: K depends on the voltage type (alternating, switching, lightning). The K-value of 43 was calculated from the experimental data for a cylindrical bushing with an external radius of R =7,5 cm, internal radius r = 5 cm. The electrode spacing is taken from 10 to 30 cm and the 50 Hz voltage is given in kV_{rms}.

3. Bushing insulators

The simplest, non-condenser bushing is a cylinder of insulating material with radial and axial clearances to suit the electric strengths of the insulating material and the surrounding media. These clearances depend on the non-uniform voltage distribution shown for ungraded bushing in figure 4. Therefore, as the voltage increases the dimensions required become so large that high voltage bushings of this simple form are not practicable.

This difficulty is overcome by the condenser bushing principle shown in figure 4 (fine graded) and in figure 5. The wall thickness is divided up into a number of capacitors by conducting layers. The conductive layer control the voltage distribution radially (lower the field near HV conductor) and axially to increase the flashover voltage for any given arcing distance. The condenser bushing construction gives much more compact design than any other construction and has been far more applied.



4. Pollution Flashover

When the surface resistance of insulator becomes small (usually due to pollution and wetting), the capacitive coupling and electrostatic voltage distribution does not determine the flashover voltage value. The voltage distribution depends on the distribution of surface conductivity which is a function of the contamination density, the wetting grade and dry band configuration. The surface leakage current is many times greater than the capacitive current.

The dry bands are build in the places where the leakage current density is the highest. When the voltage stress over a dry band exceeds the flashover voltage, the local surface discharges appear. The pre-breakdown discharges on clean insulators are very small, in the range of micro amperes. Their value on the bushing insulators is higher, about 1 mA. On the contrary, the maximum leakage current on the heavy polluted insulators can be higher than 1A.

Therefore, the voltage source used for testing of polluted insulators have to fulfil special requirements. The transformer power and short-circuit current have to be high enough and can't influence the discharge development on the insulator. In other words, the current should not cause a

high voltage drop on the source internal impedance. Thus, the object voltage will not decrease much during the testing.

The applied test circuit even with 70 kVA voltage regulator does not fulfil the requirements of IEC standard 60-507 in regard to the short-circuit current value. Therefore, the test circuit can not be used for measurement of pollution flashover voltage but only for observation of pollution discharges.

Additionally, the contamination and wetting procedure used in the tutorial does not model the field conditions. After the wetting of polluted insulator by means of hand sprayer, a very high leakage current flows after switching-on the test voltage. In this case, intensive discharges burn on every shed division (fig. 6a). Under natural conditions, the contaminated insulators work under operating voltage for a very long time. The wetting rate is often small (fog, drizzle). The rather small, concentrated discharges are observed under such conditions (fig. 6b). They cover only a small part of leakage distance.



Fig. 6. Discharges on polluted insulators [4]

- a – intensive discharges during “flow on” test on insulator VKL 75/14 in laboratory.
- b – concentrated weak discharges on polluted insulator LPZs 75/15 in very humid air.

5. References

- [1] Toepler M., Ueber die physikalische Grundgesetze der in der Isolatorentechnik auftretenden elektrischen Gleiterscheinungen. Archiv fuer Elektrotechnik 1921, Heft 5/6, S. 157-185.
- [2] Gacek Z. Technika wysokich napięć. Wydanie III, Wydawnictwo Politechniki Śląskiej 1999, pp. 140.
- [3] Chrzan K.L., Trzęsicki P., Creeping discharges. 5th Ogólnopolskie Warsztaty Doktoranckie OWD, Istebna-Zaolzie, 2003.
- [4] Chrzan K.L., Moro F., Concentrated discharges and dry bands on polluted outdoor insulators. IEEE Trans. on Power Delivery, 2007 vol. 22, No. 1, pp. 466-471.

THEORY FOR PRACTICAL 8

VOLTAGE DISTRIBUTION ALONG THE CAP AND PIN INSULATORS STRING AND ALONG THE POST INSULATOR MODEL

1. Cap and pin insulators

Transmission lines use modular *cap and pin* insulator designed since 1907 (Fig. 1). The wires are suspended from a “string” of identical disk-shaped insulators which are attached to each other with metal pin or ball and socket links. The lines with different voltages are constructed by adding a certain number of basic units in the insulator string. This is one of the advantages of cap and pin insulators.

Each unit is constructed of a porcelain or glass disk with a metal cap and pin cemented to opposite sides. The glass is heat-treated (toughened) so it will shatter, making the damaged unit visible. However the mechanical strength of the unit is unchanged, so the insulator string will stay together. Standard disk insulator units are 254 mm in diameter and 146 mm high. They can support a load of 80-120 kN. The unique feature of the cap-and-pin design is that it converts an applied tensile load into a radial compressive stress on the ceramic dielectric, which, withstands more easily than the tension load.

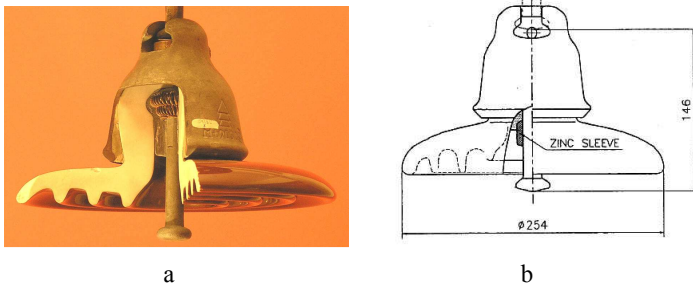


Fig. 1. Cap and pin insulators

a – manufactured by Hescho

b – IEEE standard disc manufactured by NGK insulators with a zinc sleeve as an anti-corrosion protection

2. Voltage distribution along the string of disc insulators

However, the flashover voltage of a string is less than the sum of its component disks, because the electric field is not distributed evenly across the string but is strongest at the disk nearest to the conductor, which will flashover first. Metal *grading rings* are sometimes added around the lowest disk, to reduce the electric field across that disk and improve flashover voltage.

The simplest model of a disc insulator string, useful for analytical consideration, consists of 3 capacitor kinds, i.e. insulator capacitance C_w and stray capacitances: insulator-ground C_z and insulator-phaseable C_p (Fig. 2). The capacitance value of each insulator C_w is assumed as nearly identical for all disc insulators. Under the assumption of constant values of C_p and C_z the well known analytical formula describes the voltage distribution along insulator string:

$$U_i = \frac{U}{C_p + C_z} \left[C_p + C_z \frac{\text{sh}[k(N-1)]}{\text{sh}(kN)} - C_p \frac{\text{sh}(ki)}{\text{sh}(kN)} \right] \quad (1)$$

where:

U_i – voltage between given insulator and high voltage cable,

U – voltage applied to the whole string,

i – insulator number in the string,

N – number of insulators in the string

sh – hyperbolic sine function ‘sinh’

$$k = \sqrt{\frac{C_p + C_z}{C_w}} \quad (2)$$

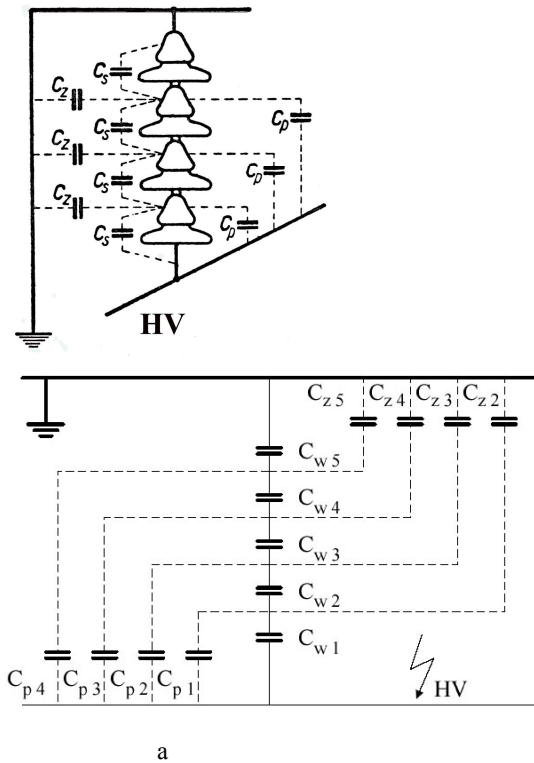


Fig. 2. String of 4 disc insulators

(a) schematic representation

(b) electrical model of disc insulator string

In reality, the capacitance to high voltage cable C_p and to the ground C_z depends on the insulator position of the string. Therefore, the voltage calculated from the formula (1) is an approximate value. Using PSPICE, it is possible to calculate the voltages along the insulator string if the value of C_{zi} and

C_{pi} are known. The estimation of stray capacitance can be carried out with professional programs based on finite element method or other methods.

The approximate stray capacitance values for typical high voltage masts can be determined from:

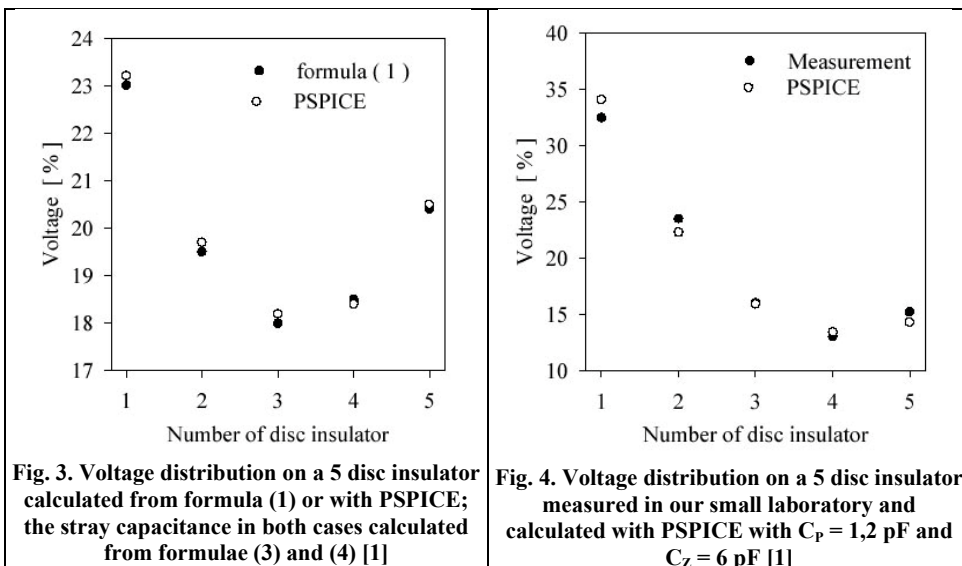
$$C_{pi} = 1,2 - 0,012 [i - (N - 1)] \quad (3)$$

$$C_{zi} = 1,7 - 0,007 (1,0 - i) \quad (4)$$

where i is the insulator number counted or numbered from the phase cable, C_{pi} and C_{zi} are given in pF. The PSPICE calculations carried out for a string of 5 insulators with the stray capacitances given by the equations (3) and (4) gave nearly the same results as the calculation found using formula (1) which considers only one value for all capacitances C_z and one value for all capacitances C_p (Fig.3). For the calculator according to formula (1), the values of $C_p = 1,218$ pF and $C_z = 1,71$ pF were used. These values are considered as the medium values of the 4 obtained values using the equations (3) and (4).

The calculated voltage distribution along the insulator string is shown in figure 3. The minimum voltage drop is on the insulator number 3. On the contrary, the measurements carried out in the high voltage laboratory have shown that the minimum voltage drop is on the insulator number 4 (Fig. 4). The discrepancy is caused by different measurement conditions in the relatively small laboratory room with dimensions of $4 \text{ m} \times 4 \text{ m}$ and height of 3,5 m. Formula (1) applies to a high voltage mast (110 kV or above) with longer dimensions. Therefore, it is obvious that the capacitance to ground in the small laboratory is greater than in the case of high voltage mast. The capacitance to high voltage cable can be assumed similar in both cases in spite of short length of the cable in the laboratory (1, m).

To prove the above observation, a few PSPICE simulations were carried out with the same capacitances $C_p = 1,3$ pF and different values of capacitance C_z . The simulation results with $C_p = 1,3$ pF and $C_z = 6$ pF (Fig. 4) show good accordance with the measurement results. Note that in both cases the minimum voltage drops on the insulator number 4.



3. Error measurement

When an air gap is connected to the disc insulator (parallel to the insulator capacitance), the voltage on this insulator and therefore the voltage on other insulators in the string changes significantly. The capacitance of the air gap and capacitance of connecting wires increase the insulator capacitance and decrease therefore its voltage.

The air gap and connecting wire capacitances were calculated according to formulae:

$$C_l \cong \frac{4\pi \cdot \varepsilon \cdot l}{\ln \frac{l}{r} + \ln \frac{l}{d} - 0,614} \quad (5)$$

$$C_k = 8\pi \cdot \varepsilon \cdot a \cdot \frac{1}{1 + \frac{a}{2 \cdot x}}$$

where:

C_l – capacitance of 2 parallel wires with the same length l , radius r and separated with the distance $d \ll l$,

C_k – capacitance of 2 spheres with the same radius a and separated with the distance x such as $a/2 \cdot x < 0,5$.

The capacitance of 2 one meter - long wires with the radius of 0,5 mm amounts to 12 pF while the capacitance of 2 spheres with the radius of 10 mm, separated by a distance of 2 mm amounts to 0,9 pF. When the wires are only 20 cm long, their capacitance decreases to 3 pF only.

The voltage calculation results, for 5 standard disc insulators having the capacitance of 29 pF without air gap and with air gap and connecting wires of 1 m length, are shown in figure 5. The voltages calculated without air gap are marked as $C = 0$ and calculated with the air gap as $C = 15$ pF. The voltage sum on 5 insulators “measured” with the air gap is only 75% of the applied voltage. When the voltage is “measured” with the air gap connected by short wires of 20 cm length, the voltage sum amounts to 97,6% of applied voltage. This means *the measurement error decreases from 25% to 4%*.

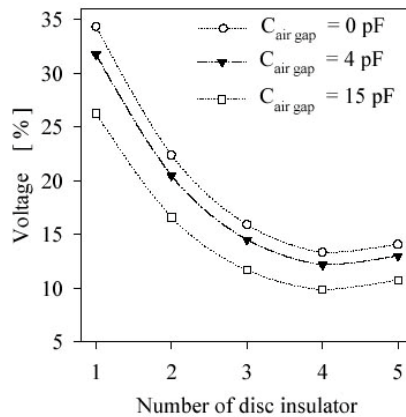


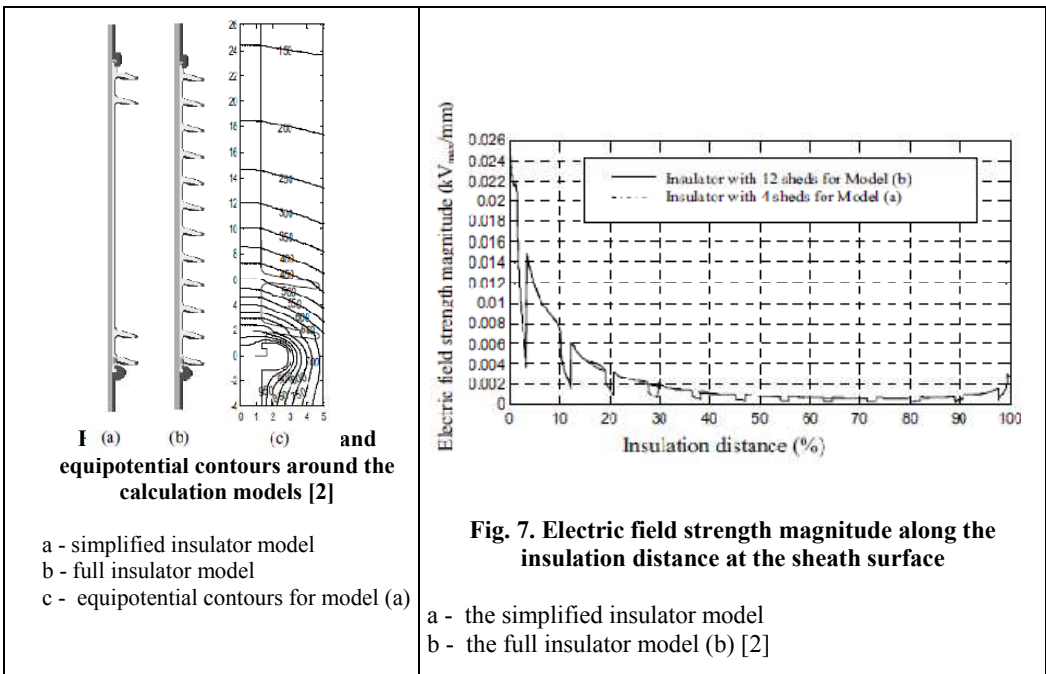
Fig. 5. Voltage distributon on 5 standard disc insulators

$C = 0$ – the true value [1]

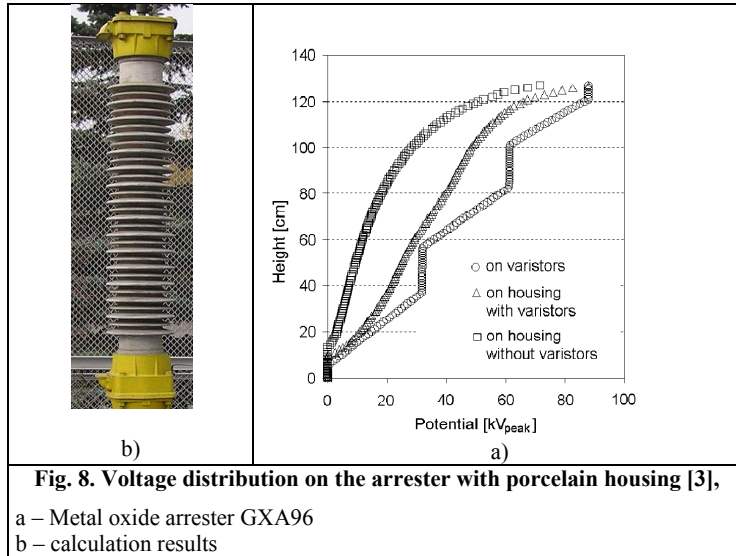
$C = 4 \text{ pF}$ (15 pF) – the values calculated with an air gap connected by 20 cm (or 100 cm) long wires.

4. Voltage distribution along long rod insulators and surge arrester housing

The voltage distribution is also non-uniform on other type of insulators, e.g. post, long rods or housings. The non-uniformity of voltage distribution increases with the operating voltages and can lead to the ignition of partial discharges and relating acoustic noises, radio and TV interferences and power losses. The corona discharges are especially dangerous for polymer insulators and great care have to be taken to avoid them. Therefore, the grading rings are widely used on composite insulators for 110 kV or higher voltages



The calculations of the electric field and voltage distribution carried out by means of program COULOMB in the vicinity of 34 kV composite insulators are shown in figures 6 and 7. The dips in the electric field strength plot of the insulator modelled with weather sheds are due to the calculation path passing through the weather shed material, which has a relative permittivity of 4.3.



Voltage distribution along the porcelain housing of 110 kV metal oxide arrester and along the varistor column is presented in figure 8. The finite element method program tools OPERA has been employed for these calculations. A remarkable influence of varistor column on the voltage distribution on porcelain housing is shown in figure 8. At the upper flange of porcelain housing, the maximum voltage gradient amounts to 2 kV_{peak}/cm. This means that the maximum voltage gradient is 2,5 times greater than the mean value of voltage gradient.

5. References

- [1] Chrzan K.L., Rebizant W., PSPICE application for modelling of cap and pin insulator string. Int. Conference on Modern Power Systems MEPS, Wrocław 2002, pp. 581-585.
- [2] Que W., Sebo S.A., Discussions of possible simplifications for the electric field and voltage distribution calculations along composite insulators. 13th Int. Symposium on High Voltage Engineering, Delft 2003, paper 230.
- [3] Chrzan K.L., Gielniak J., Voltage distribution along metal oxide surge arresters. 13th Int. Symposium on High Voltage Engineering, Delft 2003, paper 077.
- [4] Looms J.S.T., Insulators for high voltages. Peter Peregrinus Ltd, London 1990.
- [5] Chrzan K. L., Wiatrzyk M., Naito K., „Izolatory kołpakowe ze szkliwem półprzewodzącym”. VI Konf. Postępy w Elektrotechnologii, Jamrozowa Polana 2000, s. 81-87.
- [6] Mizuno Y., Naito K., Suzuki Y., Mori S., Nakashima Y., Akizuki M., „Voltage and temperature distribution along semiconducting glaze insulators strings.” IEEE Trans. on Dielectrics and Electrical Insulation, Feb. 1999, pp. 100-104.

THEORY FOR PRACTICAL 10

LEAKAGE CURRENT ON POLLUTED OVERHEAD INSULATORS

1. Preamble and development

The current on clean and dry insulators is very small, in the order of micro-amperes and depends on the capacitance between 2 flanges. After the voltage application to the polluted and wet insulator, the resistive current flows which can achieve the amplitude of 1 A, in a heavy polluted area. Initially, when a continuous pollution layer is present, the current is sinusoidal. However, in parts of the insulator where the current density is higher, the moisture dries up quicker and dry bands are formed with high surface resistance. The voltage stress over the dry bands is many times higher than that along the wet insulator part. The dry band flashover causes a sudden current increase and current shape become non-sinusoidal (fig. 1). If the arc is able to extend to about 66% of the whole leakage distance, the flashover occur and the current reach the value of short current.

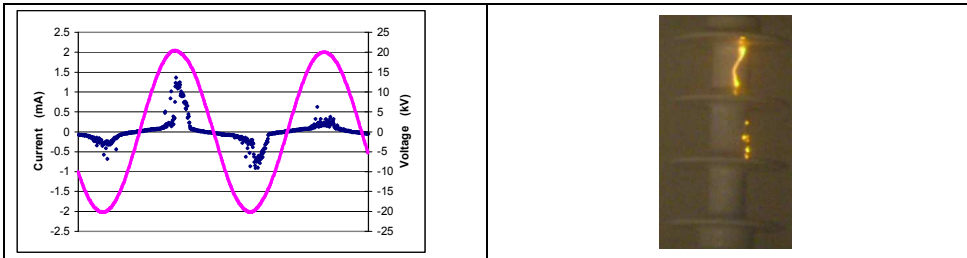


Fig. 1. Small discharge with the current amplitude of 1.4 mA on lightly polluted insulator

According to the model of Fritz Obenaus (fig. 2), the single arc burning over the dry band is connected to the *narrow wet contaminated strip*. The equations 1 and 2 are only valid for the simplified model insulator without sheds shown in figure 2. The supply voltage U is, therefore, a sum of the arc voltage and the voltage drop along the polluted strip.

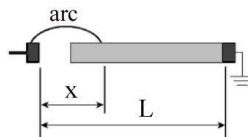


Fig. 2. Obenaus model for flashover of uniformly polluted surface

$$U = A \cdot x \cdot I^{-n} + I \cdot r_p (L - x) \quad (1)$$

where:

x – arc length in cm

L – leakage distance of insulator in cm,

r_p – per unit length resistance of pollution layer in $k\Omega/cm$,

A, n – arc constants

The arc length can be calculated as a function of current from the equation (2) :

$$x = \frac{U - r_p \cdot L \cdot I}{A \cdot I^{-n} - r_p \cdot I} \quad (2)$$

The arc length as a function of the current was calculated from equation (2) for the rod insulator with the length of 105 cm, the diameter of 3 cm, the voltage of 75 kV and for different values of pollution layer unit resistance. The arc constant $A = 140$ and $n = 0,56$ were taken from the literature. The calculations carried out by means of PC program Mathcad®6 are shown in figure 3. The critical value of pollution layer unit resistance amounts to 35 kΩ/cm.

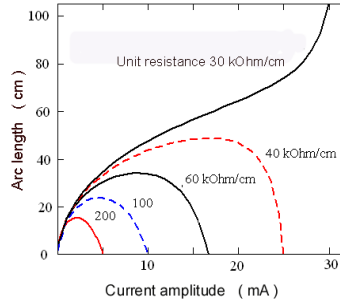


Fig. 3. Arc length as a function of current and pollution layer unit resistance calculated from equation (2) by means of Mathcad®6 for $U = 75\text{kV}$ ($105 \text{ kV}_{\text{max}}$) and $L = 105 \text{ cm}$ [1]

The critical voltage U_C (minimum flashover voltage) and critical current I_C can be calculated from the following equations :

$$U_C = L \cdot A^{\frac{1}{n+1}} \cdot r_p^{\frac{n}{n+1}} \quad (3)$$

$$I_C = \left(\frac{A}{r_p} \right)^{\frac{1}{n+1}} \quad (4)$$

The critical voltage can also be given as a function of critical current :

$$U_C = A \cdot L \cdot I_C^{-n} \quad (5)$$

The leakage currents on insulators are smaller than the critical current. It is important to know the “fictive value of flashover voltage” at the highest current value I_h recorded under the operating voltage U during the so called pollution event when insulator has been wetted. This problem was solved by Zhang [1]:

$$U_C = L \cdot \left(\frac{U}{2L} \right)^{\frac{n}{n+1}} \cdot A^{\frac{1}{n+1}} \cdot I_h^{\frac{-n}{n+1}} \quad (6)$$

The engineers responsible for maintenance of line insulators choose the value of leakage current which is treated as the warning level. This value usually differs from 100 to 250 mA.

2. References

- [1] Chrzan K.L., Leakage currents on naturally contaminated porcelain and silicone insulators. IEEE Trans. on Power Delivery, Vol. 25, Issue 2, Apr 2010, pp. 904 – 910.

THEORY FOR PRACTICAL 11

THE REVERSE POLARITY PHENOMENON OF INSULATION ARRANGEMENTS WITH WEAKLY NON- UNIFORM FIELD

1. Introduction

The positive switching flashover voltage of clean cap and pin insulators is lower than under negative polarity. An opposite performance was found 40 years ago. Under artificial rain the negative lightning flashover voltage of double long rod insulators was lower than that with positive polarity. This so called reversal polarity phenomenon was found by other researchers on cap and pin insulators, on line long rod insulators and on post insulators under artificial rain conditions.

2. Flashover voltage of cap and pin insulators

The 50% lightning 1,2/50 μ s flashover voltage with negative or positive polarity, according to up and down method, was measured on strings consisted of five standard insulators or aerodynamic insulators (fig. 1).

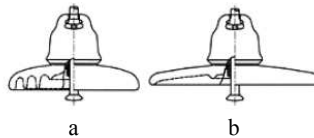


Fig. 1. The standard cap and pin insulator (a) and the aerodynamic cap and pin insulator (b) [1]

The non-uniformly polluted insulators with the measured values of surface conductivity are shown in Figure 2. The clean zones around the caps with the widths of 2,5 cm (Fig. 2a) or 3 cm (Fig. 2c) were left. The upper sides of the standard insulators shown in figure 2b were not polluted. Such non-uniform contamination models the condition of insulators which were partly cleaned by rain. In these circumstances, the discharges can burn close to the cap on the upper insulator side. Similarly, contaminated insulators were studied in South Africa under field conditions.

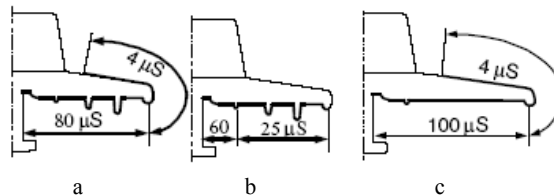


Fig. 2. The surface conductivity on non-uniformly polluted insulators.

The 50% flashover voltage of clean standard cap and pin insulators amounted to about 500 kV. This value dropped to about 410 kV under uniform contamination with the surface conductivity in the range of 7 – 15 μ s. In both cases, the negative flashover voltage was insignificantly higher than the flashover voltage with positive polarity. However, under non-uniform pollution the electrical strength decreased twice comparing to the value measured under clean conditions. **Moreover, with negative polarity, the flashover voltage is 10% lower than that with positive polarity.**

The flashover voltage of uniformly polluted standard insulators decreased of only 80 kV and that of non uniformly polluted insulators dropped to even 200 kV compared to the clean insulators. These results confirm the known influence of dry bands on electrical strength of insulators under impulse voltages.

The pictures in figure 3 show parallel discharges that burn in different spots of sheds. Flashovers on standard insulators could easily be distinguished from withstands by observation with the naked eye. The discharges, which do not lead to flashover, emit less light, have smaller diameter and are shorter.

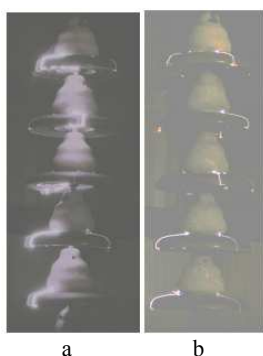


Fig. 3. Discharges on polluted standard insulators
a - flashover case
b - withstand case

3. Effect of impulse polarity on model arrangements

The lower negative flashover voltage of the non-uniformly polluted cap and pin insulators can be explained by the reversal polarity phenomenon occurring in air gaps with a weakly non-uniform electrical field. The negative breakdown voltage of sphere-sphere air gap with a uniform field (when the ratio of sphere distance S to the sphere radius R is lower than 0,7) is equal to that of positive polarity. In non-uniform field, when $S/R > 1,4$, the negative breakdown voltage is higher than the positive breakdown voltage. In the intermediate ratio $0,7 < S/R < 1,4$, the electrical strength under negative impulses is lower.

The additional measurements were carried out with round flat glasses with a diameter of 25 cm. The top electrode which modelled the cap had the diameter of 4,5 cm. The opposite electrode was in the form of a disc with the diameter of 25 cm and/or a metal band wrapped around the glass disc (tab. 1). When the high voltage electrode has the greater diameter than the grounded electrode, then the negative flashover voltage is smaller than the positive flashover voltage (tab. 1). **The highest ratio $U_{+}/U_{-} = 1,29$ was found on the model, with the thickness of 3 cm**, with an additional graphite ring with the width of 4 cm which was put on the upper surface. When the HV electrode has a smaller diameter than the grounded electrode, then the positive flashover voltage was smaller than the negative flashover voltage.

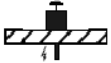
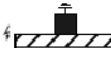
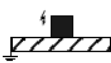
When the dry band is formed at the pin on the bottom part of insulator, then due to a small pin diameter, the electrical field in the dry zone is very non-uniform. Therefore, the negative breakdown voltage of a dry band is higher than that of a positive polarity and the reversal polarity phenomenon is

not observed. In this case, the same relation is valid for flashover voltage of a single cap and pin insulator and the whole insulator string.

The reversal polarity phenomenon appears when dry bands are formed at the cap under the operating voltage. Such conditions are possible when the upper side of the disc is lightly polluted and the bottom side is polluted more. Additionally, the preferable wetting conditions rate should be low, e.g. air humidity is very high.

The weather conditions which allow light wetting rate (drizzle, fog, high air humidity) favour the appearance of this type of phenomenon.

Tab. 1. The ratio of the positive flashover voltage to the negative flashover voltage for different insulator arrangements

Arrangement	Plate thickness (cm)	$\frac{U_+}{U_-}$
	3	1,29
	1,2	1,15
	1,2	0,82

4. References

[1] Chrzan K.L., Schwartz H., Häusler H., Effect of impulse polarity on the flashover voltage of polluted cap and pin insulators. 16th International Symposium on High Voltage Engineering, Cap Town 2010, paper E-30.

PRACTICAL 1

AC HIGH VOLTAGE MEASUREMENTS

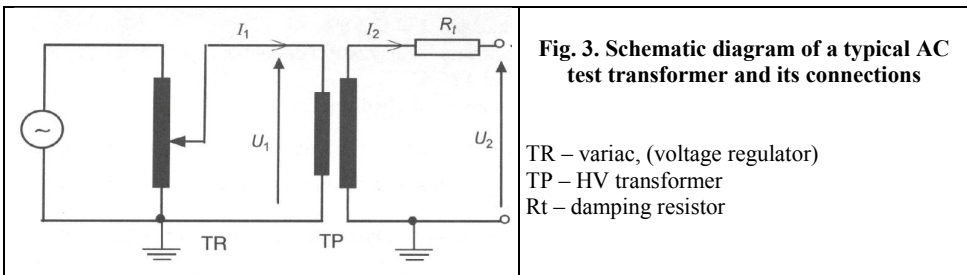
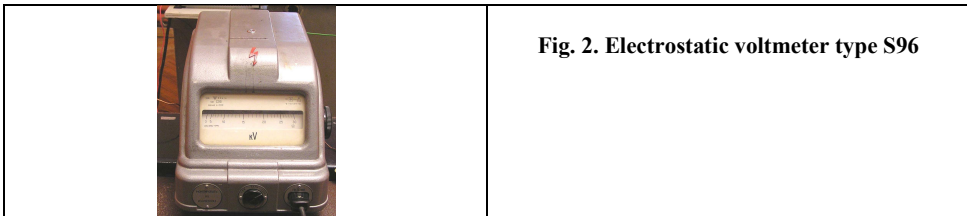
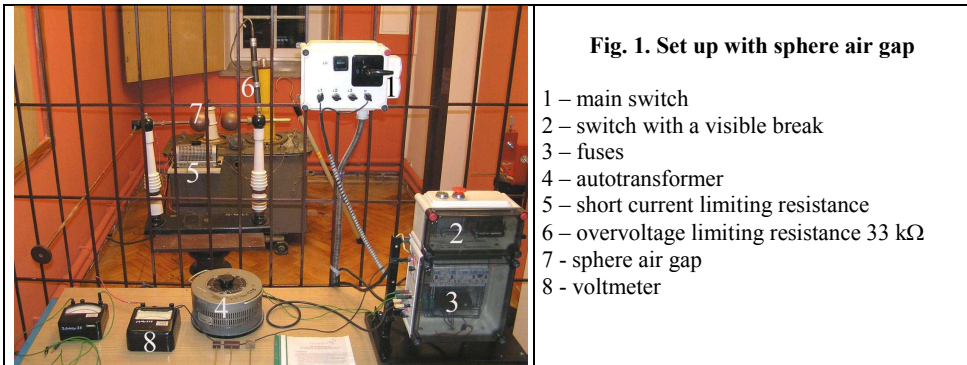
1. 1 . Purpose of the experiment

The purpose of the experiment is to carry out the AC voltage measurement by means of a sphere gap, an electrostatic voltmeter, a capacitive voltage divider, and a voltage transformer

1. 2. Measurement by means of sphere gap and electrostatic voltmeter

1. 2. 1 . Experimental set up

This experiment is carried out in the box shown in fig. 1. Figure 2 shows the electrostatic voltmeter type S96.



1. 2. 2. List of measuring devices

- Test transformer by Koch & Sterzel Dresden with symmetrical output (using 2 bushing insulators) voltage ratio 90 V/110 V/130 V / 120 kV, $I_1 = 25$ A (on low voltage side), $I_2 = 50$ mA (on high voltage side), $S = 6$ kVA
- The bushing insulators have special construction with great grounding electrode diameter (and therefore higher onset voltage of creeping discharges).
- Terminals 1 – 2: $U_1 = 90$ V, terminals 1 – 3: $U_1 = 110$ V, terminals 1 – 4: $U_1 = 130$ V
- This transformer is used here with non-symmetrical output (one end of the HV winding is being grounded at the top of the bushing).

Note, in non-symmetrical output the maximum high voltage of 90 kV is allowed.

- Air gap by Siemens & Halske with sphere diameters of 10 cm, one sphere is grounded.
- Electrostatic voltmeter type S96, Soviet Union, 7,5/15/30 kV, 20 Hz – 10 MHz
- Autotransformer 220 V/ 0 – 250 V, 10 A
- Short current limiting resistance 8,2 Ω , 2,9 A
- Overvoltage limiting resistance 33 k Ω
- Voltmeters with different ranges
- Additional elements of the test circuit: switches, fuses, lamps, safety interlock, grounding rod

1. 2. 3. Measuring tasks

1. Draw the test circuit similar to that shown in fig. 3 but containing more elements.
2. Measure the high voltage by means of sphere air gap and the low voltage by means of voltmeter for the distances of 1 and 2 cm. Repeat the measurement at 1 cm distance with connected electrostatic voltmeter.
Use the air gap characteristics (given for standard atmospheric conditions).
Make the correction of breakdown voltages for real atmospheric conditions.
3. Calculate the voltage ratio of test transformer for both breakdown distances. Remember that the breakdown voltage is given in kV_{peak} and low voltage in V_{rms} .

1. 3. Measurement by means of a capacitive voltage divider or a voltage transformer

1. 3. 1 . Experimental set up

This experiment is carried out in the box shown in fig. 4.



Fig. 4. Set up with the capacitive voltage divider and with the voltage transformer

- 1 – HV transformer
- 2 – capacitive voltage divider
- 3 – compressed gas capacitor Micafil
- 4 – inductive voltage transformer
- 5 – low voltage decade capacitance
- 6 – digital voltmeter
- 7 – electromagnetic voltmeter
- 8 – digital oscilloscope

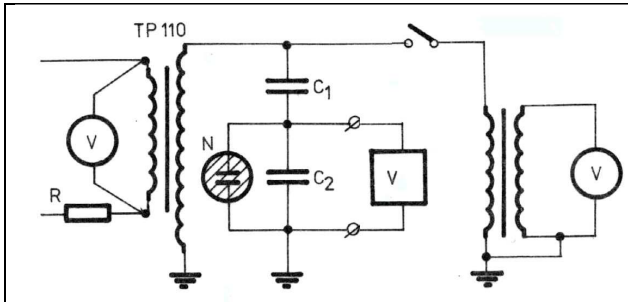


Fig. 5. Schematic diagram of test circuit containing the capacitive divider and the inductive voltage transformer

1. 3. 2. List of measuring devices

- Test transformer TP 110,
- L V/HV 220 V/ 110 kV, 50 Hz
- Continuous power 10 kVA Temporary power (15 min) 40 kVA
- Continuous secondary current 0,09 A Temporary secondary current (15 min) 0,36 A
- Test voltage 50 Hz, 5 min 143 kV Voltage ratio accuracy $\pm 5\%$
- Voltage transformer by ZWAWN Warszawa
- Nominal voltage $U_n = 60$ kV Continuous power $S_g = 2$ kVA
- Test voltage 50 Hz $U = 130$ kV Test voltage 1,2/50 μ s 325 kV
- $U_{2n} = \frac{100 V}{\sqrt{3}}$ $S_{2n} = 120$ VA, class 0,5
- Voltage ratio $\frac{60 kV}{\frac{100 V}{\sqrt{3}}} = 600$
- Compressed gas capacitor (standard capacitor) $U_{max} = 190$ kV, $C_{1w} = 107,9$ pF, class 0,1, $tg \delta < 10^{-5}$. **Note: Use this gas capacitor only up to 90 kV !**
- Low voltage decade capacitor $U_{max} = 250$ V, class 1
- Digital voltmeter with very high input resistance (for measurement with capacitive voltage divider)
- Electromagnetic voltmeter (for measurement with voltage transformer)
- Voltmeter with digital display Lumel N15Z, 300 V, $R > 2$ M Ω , Error $0,5\% \pm 1$ digit
- Digital oscilloscope

1. 3. 3. Measuring tasks

1. Choose the value of low voltage capacitance so that the ratio of capacitive voltage divider is equal to (about) 10 000.
2. Set the value of high voltage to 30 kV and measure the low voltage at capacitive voltage divider and voltage transformer. Calculate the voltage ratio of test transformer based on both voltmeter readings. Observe the voltage shape on the oscilloscope.
3. Increase the value of high voltage to the value considerably greater than $60 \text{ kV} / \sqrt{3}$ (up to 60 kV) . Observe the voltage shape. Calculate the voltage ratio of test transformer based on both voltmeter readings.

1. 4. Report contents

- Purpose of the experiments, measuring circuits
- List of measuring equipments with main technical data and numbers
- Measurement readings and calculation results, calculation examples, conclusions
- Manual measuring report signed by the tutor.

1. 5. Control questions

1. Parameters of AC voltage
2. Constructions of test transformers
3. Typical test circuits
4. Regulation of test voltage amplitude
5. Overvoltages in test circuits
6. Damping resistors
7. High voltage measurements
8. Construction of compressed gas capacitors

1. 6. References

[1] Holtzhausen J. P., Vosloo W. L., High Voltage Engineering, Practice and Theory, Stellenbosch University, 2008, Chapter 1, Chapter 4

[2] Ryan H.M., (editor), High voltage engineering and testing, second edition, The Institution of Electrical Engineers, London 2001, Chapter 13, Chapter 15

PRACTICAL 1 : AC HIGH VOLTAGE MEASUREMENT

Manual measuring report date :

Laboratory team number

1. Reporter
2. Student
3. Student
4. Student
5. Student
6. Student

Tutor's signature

Climatic conditions: T =°C, p = hPa, RH =%

$\delta =$

Table 1. Sphere air gap measurement

No	a	U_1	$U_{1 \text{ mean}}$	$U_{2 \text{ stand}}$	$U_{2 \text{ pT}}$	η	Remarks
	cm	V	V	kV	kV	-	
1	1						
2							
3							
1	1					-	With electrostatic voltmeter
2						-	
3						-	
1	2						
2							
3							
Mean value of transformer voltage ratio $\eta =$							

- U_1 - low voltage, $U_{1 \text{ mean}}$ - mean value of low voltage (for three consequence readings)
 $U_{2 \text{ stand}}$ - HV for standard atmospheric conditions as read from characteristics of sphere air gap
 $U_{2 \text{ pT}}$ - corrected high voltage taken into account the real atmospheric conditions
 η - transformer voltage ratio a - distance between air gap

Table 2. Capacitive voltage divider and voltage transformer measurements

Capacitive voltage divider			Voltage transformer			
No	U_1 V	U_2 kV	η_c -	U_1 V	U_2 kV	η_t -
1						
2						

U_1 - low voltage, U_2 - high voltage

η_c - voltage ratio of transformer calculated from measurements by means of capacitive voltage divider

η_t - voltage ratio of transformer calculated from measurements by means of voltage transformer

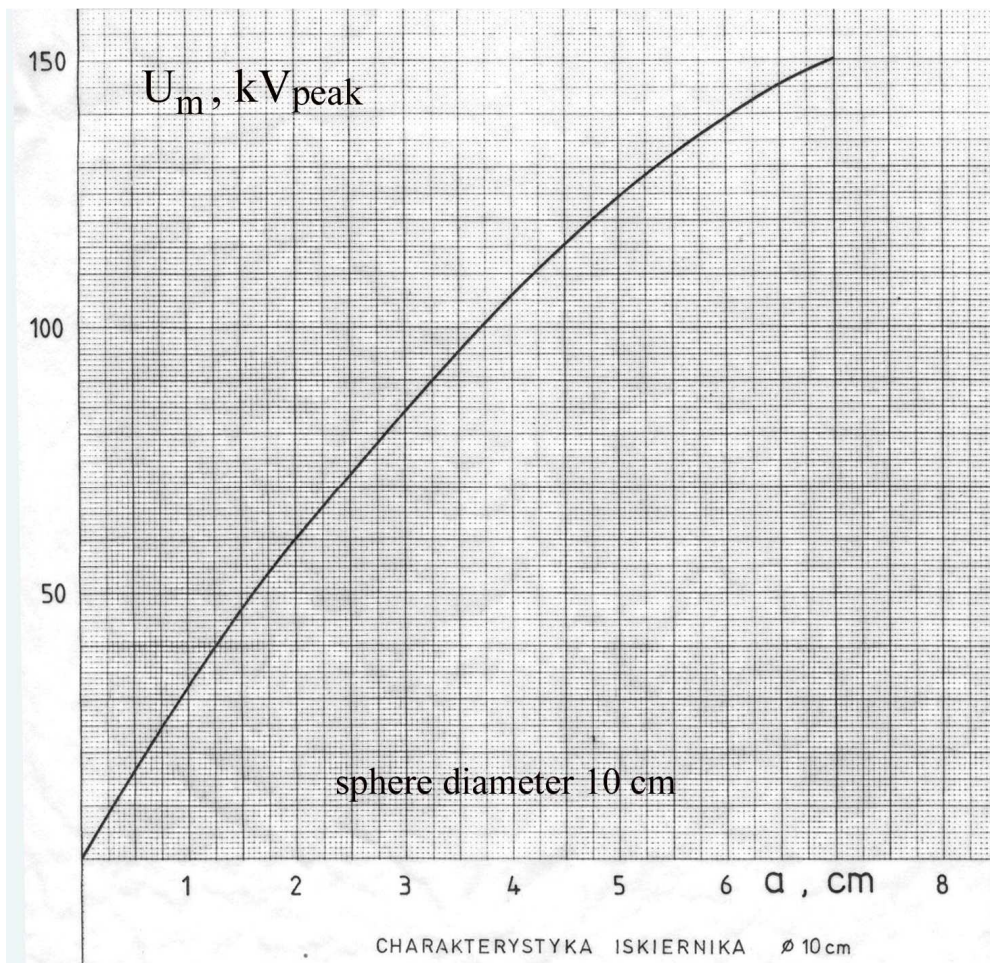


Fig. 6. Characteristic of sphere air gap

PRACTICAL 2

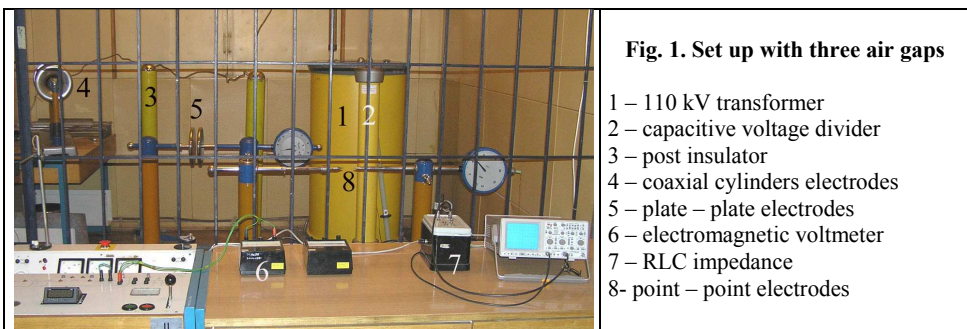
AIR BREAKDOWN IN UNIFORM OR NON-UNIFORM FIELD

2. 1. Purpose of the experiment

The purpose of the experiment is to measure the onset voltage of partial discharges and breakdown voltages in 3 air gaps arrangements: plate – plate, point – point and coaxial cylinders.

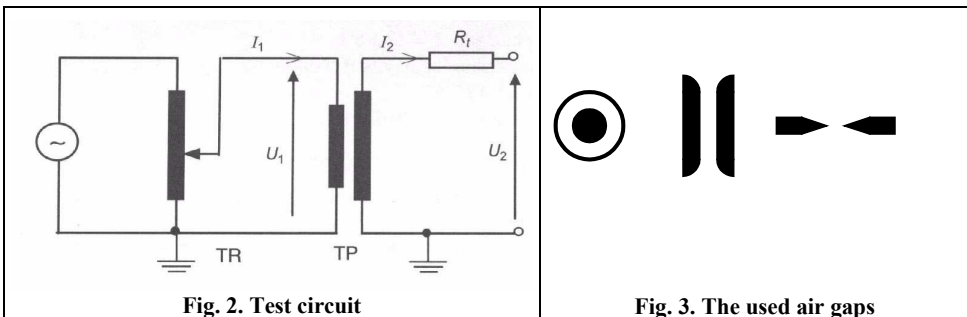
2. 2. Experimental set up

This experiment is carried out in the box shown in fig. 1.



2. 3. List of measuring devices

- Test transformer TP 110, voltage ratio $\eta = 475$
- Damping resistance 480Ω
- Voltmeter with digital display Lumel N15Z, 300 V, $R > 2 \text{ M}\Omega$, Error $0,5\% \pm 1 \text{ digit}$
- Electromagnetic voltmeters
- Oscilloscope
- RLC impedance (for description and parameters see fig. 4)



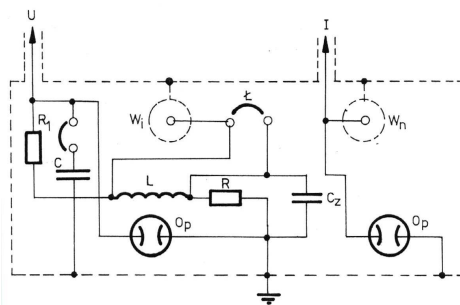


Fig. 4. Electrical circuit of RLC impedance used for measurement of voltage and corona currents of point –point electrodes.

W_i – output for current channel (connected to air gap)

W_n – output connected to voltage divider

L – short circuit switches

O_p – overvoltage protection element (gas tube)

R_1 – 2000 Ω , L = 3 mH, C_1 - 100 nF, C_2 - 100 nF.

2. 4. Measuring and calculation tasks

1. Measure the breakdown voltage of plate – plate arrangement for the distance of 1 cm and for 3 cm.
2. Measure the onset voltage of corona discharges and breakdown voltages of the coaxial arrangement with different radius of internal electrode. From the following diameters of internal electrodes: 1, 3, 8, 12, 20, 25, 50, 55 mm use at least: **1, 3, 8, 25** and **55** mm. The diameter of external electrode is equal to 75 mm. Find the onset voltage of corona based on acoustic noise – method.
3. Measure the onset voltage of corona and the breakdown voltage of point – point arrangement as a function of electrode distance. Use at least the following distances **2, 6, 12, 22** cm. Find the onset voltage of corona by optical method in dark room.
4. Connect the RLC impedance to the point – point arrangement and find the onset voltage of corona for positive and negative polarity of voltage wave. Fix the electrode distance for 12 cm before this measurement. Avoid the breakdown, do not increase the voltage over the value of 80% of breakdown voltage. Breakdown is dangerous for RLC impedance and for oscilloscope.
5. Calculate the breakdown voltages of point – point arrangement for the distances used at the measurements from the ABB formula. Compare the calculations with the experimental data in the separate figure.
6. Calculate the maximum electrical field in point to point air gap for the same distances assuming the angle $\alpha = 6^\circ$, draw the function $E_{max} = f(s)$.

2. 4. Additional informations

The BBC formula for the non-symmetric point – point air gap for the distances $s > 6$ cm under the following atmospheric conditions: $T = 293$ K, $p = 950$ hPa, absolute humidity of 13 g/m^3 .

$$U_b = 3,16 \cdot s + 14$$

where U_b is the breakdown voltage in kV_{rms} and s is the distance between electrodes in cm.

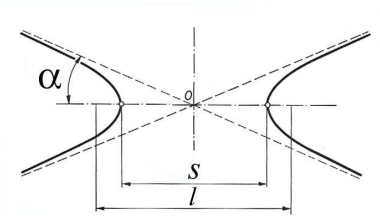


Fig. 5. Approximation of point electrodes to rotational hyperboloids

The maximum electrical field intensity of point – point air gap can be estimated if the electrode tips are modelled by hyperboloids. The cross section of such volume forms a hyperbola described by the axis “s” and the focus “l” where the angle α is measured between axis l and the asymptote crossing the point O (fig. 5).

$$E_{\max} = E_{\text{mean}} \cdot \beta = \frac{U}{s} \cdot \frac{\cos \alpha}{\sin^2 \alpha \cdot \ln \operatorname{ctg} \frac{\alpha}{2}} \quad (1)$$

$$\beta = \frac{\cos \alpha}{\sin^2 \alpha \cdot \ln \operatorname{ctg} \frac{\alpha}{2}} \quad (2)$$

For small angles ($\alpha < 7^\circ$), formula (1) can be simplified to:

$$E_{\max} = \frac{U}{s} \cdot \frac{1}{\alpha^2 \cdot \ln \frac{2}{\alpha}} \quad (3)$$

Let calculate E_{\max} for $\alpha = 6^\circ$ (0,105 rad).

2. 5. Report contents

1. Purpose of the experiments, measuring circuits.
2. List of measuring equipment with main technical data and numbers.
3. Measurement readings and calculation results, calculation examples, conclusions.
4. Manual measuring report signed by the tutor.
5. Draw the functions $U_b = f(s)$ and $E_{\max} = f(s)$ for point – point air gap.

2. 6. Control questions

1. Give the definition of the non-uniformity factor β , write the formula for medium value of electrical field between the electrodes of an air gap.
2. Breakdown in uniform and non-uniform field.
3. Explain the terms: glow, streamer, lider, arc.
4. Pashen’s law.
5. Normal atmospheric conditions.
6. Correction of breakdown voltage to normal atmospheric conditions.
7. Rogowski profile.

8. Optimum ratio of radiuses in coaxial electrodes.

2. 7. References

[1]J.P. Holtzhausen, W.L. Vosloo, High Voltage Engineering, Practice and Theory, Stellenbosch University, 2008, Chapter 2, Chapter 3.1.

[2]Arora R., Mosch W., High Voltage Insulation Engineering, New Age, New Dehli (1995) 2004, Chapter 1, Chapter 2,

[3] Ryan H.M., (editor), High voltage engineering and testing, second edition, The Institution of Electrical Engineers, London 2001, Chapter 20.

PRACTICAL 2 : AIR BREAKDOWN IN UNIFORM OR IN NON-UNIFORM FIELD

Manual measuring report date :

Laboratory team number

- 1. Reporter
- 2. Student
- 3. Student
- 4. Student
- 5. Student
- 6. Student

Tutor's signature

Climatic conditions: T =°C, p = hPa, RH =%

$\delta =$

Table 1. Measurement of the breakdown voltage of plate – plate air gap

No	s	U_1	$U_{1\text{ mean}}$	$U_{2\text{ pT}}$	$U_{2\text{ N}}$	η	Remarks
	cm	V	V	kV	kV	-	
1	1						
2							
3							
1	3						
2							
3							

U_1 - low voltage

$U_{1\text{ mean}}$ – mean value of low voltage (for three consequence readings)

$U_{2\text{ pT}}$ - breakdown voltage in real atmospheric conditions, $U_{2\text{ pT}} = U_{1\text{ mean}} \cdot \eta$

$U_{2\text{ N}}$ – high voltage corrected to normal atmospheric conditions

η - transformer voltage ratio a (s) - distance between air gap

Table 2. Measurement with coaxial air gaps

No	d	U _o	U _{o mean}	U _o	U _b	U _{b mean}	U _{b N}	E _{max}	Remarks
	mm	V	V	kV	V	V	kV	kV/cm	
1	1								
2									
3									
1	3								
2									
3									
1	8								
2									
3									
1	12								
2									
3									
1	20								
2									
3									
1	25								
2									
3									
1	50								
2									
3									
1	55								
2									
3									

E_{max} – calculated maximum value of electrical field from formula (3)

U_o – onset voltage of corona

U_b – Breakdown voltage in real atmospheric conditions

U_{bN} – Breakdown voltage in normal atmospheric conditions (after the correction of measurement results)

Table 3. Measurement with point - point air gap

No	s	U_o	$U_{o \text{ mean}}$	U_o	U_b	$U_{b \text{ mean}}$	U_{bN}	Remarks
	mm	V	V	kV	V	V	kV	
1	2							
2								
3								
1	6							
2								
3								
1	12							
2								
3								
1	22							
2								
3								

U_o – onset voltage of corona

U_b – Breakdown voltage in real atmospheric conditions

U_{bN} – Breakdown voltage in normal atmospheric conditions (after the correction of measurement results)

Table 4. Onset voltage measurement of corona by means of an oscilloscope and RLC impedance

s	U_{o+}	U_{o+}	U_{o-}	U_{o-}
cm	V	kV	V	kV
12				

PRACTICAL 3

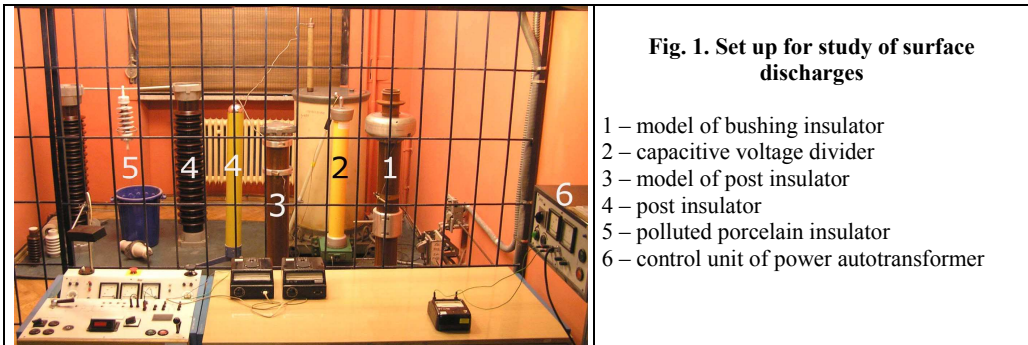
SURFACE DISCHARGES AND SURFACE FLASHOVER

3. 1. Purpose of the experiment

The purpose of the experiment is to study the different form of surface discharges on three model insulators: a post, a bushing and on contaminated porcelain insulator.

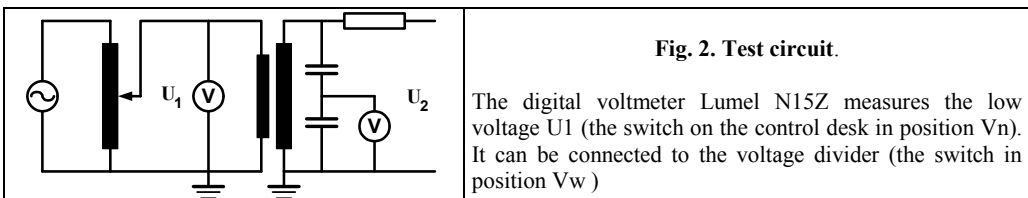
3. 2. Experimental set up

This experiment is carried out in the box shown in fig. 1.



3. 3. List of measuring devices

- Test transformer TP 110, voltage ratio $\eta = 479$
- Damping resistance 500Ω
- Capacitive voltage divider voltage ratio **311** (without short-circuiting gear), **822** (with short-circuiting gear)
- Vvoltage with digital display Lumel N15Z, 300 V, $R > 2 \text{ M}\Omega$, Error $0,5\% \pm 1$ digit
- Electrostatic voltmeter type C50, 75 V, 20 Hz – 10 MHz
- Electrostatic voltmeter type C50, 150 V, 20 Hz – 10 MHz
- Electromagnetic voltmeter



3. 4. Measuring and calculation tasks

1. Measure the flashover voltage U_F of post insulator for the electrode distance of 5, 10 and 15 cm. The voltage should be measured by means of the electrostatic voltmeter connected to the low side of voltage divider
2. Find optically the onset voltage of ionisation U_0 for the electrode distance of 15 cm in the darkened room.
3. Calculate the flashover voltage of post insulator for the same distances from the equations (1) and (2)

4. Find optically in the dark room the onset voltage of ionisation U_o , the onset voltage of creeping discharges U_C , and the flashover voltage U_F of bushing insulator for the electrode distance of 5, 10, 15 and 40 cm.
5. For the electrode distances of 10, 15 and 40 cm calculate the flashover voltage U_F of bushing insulator from equation (3). Assume the K value in the equation (3) as equal to 43.
6. Carry out 2 or 3 voltage test of polluted insulator to produce partial arcs and estimate the pollution flashover voltage. The test transformer should be connected to the external 70 kVA autotransformer. At the opened disconnecting switch fix the selected value of voltage and then close promptly the disconnecting switch. In the case of flashover, choose the lower voltage for the next trial. In the case of withstand, choose the higher voltage for the following trial. (up and down procedure)

3. 5. Additional information

The flashover voltage U_F (kV) of a post insulator as a function of electrode distance l can be calculated from the following empirical formulas:

$$U_F = 3,35 \cdot l + 20 \quad \text{for } l > 10 \text{ cm} \quad (1)$$

$$U_F = 7,3 \cdot l - 0,2 \cdot l^2 \quad \text{for } l \leq 10 \text{ cm} \quad (2)$$

The flashover U_F of bushing insulator :

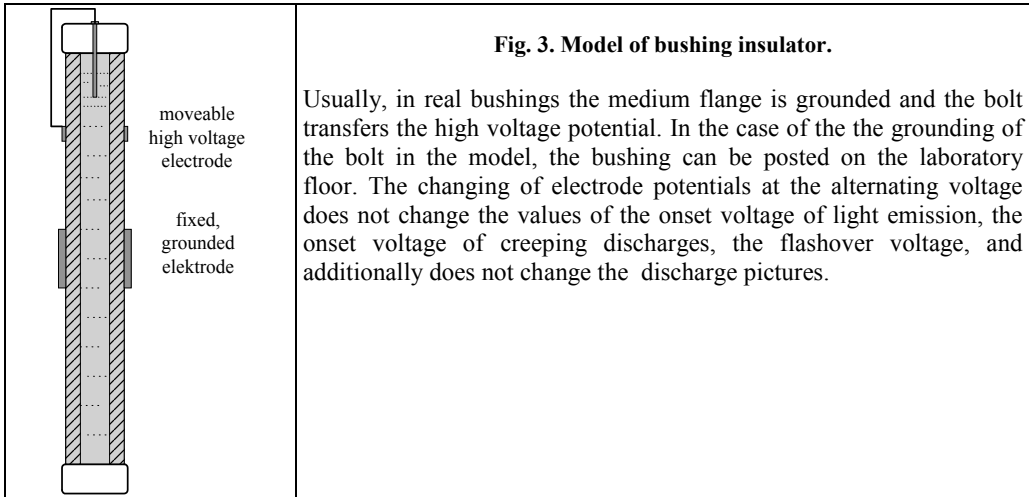
$$U_F = K \cdot l^{0,2} \cdot \left(\frac{R \cdot \ln \frac{R}{r}}{\epsilon_r} \right)^{0,4} \quad (3)$$

For cylindrical bushing with the radiuses $R = 7,5$, $r = 5$ cm, and the electrode distance l from 10 to 30 cm, under AC voltage measured in kV_{rms} the constant $K = 43$.

Table 1. Parameters of model insulators

Model type	Dimensions (cm)	ϵ_r
Post insulator	D = 15, d = 10	7
Bushing insulator	D = 15, d = 10	7
line insulator LP 60/5U	H = 26, L = 52, f = 3,0	-

D – external diameter, d – internal diameter, H = electrode distance, L = leakage distance



3. 6. Report contents

- Purpose of the experiments, measuring circuits,
- List of measuring equipment with main technical data and numbers.
- Measurement readings and calculation results, calculation examples, conclusions,
- Manual measuring report signed by the tutor
- Draw the experimental and theoretical functions $U_F = f(l)$ for the post insulator on one figure.
- Draw a similar figure for the bushing insulator, with experimental data for the $l = 5, 10, 15$ and 40 cm and with calculated results for the $l = 10, 15$ and 40 cm

3. 7. Control questions

1. Influence of dielectric material on the flashover voltage of a clean post insulator.
2. Mechanisms of surface discharges:
 - on post insulator
 - on bushing insulator
 - on contaminated insulator
3. Requirements for test voltage sources including the sources used for testing of polluted insulators
4. Parameters of outdoor insulators
5. Up and down method

3. 8. References

- [1] Kuffel E., Zaengl W.S., Kuffel J., High Voltage Engineering Fundamentals, Newnes 2004, Chapter 9
- [2] Looms J.S.T., Insulators for High Voltages, Peter Peregrinus Ltd, 1990

PRACTICAL 3 : SURFACE DISCHARGES AND SURFACE FLASHOVER

Manual measuring report date :

Laboratory team number

1. Reporter
2. Student
3. Student
4. Student
5. Student
6. Student

Tutor's signature

Climatic conditions: T =°C, p = hPa, RH =%

$\delta =$

Table 1. Flashover voltage of post insulators

No	l	U_1	$U_{1\text{ mean}}$	$U_{2\text{ pT}}$	$U_{2\text{ N}}$	Remarks
	cm	V	V	kV	kV	
1	5					
2						
3						
1	10					
2						
3						
1	15					$U_o =$
2						$U_o =$
3						$U_o =$

U_1 - low voltage

$U_{1\text{ mean}}$ - mean value of low voltage (for three consequent readings)

$U_{2\text{ pT}}$ - breakdown voltage in real atmospheric conditions, $U_{2\text{ pT}} = U_{1\text{ mean}} \cdot \eta$

$U_{2\text{ N}}$ - high voltage corrected to normal atmospheric conditions

η - transformer voltage ratio l - distance between electrodes

Table 2. Onset voltage of creeping discharges and flashover voltage of bushing insulator

No	<i>l</i>	U_c	$U_{c\ mean}$	U_c	U_F	$U_{F\ mean}$	U_{FN}	Remarks
	cm	V	V	kV	V	V	kV	
1	5							
2								
3								
1	10							
2								
3								
1	15							
2								
3								
1	40							
2								
3								

U_c – onset voltage of creeping discharges

U_F – Flashover voltage in real atmospheric conditions

U_{FN} – Flashover voltage in normal atmospheric conditions (after the correction of measurement results)

Note : The onset voltage of creeping discharges U_c is not the onset voltage of ionisation U_o (when a small optical light is visible). The creeping discharges are yellow sparks associated by a characteristic clics (acoustic signal). Ionisation is associated by a blue weak light.

Estimation of 50% pollution flashover voltage

Example :

32	kV																				
30										F				F							
28								F	W		F		W		F					F	
26			F		F		W		W				W			F		W			
24		W		W		W												W			
22		W																			
		1	2	3	4	5	6	7	8	9	10	11	12	13	14	15	16	17	18	19	20

W – withstand F – flashover

Simulate the test results according to up and down method and calculate the 50% pollution flashover voltage :

	kV																				
		1	2	3	4	5	6	7	8	9	10	11	12	13	14	15	16	17	18	19	20

PRACTICAL 4

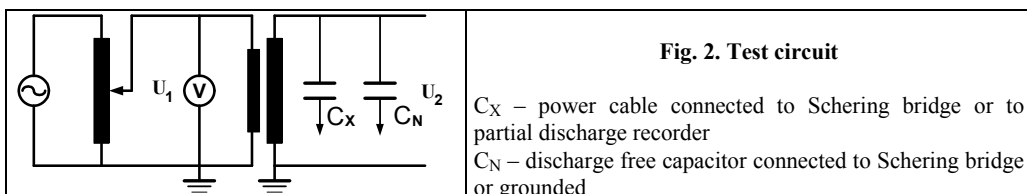
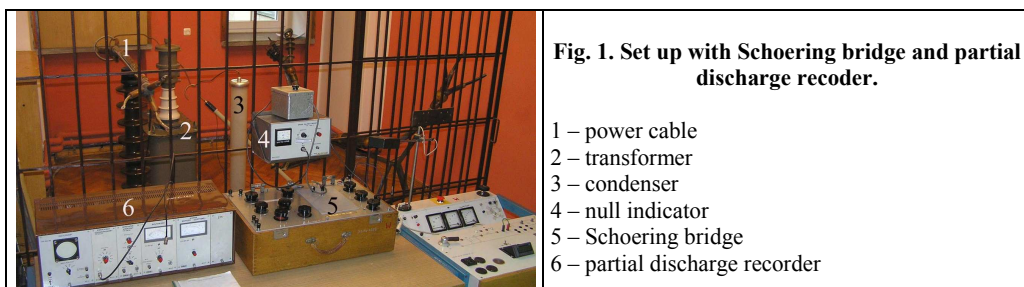
MEASUREMENT OF DIELECTRIC LOSSES AND PARTIAL DISCHARGES

4. 1. Purpose of the experiment

The purpose of the experiment is to measure the onset voltage of partial discharges in a power cable by means of Schering bridge and partial discharge recorder. The dissipation factor $\tan \delta$ and the apparent charge will be estimated as a function of voltage.

4. 2. Experimental set up

This experiment is carried out in the box shown in fig. 1.



4. 3. List of measuring devices

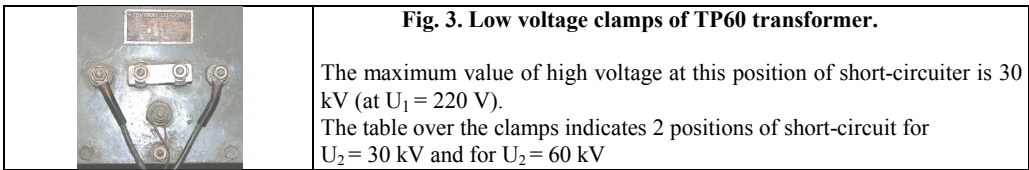
- Test transformer TP 60, manufactured by ZWAR
- Low voltage 220 V, 50 Hz, High voltage 60 kV/30 kV
- Continuous power 10/5 kVA Temporary power (15 min) 20/10 kVA
- Continuous secondary current 0,17 A Temporary secondary current (15 min) 0,34 A
- Test voltage 50 Hz, 78 kV Discharge free capacitor 500 pF \pm 1%, 50 kV, 50 Hz, Robinson Electronic Instruments, Manchester
- Voltmeter with digital display Lumel N15Z, 300 V, $R > 2 \text{ M}\Omega$, Error 0,5% \pm 1 digit
- Electromagnetic voltmeter

4. 4. Measuring and calculation tasks

1. Connect the Schering bridge to the test circuit and estimate:
 - the capacitance of power cable based on data given below (in additional information)
 - maximum current flowing through the bridge resistance R_3 (under the maximum allowable voltage)
2. Find the balance of the bridge for different value of the test voltage and then calculate C_X and $\tan \delta_X$
3. Connect the partial discharge recorder to the test circuit according to the instruction of the set up
4. Determine the calibration factor K of measuring arrangement
5. Find the onset voltage of partial discharges and measure the maximum apparent charge Q_X as a function of voltage.

6. Observe on the oscilloscope how the pictures of partial discharges change.

4. 5. Additional information



The maximum test voltage have to be smaller than 11, 5 kV.

Carry out the measurements with the Schering bridge and with the partial discharge recorder in the voltage range of 5 – 11 kV.

Parameters of tested power cable

Type HAKFtA 3 × 150, nominal voltage $U_n = 20$ kV (phase to phase !)

Length = 2 m, unit capacitance 0,3 μ F/km

4. 6. Report contents

- Purpose of the experiments, measuring circuits,
- List of measuring equipment with main technical data and numbers.
- Measurement readings and calculation results, calculation examples, conclusions,
- Manual measuring report signed by the tutor
- Introductory calculations dealing with approximate value of C_x , R_3 , and maximum value of current flowing through the resistance R_3 .
- Draw the following functions: $\tan \delta_x = f(U)$, $C_x = f(U)$, $Q_x = f(U)$, P (W/km) = $f(U)$ in one figure,
- Determine the onset voltage of ionization from the functions: $\tan \delta_x = f(U)$, $Q_x = f(U)$,
- Based on the above relationships and the nominal voltage of the power cable evaluate its technical state (can this underground cable be used in the power system ?)

4. 7. Control questions

1.	Reasons of dielectric losses in electrical insulation
2.	A typical relation between voltage and $\tan \delta$
3.	High voltage Schering bridge, basic types, balance conditions
4.	Partial discharges, the role for ageing process
5.	Model of solid insulation with a gas cavity, definition of $\tan \delta$
6.	Partial discharge measurement, explain the term “apparent charge”
7.	What maximum voltage value of transformer is used here ? What is the maximum permissible voltage value of the power cable ?
8.	The power losses in the underground cables

4. 8. References

[1] BICC cables, Electric cables handbook, third edition, Wiley-Blackwell 1997, available in Knovel data bank.

[2] Naidu M.S., Kamaraju V., High Voltage Engineering, second Ed., McGraw-Hill, 1996, Chapter 9.

[3] J.P. Holtzhausen, W.L. Vosloo, High Voltage Engineering, Practice and Theory, Stellenbosch University, 2008, Chapter 4

INSTRUCTION MANUAL OF PARTIAL DISCHARGE RECORDER MWN

The partial discharge recorder MWN (Fig. 4) manufactured by Scientific and Dydactic Apparatus Manufacturer ZANID can measure maximum apparent charge of partial discharges Q . The recorder consists of the following parts:

- oscilloscope POS-302
- wide band amplifier WS-401
- standard generator GW-201
- electronic voltmeter WE-201
- peak value meter DWS-201.

The measuring impedance ZUW-1 (Fig. 5) is an additional, element belonging to the partial discharge recorder.

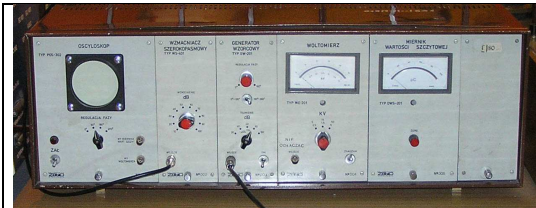
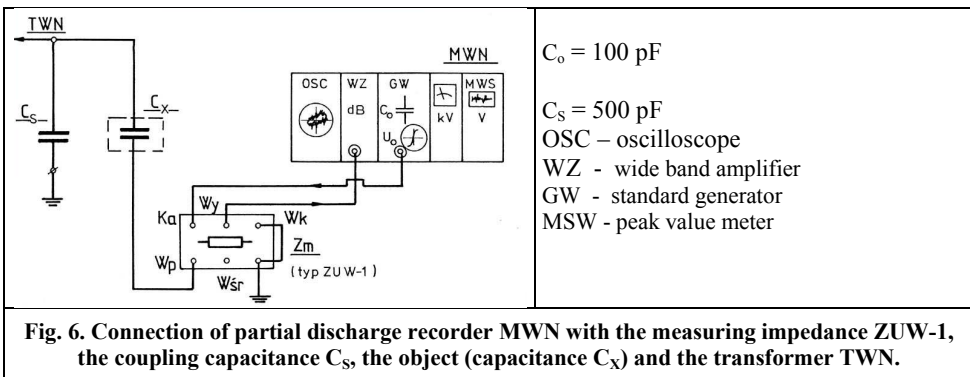


Fig. 4. Partial discharge recorder MWN



Fig. 5. Measuring impedance ZUW-1

The standard generator, connected to the capacitance C_o , produces the rectangular impulses with regulated voltage amplitude U_o . The capacitance C_o is usually many times smaller than the object capacitance C_x (Fig. 6). In this tutorial the calibrator is connected to the measuring impedance. This method is called the indirect calibration, (Fig. 6).



CALIBRATION PROCEDURE

Build the circuit according to figure 6:

- connect the input of wide band amplifier WZ with the output (WY) of measuring impedance ZUW-1 using the coaxial cable,
- connect the output of standard generator GW with BNC jack KA (calibration) of measuring impedance ZUW-1,
- connect the object C_x to the BNC jack Wp (wejście początek) of measuring impedance ZUW-1,
- connect the BNC jack Wk (wejście koniec) and earth terminal with the earth potential,
- connect the output of the coupling capacitance C_s to the earth potential.

The reactance of the coupling capacitance C_s and the object capacitance C_x are negligible for partial discharge signals ($C_s, C_x \gg C_o$). In this case, the charge in the circuit depends only on the value of C_o and on the voltage U_o .

$$Q_o = U_o \cdot C_o \quad (1)$$

The circuit calibration factor K is given by the quotient

$$K = \frac{Q_o}{\Delta U_{we}} \quad (2)$$

where ΔU_{we} is the maximum value of impulses measured by peak value meter MWS during the calibration.

The voltage value of standard generator depends on the position of attenuation knob (tłumienie) and can be read from table 1

Table 1. The voltage U_o of standard generator

Attenuation (dB) (Tłumienie)	20	40	60	80	100
calibration voltage U_o (V)	10	1,0	0,1	0,01	0,001

The peak voltage value ΔU_{we} during the calibration procedure (and later during the measurement of apparent charge) can be calculated based on the indication of the peak value meter MWS and then using table 2. The voltage ranges (100 scale divisions) correspond to amplification in decibels dB of wide band amplifier WZ.

Table 2. Voltage ranges of the peak value meter MWS corresponding to the amplification value of wide band amplifier WZ

Amplification dB	100	90	80	70	60	50	40	30	20	10
U_{we} (mV)	0,1	0,316	1,0	3,16	10	31,6	100	316	1000	3160

ESTIMATION OF THE CALIBRATION FACTOR K

Set the positions of the following switches:

- phase of the standard generator in position 0 - 180°,
- attenuation of the standard generator in position 20 dB,
- amplification of the wide band amplifier in position 60 dB,
- the power switches of the partial discharge recorder and the standard generator in position 'ON' (Za).

The ellipse with 2 scaling marks will appear on the oscilloscope lamp after 1 minute of warming time. Then, do the following:

- read the pointer indication in scale divisions α on the peak value meter MWS,
- read U_o from table 1 and U_{we} from table 2,
- calculate the the charge Q_o from equation (1) and the calibration factor K using equation (2).

MEASUREMENT OF THE PARTIAL DISCHARGE ONSET VOLTAGE AND OF THE APPARENT CHARGE Q

- switch off the standard generator GW,
- set the amplification of wide band amplifier in position 80 dB,
- switch on the high voltage,
- increase slowly the voltage up to the moment when the spikes appear on the oscilloscope lamp. Then, note the onset voltage value U_i indicated by the voltmeter on the low side of the transformer),
- set the amplification to the position where pointer indication is smaller than 100 scale divisions,
- calculate the maximum value of apparent charge Q ,
- repeat the charge measurement for a few set of voltages.

EXAMPLE OF CALIBRATION FACTOR K CALCULATION

Given data: attenuation of standard generator equal to 20 dB \Rightarrow from table 1: $U_o = 10$ V.

Given $C_o = 100$ pF and $U_o = 10$ V $\Rightarrow Q_o = U_o \cdot C_o = 10 \cdot 100 = 1000$ pC.

Now let's take a practical example: Suppose that the peak value meter MWS indicates 75 scale divisions that is $\alpha = 75$

Then, if the amplification of wide band amplifier = 60 dB \Rightarrow from table 2, $\Delta U_{we} = 10$ mV (for $\alpha = 100$ divisions)

For $\alpha = 75$ divisions $\Rightarrow \Delta U_{we} = 10 \text{ mV} \cdot \frac{75}{100} = 7,5 \text{ mV}$

$$K = \frac{Q_o}{\Delta U_{we}} = \frac{1000}{7,5} = 133 \frac{\text{pC}}{\text{mV}}$$

EXAMPLE OF APPARENT CHARGE Q CALCULATION

The peak value meter MWS indicates 90 scale divisions, $\alpha = 90$ divisions.

The amplification of wide band amplifier = 80 dB \Rightarrow from table 2, $\Delta U_{we} = 1$ mV (for $\alpha = 100$ divisions).

For $\alpha = 90$ divisions $\Rightarrow \Delta U_{we} = 1 \text{ mV} \cdot \frac{90}{100} = 0,9 \text{ mV}$

$Q = K \cdot \Delta U_{we} = 133 \cdot 0,9 = 120$ pC

PRACTICAL 4 : MEASUREMENT OF DIELECTRIC LOSSES AND PARTIAL DISCHARGES

Manual measuring report date

Laboratory team number

1. Reporter
2. Student
3. Student
4. Student
5. Student
6. Student

Tutor's signature

Tab. 1. Selection of Schering bridge elements.

Length of power cable $l = 2$ m Unit capacitance of power cable $C_U = 0,3 \mu\text{F}/\text{km} = \dots\dots\dots\text{pF}/\text{m}$

C_X	R_4	R_3	C_N	U_2	η_{TR}	U_1	f	I_{load}	I_{perm}
pF	Ω	Ω	pF	kV	-	V	Hz	mA	mA
	$1000 / \pi$		500	11,5					70

- C_X – estimated capacitance of power cable under test
- R_3 - estimated value of resistance from the bridge balance equation (formula 1, next page)
- U_1 - maximum permissible value of test voltage calculated for the low voltage side of transformer
- η_{TR} – voltage ratio of test transformer
- f - voltage frequency
- I_{load} – calculated load current of the bridge
- I_{perm} – permissible load current of the bridge at the shunt position „ ∞ „

Table 2. Estimation of function $C_X = f(U_2)$ and $\tan \delta = f(U_2)$

	U_1	U_2	R_3	C_4	$\tan \delta$	C_X	p	Remarks
	V	kV	Ω	μF	-	pF	W/km	
1								
2								
3								
4								
5								
6								
7								
8		11,5						

p – power loss in cable insulation per unit length

U_1 – onset voltage of ionization estimated from the function $\tan \delta = f(U_2)$

Table 3. Calibration of partial discharge recorder

C_0	U_0	Q_0	α	Amplification	U_{100}	ΔU_{input}	K
pF	V	pC	units	dB	mV	MV	pC / mV
100							

C_0 - capacitor capacitance of calibrator

U_0 - impulses amplitude from calibrator

Q_0 - charge flowing through cable capacitance C_X , ($Q_0 = C_0 \cdot U_0$)

α - indication of peak value meter at a given amplification

U_{100} - voltage range at a given amplification suitable to the full swing of indicating needle

ΔU_{input} – peak of voltage impulses measured by partial discharge recorder $\Delta U_{input} = U_{100} \frac{\alpha}{100}$

K - calibration coefficient $K = \frac{Q_0}{\Delta U_{input}}$

Table 4. Estimation of function $Q_a = f(U_2)$

	U_1	U_2	α	Amplification	U_{100}	ΔU_{input}	K	Q_a	Remarks
	V	kV	units	dB	MV	mV	pC / mV	PC	
1									
2									
3									
4									
5									
6									
7									
8									

Q_a – apparent charge

Formulas for calculation of C_X , $\tan \delta$ and power dissipated in the cable insulation :

$$C_X = C_N \frac{R_4}{R_3} \tag{1}$$

$$\tan \delta = \omega \cdot C_4 \cdot R_4 \tag{2}$$

$$P = U^2 \cdot \omega \cdot C_X \cdot \tan \delta \tag{3}$$

PRACTICAL 5.

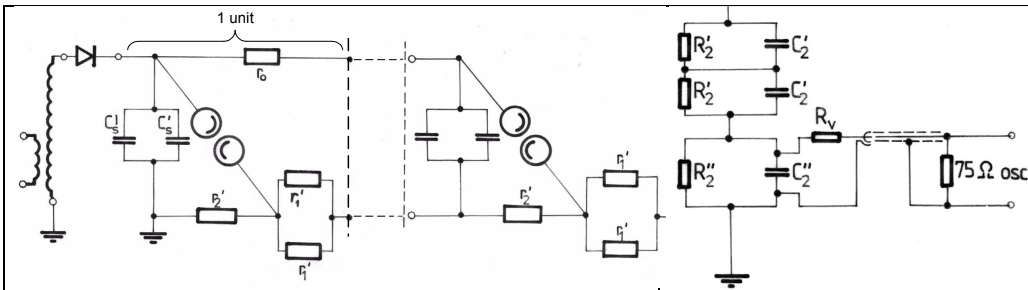
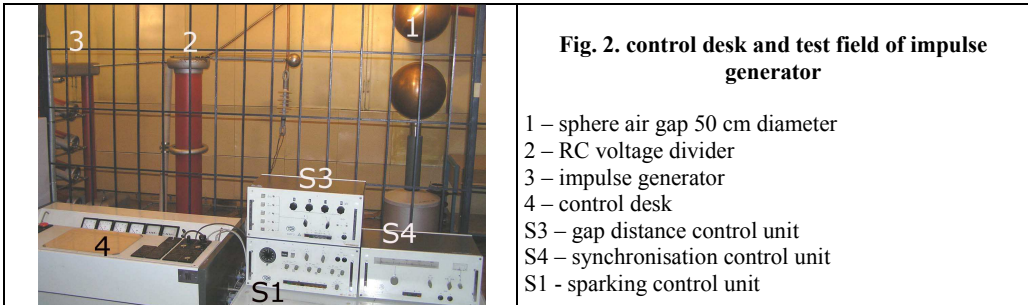
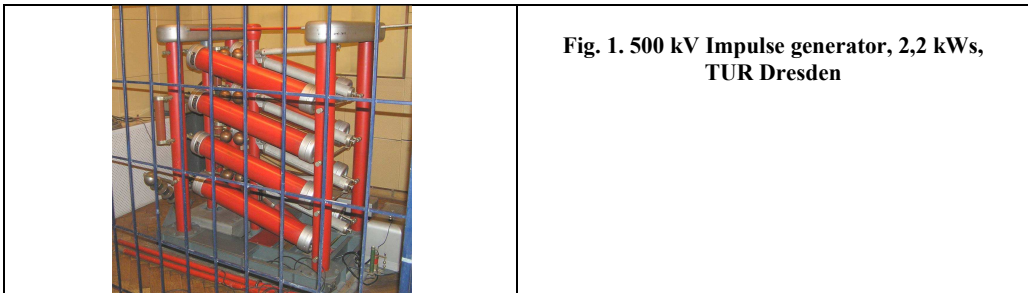
GENERATION OF IMPULSE VOLTAGES, IMPULSE FLASHOVER

5.1. Purpose of the experiment

The purpose of the experiment is the estimation of flashover voltage of 20 kV composite insulator under lightning impulses according to the serial method. Additionally, the construction and elements of multi-stage Marx generator will be analysed.

5.2. Experimental set up

This experiment is carried out in the box shown in fig. 1 and fig. 2.



$$C'_S = 0,035 \mu\text{F} \quad r'_1 = 122 \Omega \quad r_0 = 16,5 \text{ k}\Omega \quad r'_2 = 1360 \Omega$$

Fig. 3. Electrical circuit of 4-unit impulse generator GU500

$$C'_2 = 2966 \text{ pF} \quad R'_2 = 4026 \Omega$$

$$C''_2 = 888 \text{ nF} \quad R''_2 = 36,8 \Omega$$

$$r_v = 94 \Omega$$

Fig. 4. RC voltage divider

5.3. List of measuring devices

- RC voltage divider type SMCR 1500/500 TUR Dresden, voltage ratio **631** with cable having characteristic impedance of 75 Ω
- Precision impulse peak voltmeter SV642 Haefely, measuring range: low input: 16 V – 160 V, 1 M Ω
High input: 160 V – 1600 V, 2 M Ω

5.4. Measuring and calculation tasks

1. Make familiar with the construction of 4 - stage Marx generator and with its operation and remote control.
2. Calculate the time parameter T_1 and T_2 of generator based on values of capacitors and resistors given on the electrical circuit of generator.
Use the following relations: $T_1 \approx 2,5 \cdot R_1 \cdot C_2$ $T_2 \approx 0,7 \cdot R_{2E} \cdot C_1$
3. Estimate the 50% flashover voltage of 20 kV composite insulator according to serial method.
4. Based on the result of the voltage test and the Gauss grid estimate:
 - 50% flashover voltage – $U_{50\%}$
 - standard deviation – s
5. Estimate the withstand voltage U_W (the voltage at which the probability of flashover voltage is very low (less than 1%),
- $U_W = U_{50\%} - 3 \cdot s$
6. Calculate the impulse coefficient of composite insulator, knowing that its AC flashover voltage is kVrms.
7. Estimate the voltage efficiency of impulse generator, measure the charging DC voltage and the peak value of generated impulse.

5.5. Additional information

50% impulse flashover voltage. $U_{50\%}$ is the amplitude of impulse series applied to the test object (e.g. to the insulator) at which the probability of flashover occurrence is equal to 0,5 (50%). $U_{50\%}$ is estimated according to series method or according to up and down method.

Impulse coefficient k_i :
$$k_i = \frac{U_{50\%}}{U_{AC\ peak}}$$

where the so called static flashover voltage (peak value) $U_{AC\ peak}$ could be the AC 50 Hz voltage or DC voltage.

Impulse voltage – time characteristics is the dependence of impulse flashover voltage on time to flashover

Voltage efficiency of impulse generator η_v -
$$\eta_v = \frac{V_{LI}}{V_{Ch}} \cdot 100\%$$

where :

V_{LI} - amplitude of lightning impulse produced by the generator,

V_{Ch} – charging voltage of impulse generator. In the case of multi-unit generator it is the charging voltage of one unit multiplied by number of units

Transformation of 4-unit generator into an equivalent 1-unit generator

The simplified procedure for calculation of parameters of one unit generator equivalent to 4 unit generator and estimation of times T_1 and T_2 is given below.

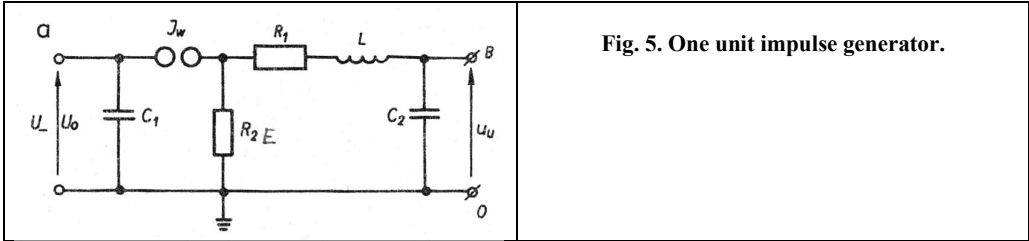


Fig. 5. One unit impulse generator.

$$C'_S = 0,035 \mu F \rightarrow C_1 = \frac{0,035 \times 2}{4} = 0,0175 \mu F$$

$$T_1 \approx 2,5 \cdot R_1 \cdot C_2$$

$$C'_2 = 2966 \text{ pF} \rightarrow C_2 = \frac{2966}{2} = 1483 \text{ pF}$$

$$T_2 \approx 0,7 \cdot R_{2E} \cdot C_1$$

$$r'_1 = 122 \Omega \rightarrow R_1 = \frac{122 \times 4}{2} = 244 \Omega$$

$$r'_2 = 1360 \Omega \rightarrow r_2 = 4 \times 1360 = 5440 \Omega$$

$$R'_2 = 4026 \Omega \rightarrow R_2 = 2 \times 4026 = 8052 \Omega$$

$$r_2 \text{ and } R_2 \text{ are connected parallel} \rightarrow R_{2E} = 3246 \Omega$$

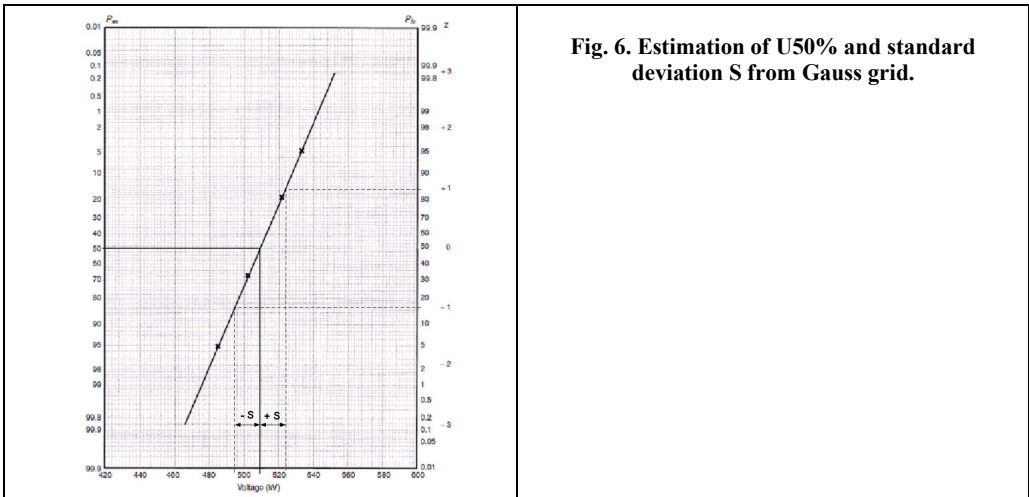


Fig. 6. Estimation of U50% and standard deviation S from Gauss grid.

5. 5. Control questions

1.	Parameters of lightning impulse voltage and switching impulse voltage
2.	Working principle of Marx impulse generator
3.	Electrical parameters of impulse generators and their relations to time parameters of impulse voltage
4.	Voltage efficiency of impulse generator
5.	Measurement of impulse voltage by means of sphere – sphere air gap, errors, advantages and disadvantages
6.	Voltage dividers for measurement of impulse voltages
7.	Peak value voltmeter
8.	50% impulse flashover voltage, definition, estimation methods, withstand voltage, 100% flashover voltage
9.	Impulse voltage – time characteristics, estimation method, the dependence on the electric field uniformity of tested insulation arrangements
10.	What is the time delay of flashover and its practical importance

5. 6. References

- [1] E. Kuffel, W.S. Zaengl, J. Kuffel, High Voltage Engineering Fundamentals, Newnes 2000, Chapter 2
- [2] J.P. Holtzhausen, W.L. Vosloo, High Voltage Engineering, Practice and Theory, Stellenbosch University, 2008, Chapter 4

PRACTICAL 5 : GENERATION OF IMPULSE VOLTAGES, IMPULSE FLASHOVER

Manual measuring report date.....

Laboratory team number

1. Reporter
2. Student
3. Student
4. Student
5. Student
6. Student

Tutor's signature

Climatic conditions: T =°C, p = hPa, RH =% δ =

1. Calculation of front time T_1 and time to half value T_2

$$T_1 \approx 2,5 \cdot R_1 \cdot C_2 =$$

$$T_2 \approx 0,7 \cdot R_{2E} \cdot C_1 =$$

2. Estimation of flashover voltage according to serial method

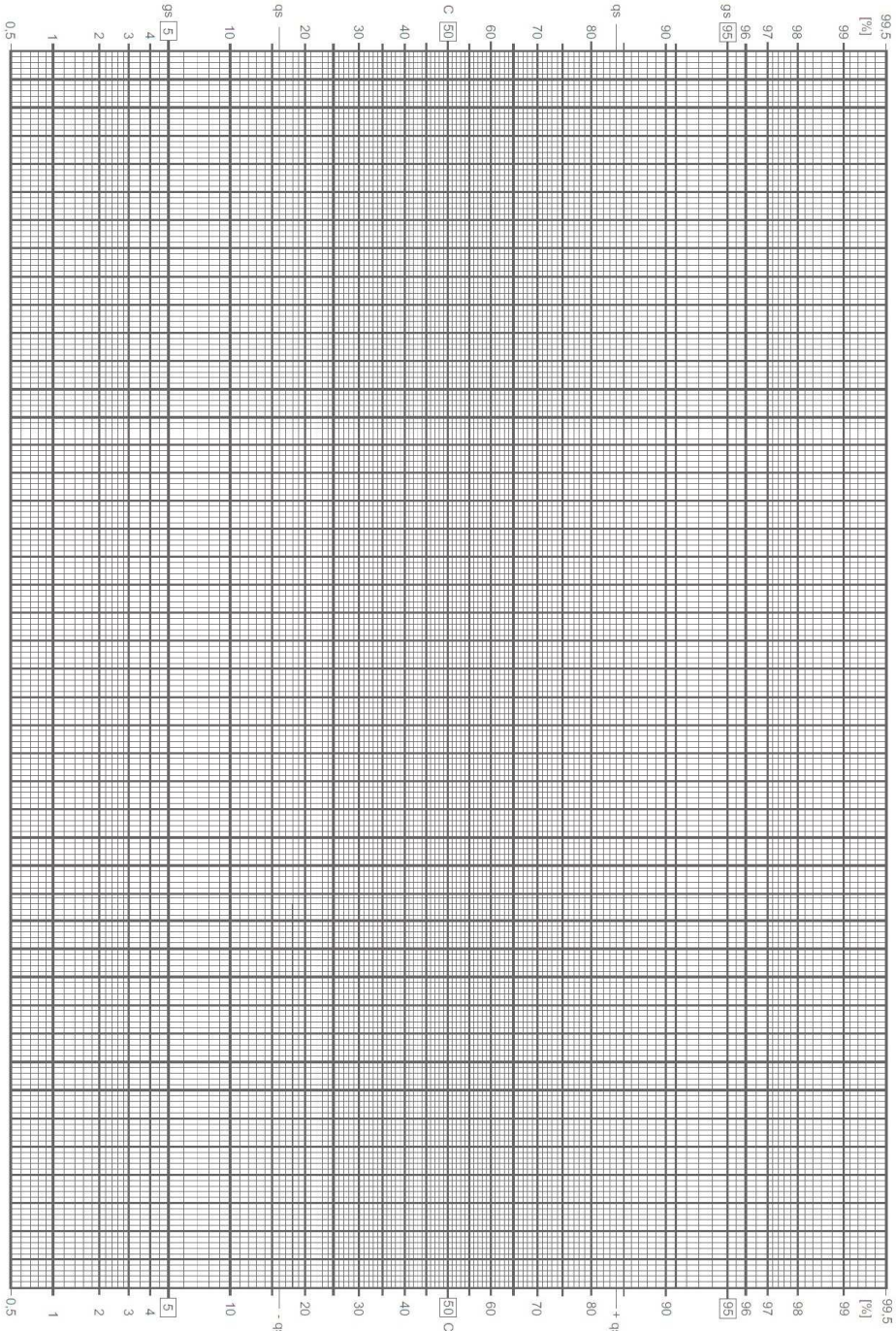
Charging DC voltage of one unit = kV										Distance between spark gaps mm										
	1	2	3	4	5	6	7	8	9	10	11	12	13	14	15	16	17	18	19	20
U	kV																			
F or W																				
Mean value of peak voltage from withstands U = kV													Flashover probability =							
Corrected value to normal atmospheric conditions $U_N =$ kV																				

Charging DC voltage of one unit = kV										Distance between spark gaps mm										
	1	2	3	4	5	6	7	8	9	10	11	12	13	14	15	16	17	18	19	20
U	kV																			
F or W																				
Mean value of peak voltage from withstands U = kV													Flashover probability =							
Corrected value to normal atmospheric conditions $U_N =$ kV																				

Charging DC voltage of one unit = kV										Distance between spark gaps mm										
	1	2	3	4	5	6	7	8	9	10	11	12	13	14	15	16	17	18	19	20
U	kV																			
F or W																				
Mean value of peak voltage from withstands U = kV										Flashover probability =										
Corrected value to normal atmospheric conditions U _N = kV																				

Charging DC voltage of one unit = kV										Distance between spark gaps mm										
	1	2	3	4	5	6	7	8	9	10	11	12	13	14	15	16	17	18	19	20
U	kV																			
F or W																				
Mean value of peak voltage from withstands U = kV										Flashover probability =										
Corrected value to normal atmospheric conditions U _N = kV																				

Gaus grid for estimation of 50% flashover voltage and withstand voltage



PRACTICAL 6

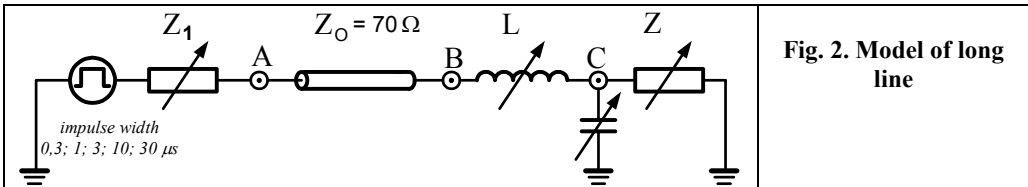
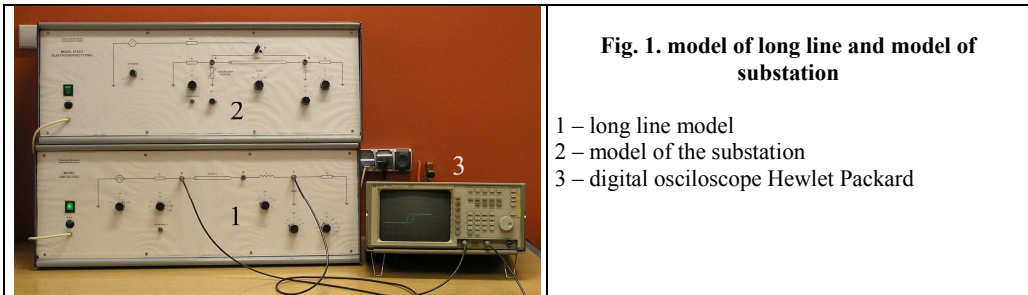
TRAVELLING WAVES ON A MODEL LONG LINE

6. 1. Purpose of the experiment

The purpose of the experiment is to measure and to calculate the amplitudes of waves on a long line model and to study the phenomena as reflections or elimination of surge impedance.

6. 2. Experimental set up

This experiment is carried out on the set up shown in fig. 1. The electrical circuit of long line model is presented in the figure 2.



6. 3. Measuring and calculation tasks

1.	Make familiar with operating manual of long line model and with the digital oscilloscope. At the values of parameters $Z_1 = Z_2 = 70 \Omega$, $L = 0$, $C = 0$, measure the amplitude of travelling wave coming to the line - u_1' . Measure the travel time of wave from the transition point A to the transition point B. Based on this measurement, calculate the cable length having the surge impedance $Z_1 = 70 \Omega$ between points A and B. Assume the wave velocity in the cable $v = 150 \text{ m}/\mu\text{s}$.
2.	At the fixed $Z_1 = 70 \Omega$, $L = 0$, $C = 0$ <ol style="list-style-type: none"> a) simulate the transition of travelling wave from the underground cable line to the overhead line ($Z_2 = 500 \Omega$) and b) the opposite case. It is impossible to regulate at this model the value of Z_0. Therefore, in this case, choose $Z_2 = 10 \Omega$ (the ratio $500/70 \Omega \cong 70/10 \Omega$). Estimate experimentally the values of transmission coefficient α_{o2} at the transition point B. Compare the α_{o2} values got from the measurements to the theoretical values calculated from the known values of Z_0 and Z_2 .
3.	At the fixed values $Z_1 = Z_2 = 70 \Omega$, study the influence of serial inductance L or the parallel capacitor C on the wave shape in transition point B. Explain this behaviour.
4.	Study the phenomenon called elimination of surge impedance at junction of the overhead line ($Z_1 = 500 \Omega$) to the transformer at the line end ($Z_2 = 2000 \Omega$). Measure the amplitudes for the first three reflections and the wave amplitude of the end state.

6. 4. Additional information

Amplitude u_2' of the wave traversing from the Z_1 line to the Z_2 line is expressed by the formula:

$$u_2' = \alpha_{12} \cdot u_1' \quad \text{where: } u_1' - \text{arriving wave amplitude} \quad \alpha_{12} - \text{transmission coefficient}$$

$$\alpha_{12} = \frac{2Z_2}{Z_1 + Z_2}$$

Amplitude of reflected wave:

$$u_1'' = u_2' - u_1' \quad u_1'' = \beta_{12} \cdot u_1' \quad \text{where: } \beta_{12} - \text{reflection coefficient}$$

$$\beta_{12} = \frac{Z_2 - Z_1}{Z_1 + Z_2}$$

6. 5. Report contents

- Purpose of the experiments, measuring circuit
- List of measuring equipment with main technical data and numbers
- Manual measuring report signed by the tutor
- Result of particular measuring tasks, drawings or photographs of observed waves,
- Values of transmission coefficients estimated experimentally and calculated from the chosen values of surge impedances.
- Control if the measured wave amplitude in end state at transition point B is similar to the wave amplitude calculated for the direct connection of line Z_1 to line Z_2 .
- Calculation examples
- Conclusions

6. 6. Control questions

1.	Overvoltages in the power system
2.	Circuit with lumped parameters and with distributed parameters
3.	Define the surge impedance
4.	Relation between current waves and voltage waves, graphical representation of waves
5.	Case I. wave transition from line having the surge impedance Z_1 to the line with surge impedance Z_2 , coefficient of transmission and reflection.
6.	Case II: open ended transmission line
7.	Case III: Short circuited line
8.	Attenuation and distortion of traveling waves in real power lines
9.	The phenomenon called elimination of surge impedance

6. 7. Literature

[1] Naidu M.S., Kamaraju V., High Voltage Engineering, second Ed., McGraw-Hill, 1996, Chapter 8, (8.1.5 and further)

[2] van der Sluis, L. Travelling Waves, in Transients in Power Systems, John Wiley & Sons, Ltd, 2002

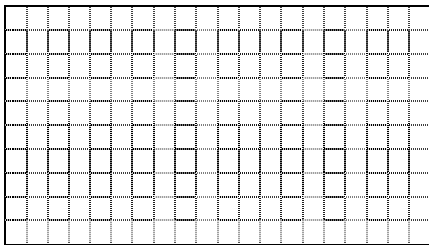
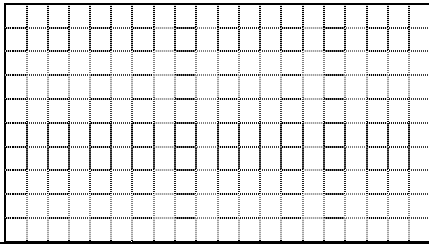
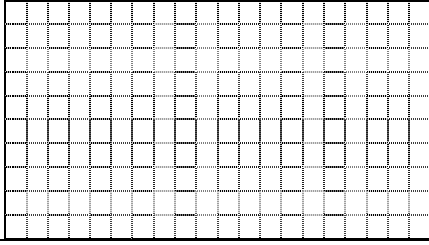
PRACTICAL 6 : TRAVELLING WAVES ON A LONG LINE MODEL

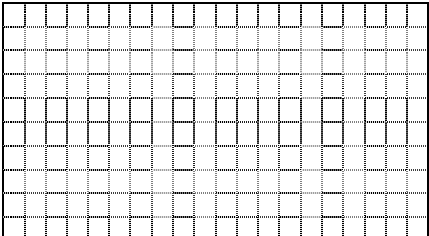
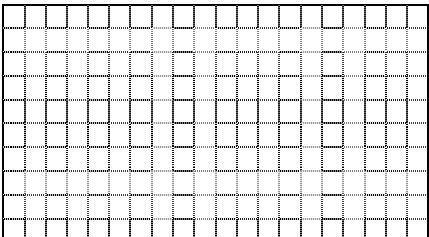
Manual measuring report date

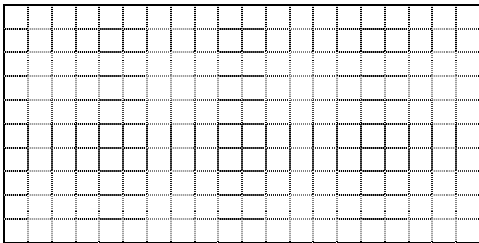
Laboratory team number

- 1. Reporter
- 2. Student
- 3. Student
- 4. Student
- 5. Student
- 6. Student

Tutor's signature

Observed wave shape	Parameters of model	The measured values
<p>Task 1</p> 	<p>Z1 =</p> <p>Z2 =</p> <p>L =</p> <p>C =</p>	
<p>Task 2a</p> 	<p>Z1 =</p> <p>Z2 =</p> <p>L =</p> <p>C =</p>	
<p>Task 2b</p> 	<p>Z1 =</p> <p>Z2 =</p> <p>L =</p> <p>C =</p>	

Observed wave shape	Parameters of model	The measured values
Task 3 	Z1 = Z2 = L = C =	
Task 4 	Z1 = Z2 = L = C =	



PRACTICAL 7

GENERATION AND MEASUREMENT OF DC VOLTAGE

7. 1. Purpose of the experiment

The purpose of the experiment is to study the Grainacher DC voltage source and the polarity dependence of breakdown voltage of point – plate air gap. Additionally, the DC voltage quality will be analysed.

7. 2. Experimental set up

This experiment is carried out in the box shown in fig. 1.

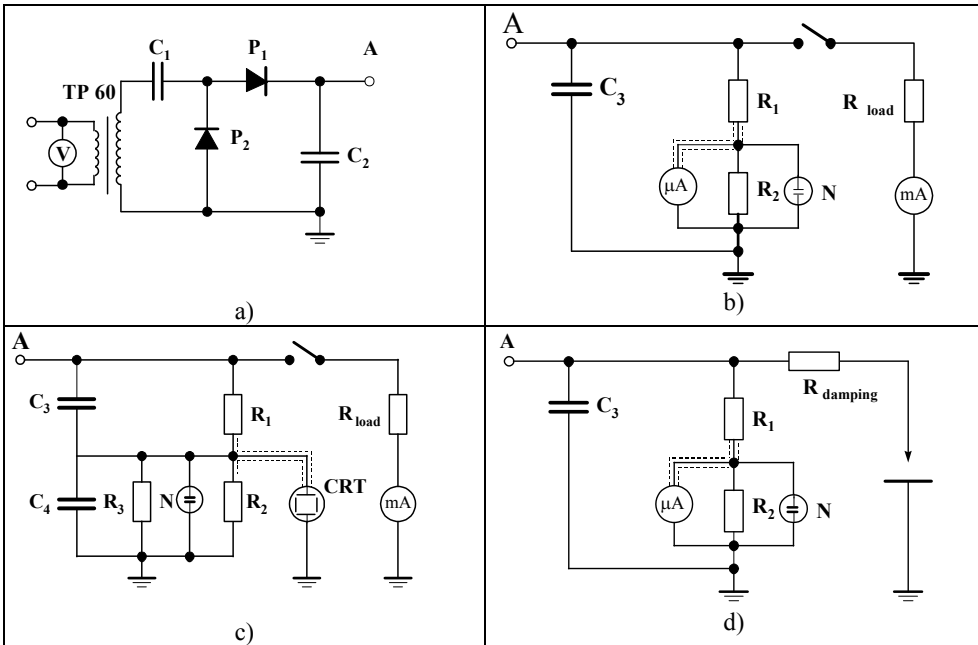
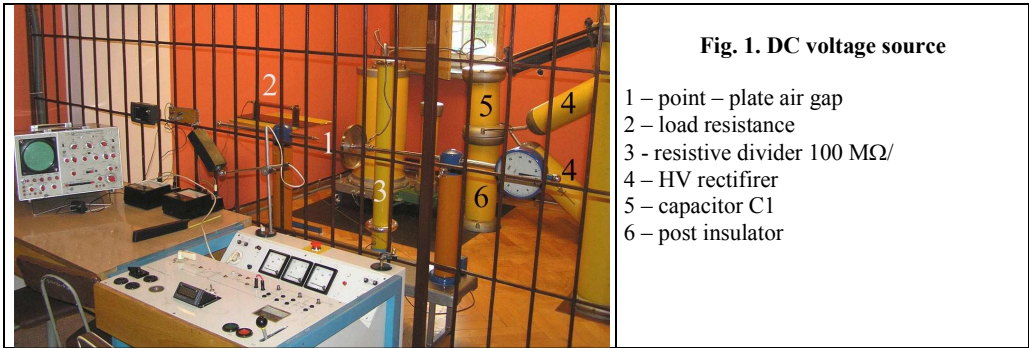


Fig. 2. Electrical circuit of DC source (a) and measuring circuits used in this training (b, c, d).

$C_1 = C_2 = 50 \text{ nF}$, $R_{\text{damping}} = 6 \text{ k}\Omega$, $R_{\text{load}} = 25 \text{ M}\Omega$

$C_3 = 2,35 \text{ nF}$, $C_4 = 2,286 \text{ mF}$, $R_1 = 100 \text{ M}\Omega$, $R_2 = 85 \text{ k}\Omega$ - elements of voltage dividers

7. 3. List of measuring devices

- Test transformer TP60, voltage ratio $\eta = 60\text{kV}/220 \text{ V} = 273$
- Moving-coil microammeter LM-3 class 0,5,
- Moving-coil miliammeter LM-1 class 0,5,
- Ddigital voltmeter Lumel N15Z, 300 V, $R > 2 \text{ M}\Omega$, Error $0,5\% \pm 1$ digit
- Two-channel oscilloscope OKD-514 A, 0 – 14 MHz
- Electromagnetic voltmeter

7. 4. Measuring and calculation tasks

1	Be acquainted with high vltage DC test set up (fig. 1a) and with measuring circuits (fig. 1a, b, c and calculate: <ul style="list-style-type: none"> - voltage constant „c” of DC measuring circuit shown in fig. 1b expressed in $\text{kV}/\mu\text{A}$ - current flowing through the resistor R_1 (fig. 1) and voltage U_1 at the primery side of transformer when the DC voltage is equal to 100 kV. - Assume that the Grainacher circuit increases 2 times the voltage and that the ratio peak voltage to the rms value is equal to $\sqrt{2}$. The voltage ratio of transformer is equal to 273.
2	Measure the dependence of HVDC on the AC primary voltage of test transformer TP60 (use the measuring circuit shown in fig. 1b) <ul style="list-style-type: none"> - Carry out the measurement with load resistance R_{load}, the load current should be less or equal to 2 mA - Without load resistance but in the same range of primery voltage U_1 (HVDC can not be higher than 75 kV)
3	Estimate the ripple factor of DC source with load resistance R_{load} an without load resistance (measuring circuit from fig. 1c). Do measurements for two values of voltage similar that from the task 2.
4	Measure the onset voltage of ionization and the breakdown voltage as a function of disance of point-plate air gap for both polarities (measuring circuit from fig. 1d)

7. 5. Report contents

- Purpose of the experiments, measuring circuits,
- list of measuring equipment with main technical data and numbers.
- Measurement readings and calculation results, calculation examples, conclusions,
- Manual measuring report signed by the tutor
- Introductory calculations from task 1.
- The measurement results from task 2 drawn in one figure.
- Drawing or photograph of oscillogram of voltage ripples

7. 6. Control questions

1. Parameters and application of HVDC
2. One unit DC circuits
3. HVDC cascade
4. Electrostatic voltmeters
5. DC voltage dividers
6. Influence of point electrode polarity on the onset voltage of ionization U_0 and on the breakdown voltage U_b of point-plate air gap.

7. 7. Literature

[1] E. Kuffel, W.S. Zaengl, J. Kuffel, High Voltage Engineering Fundamentals, Newnes 2000, Chapter 2

[2] Holtzhausen J.P., Vosloo W.L., High Voltage Engineering, Practice and Theory, Stellenbosch University, 2008, Chapter 4

PRACTICAL 7 : GENERATION AND MEASUREMENT OF DC VOLTAGE

Manual measuring report date

Laboratory team number

- 1. Reporter
- 2. Student
- 3. Student
- 4. Student
- 5. Student
- 6. Student

Tutor's signature

Climatic conditions: T =°C, p = hPa, RH =%

$\delta =$

Table 1. Estimation of DC source characteristics

	U_1	I	c	U_2	Remarks
	V	μA	kV / μA	kV	
1	with load $I_{load} = \dots\dots\dots$ $R_{load} = \dots\dots\dots$
2	
3	
4	
5	
1	without load
2	
3	
4	
5	

U_1 – primary voltage of transformer
 I – current flowing through the resistance
 $R_1 = 100 \text{ M}\Omega$
 c - voltage constant of test circuit U_2 - HVDC

Table 2. Estimation of ripple factor

	U_1	U_+	η_R	U_+	$U_{\max} - U_{\min}$	η_C	$U_{\max} - U_{\min}$	S	Remarks
	V	V	-	kV				%	
1									
2									
1									
2									

U_1 – primary voltage of transformer

U_+ - DC component of rectified voltage

$U_{\max} - U_{\min}$ - two ripple amplitudes

$$S = \frac{U_{\max} - U_{\min}}{2 \cdot U_+} \cdot 100\% \quad \text{- ripple factor of the rectified voltage}$$

η_R – calculated voltage ratio of capacitive divider

η_R - calculated voltage ratio of resistive divider

Table 3. Characteristics of point – plate air gap $U_0 = f(s)$ and $U_b = f(s)$

	s	I_0	U_0	I_b	U_b	U_{bN}	Remarks
	cm	μA	kV	μA	kV	kV	
1							
2							
3							
1							
2							
3							
1							
2							
3							
1							
2							
3							

U_0 - Onset voltage of ionization

U_b - breakdown voltage of air gap in real atmospheric conditions

U_{bN} - breakdown voltage of air gap in normal atmospheric conditions

PRACTICAL 8

VOLTAGE DISTRIBUTION ALONG THE CAP AND PIN INSULATOR STRINGS AND ALONG THE MODEL POST INSULATOR

8. 1. Purpose of the experiment

The purpose of the experiment is to study the voltage distribution along the insulators and grading methods for improvement of electric field distribution.

8. 2. Experimental set up

This experiment is carried out in the box shown in fig. 1.

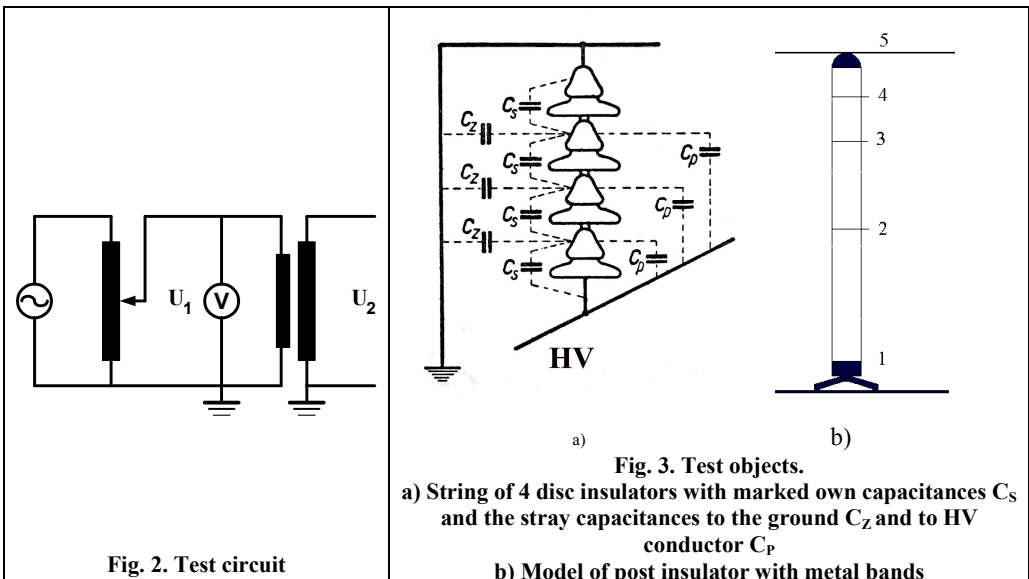
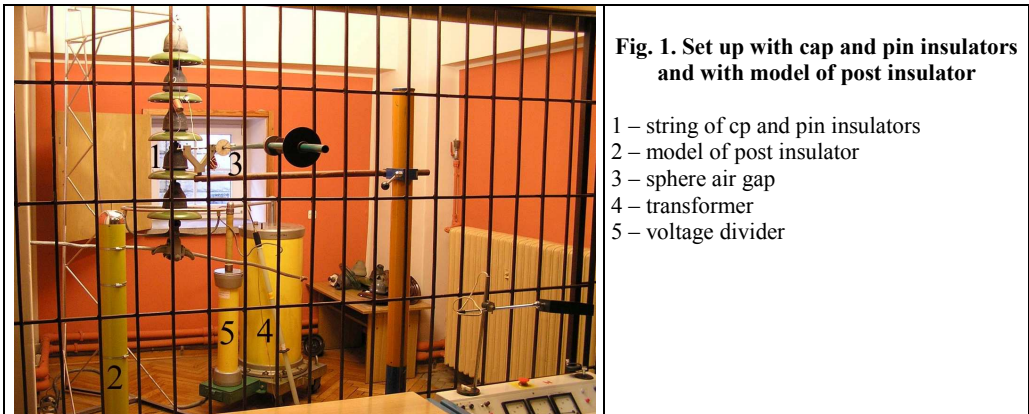


Fig. 2. Test circuit

8.3. List of measuring devices

- Test transformer TP60, voltage ratio $\eta = 60\text{kV}/220\text{ V} = 273$
- Digital voltmeter Lumel N15Z, 300 V, $R > 2\text{ M}\Omega$, Error $0,5\% \pm 1$ digit
- Electromagnetic voltmeter
- Sphere – sphere air gap with diameter of 10 mm

8.4. Measuring and calculation tasks

1	<p>Measure the voltages on every disc of strings consisting of 5 disc insulators LK280/170 by means of the sphere air gap with 10 mm diameter. Use the same high voltage during every measurement, e.g. 27,2 kV ($U_1 = 100\text{ V}$):</p> <ol style="list-style-type: none"> use the conductor without the grading ring use the conductor with the grading ring exchange the centrally situated disc insulator number 3 on the failed insulator number 3a and try to measure the voltage only on this insulator
2	<p>Elaboration of the above measurements</p> <ol style="list-style-type: none"> Check if the sum of measured ΔU voltages is equal to the high voltage U_2 applied to the string (compare the voltage peaks), Calculate the non-uniformity coefficients of voltage distribution „k” for measurements carried out in points 1a and 1b. Show in one figure the functions $\Delta U = f(i)$, $i = 1 \dots 5$ for the task 1a and 1b
3	<p>Fix the high voltage of 27,2 kV ($U_1 = 100\text{ V}$). Measure the voltage along the distance of 10 cm between the top electrode and the first metal band. Repeat the measurement between the bands situated 15 cm apart.</p> <p>Increase the high voltage to 54, 4 kV ($U_1 = 200\text{ V}$) and measure the voltage on the third 30 cm distance. „Re-calculate” the result of last third measurement to the value relevant to 27,2 kV, that means, divide the measurement result by 2.</p> <p>The voltage drop between the metal bands 3 – 2 (fig. 3b) is very low. Therefore, to produce the breakdown between spheres of air gap, the applied high voltage have to be increased.</p>
4	<p>Draw the voltage distribution along the surface of post insulator $U = f(x)$. Calculate the part of total voltage sharing along the distance of 10 cm, between the electrodes 5 – 4 (fig. 3b). fig. 4 shows an example of voltage distribution along the surface of post insulator.</p>

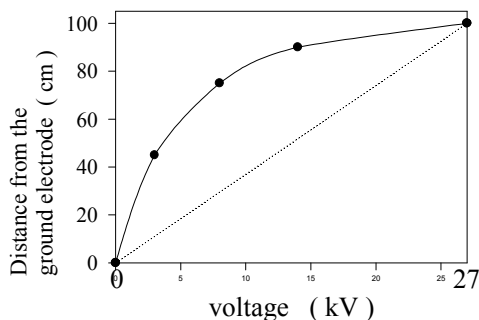


Fig. 4. Voltage distribution along the post insulator

8. 5. Control questions

1	Outdoor insulators, types, materials used.
2	Construction of cap and pin insulators
3	Electrical model of string of cap and pin insulators
4	Measurement of HV by means of sphere air gap
5	Methods for improvement of voltage distribution along string of cap and pin insulators and along long rod insulators

8. 6. Literature

- [1] Babikow M.A., Komarow N.S., Siergiejew A.S., Technika wysokich napięć. WNT Warszawa 1967, Chapter 10.3 (Polish translation from Russian)
- [2] S. M. Al Dhalaan, M. A. Elhirbawy, Simulation of Voltage Distribution Calculation Methods Over a String of Suspension Insulators. [Transmission and Distribution Conference and Exposition, 2003 IEEE PES](#), Vol. 3, pp. 909 – 914
- [3] Chrzan K.L., Rebizant W., PSPICE application for modelling of cap and pin insulator strings. International Symposium Modern Electric Power Systems, MEPS, Wrocław 2002, pp. 581-585
- [4] Chrzan K.L., Gielniak J., Voltage distribution along metal oxide surge arresters. 13th International Symposium on High Voltage engineering ISH, Delft 2003, paper 077.

PRACTICAL 8 : VOLTAGE DISTRIBUTION ALONG THE CAP AND PIN INSULATORS STRING AND ALONG THE MODEL POST INSULATOR

Manual measuring report date

Laboratory team number

- 1. Reporter
- 2. Student
- 3. Student
- 4. Student
- 5. Student
- 6. Student

Tutor's signature

Climatic conditions: T =°C, p = hPa, RH =% δ =

Tab. 1. Voltage distribution along the string of disc insulators with the conductor without the grading ring.

Lp	No of insulator	S	S _{mean}	ΔU _{mean}	ΔU _{pT}	ΔU	Remarks
		mm	mm	kV _p	kV	%	
1	1	-----					-----
2		-----					-----
3		-----					-----
1	2	-----					-----
2		-----					-----
3		-----					-----
1	3	-----					-----
2		-----					-----
3		-----					-----
1	4	-----					-----
2		-----					-----
3		-----					-----
1	5	-----					-----
2		-----					-----
3		-----					-----

- s – measured distance between electrodes of sphere air gap Φ = 10 mm,
- ΔU_{mean} – voltage amplitude read from the air gap characteristics (in kV_p)
- ΔU_{pT} – voltage drop on disc insulator calculated for rms value and for real atmospheric conditions (air gap characteristics is given for normal conditions)
- ΔU - voltage sharing on a given disc insulator in per cent. 100% relates to the total voltage along the whole string.

Tab. 2. Voltage distribution along the string of disc insulators with the grading ring conductor

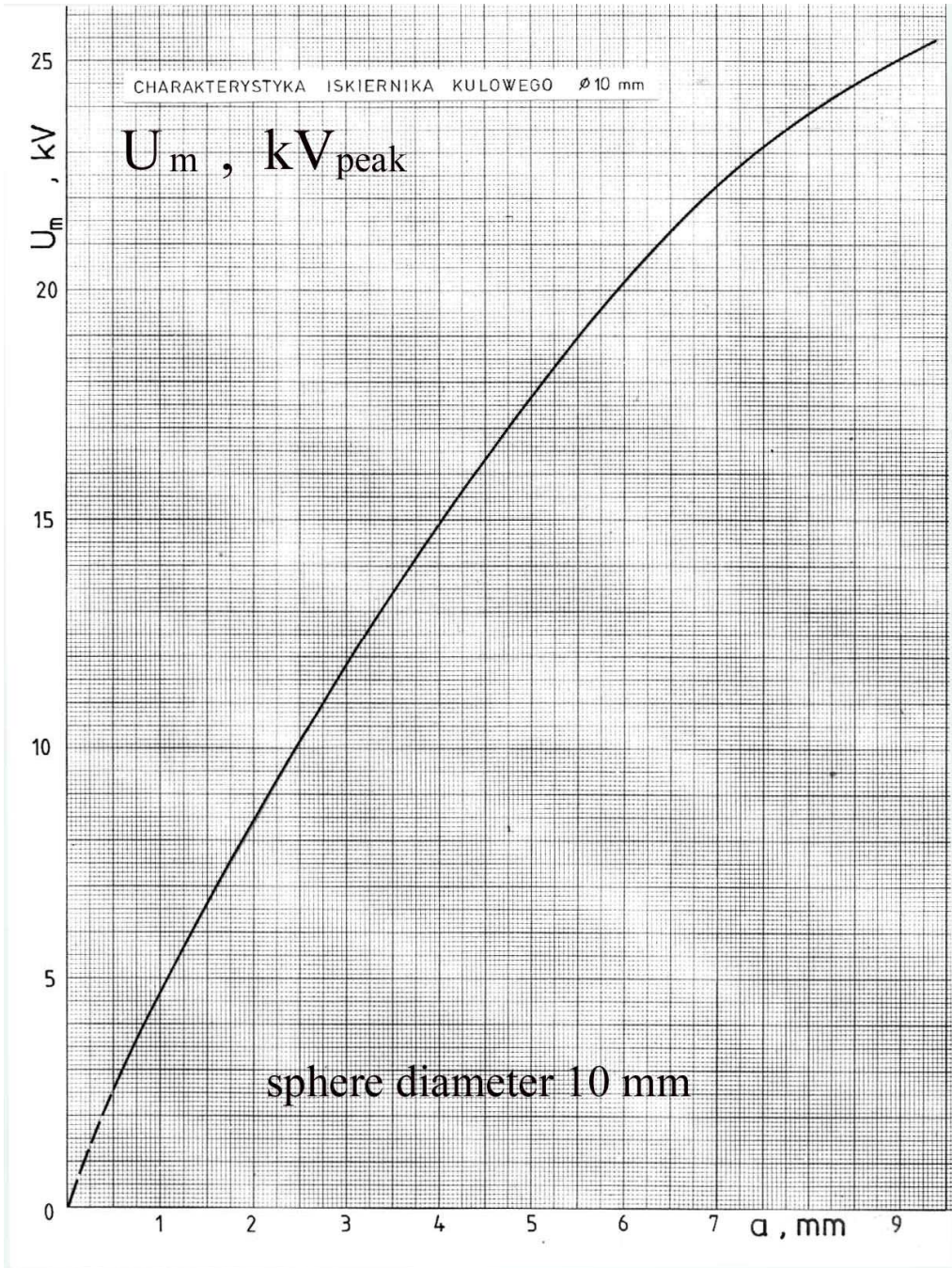
Lp	No of insulator	s	S _{mean}	ΔU _{mean}	ΔU _{pT}	ΔU	Remarks
		mm	mm	kV _p	kV	%	
1	1	-----					-----
2		-----					
3		-----					
1	2	-----					-----
2		-----					
3		-----					
1	3	-----					-----
2		-----					
3		-----					
1	4	-----					-----
2		-----					
3		-----					
1	5	-----					-----
2		-----					
3		-----					

The measured voltage on the insulator number 3a -

Tab. 3. Voltage distribution along the model post insulator

	Measurement between points shown in fig. 3b at the distance	s	S _{mean}	ΔU _{mean}	ΔU _{pT}	ΔU	Remarks
		mm	mm	kV _p	kV	%	
1	5-4 10 cm	-----					-----
2		-----					
3		-----					
1	4-3 15 cm	-----					-----
2		-----					
3		-----					
1	3-2 30 cm	-----					-----
2		-----					
3		-----					
	2-1 45 cm						Calculate this voltage according to: $\Delta U_{2-1} = \Delta U_{5-1} - \Delta U_{5-2}$

Characteristic of sphere air gap with the diameter of 10 mm



PRACTICAL 9

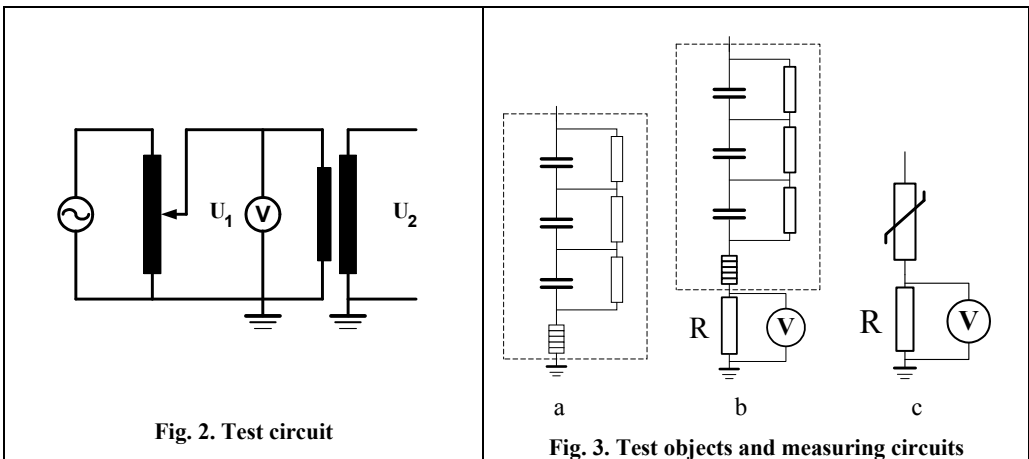
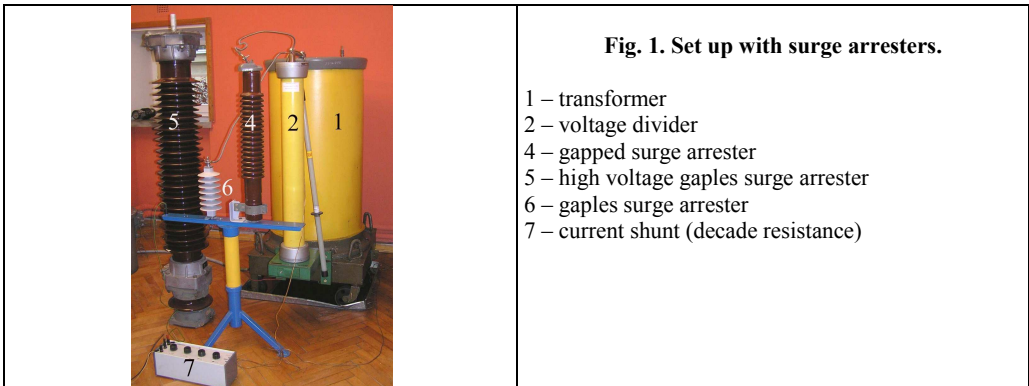
DIAGNOSTICS OF SURGE ARRESTERS

9. 1. Purpose of the experiment

The purpose of the experiment is to check the condition state of gapped surge arrester with silicone carbide varistors and the conditions of gapless surge arrester – metal oxide surge arrester.

9. 2. Experimental set up

This experiment is carried out in the box shown in fig. 1.

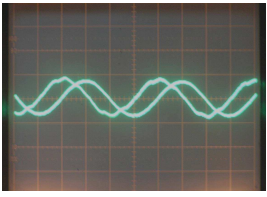


9. 3. List of measuring devices and test objects

- Test transformer TP100, voltage ratio $\eta = 470$
- Digital voltmeter Lumel N15Z, 300 V, $R > 2 \text{ M}\Omega$, Error $0,5\% \pm 1$ digit
- Digital multimeter 4150 PeakTech, AC 200 mV – 750 V
- Decade resistance DR 4c – 16 INCO Pyskowice
- Digital oscilloscope
- Oscilloscope probe model HC-OP20 manufactured by Hung Chang Products Co., LTD

- Gapped surge arrester GZSc 30/5 In = 5 kA manufactured by ZWAR (maximum continuous operating voltage phase-phase $U_c = 30$ kV)
- Metal oxide surge arrester (gapless) POLIM-D In = 10 kA manufactured by ABB, U_c - unknown

9. 4. Measuring and calculation tasks

1	<p>Measurement of sparking voltage of air gaps. Connect the gapped surge arrester to the test circuit and to the ground (fig. 3a). Increase the voltage up to the sparking of air gaps. Repeat this procedure 10 times and calculate the mean value $U_{50\%}$ and standard deviation S. Maximum continuous operating voltage $U_c = 30$ kV, what is the ratio of sparking voltage U_1 to U_c voltage? Is this value in the permissible range? $1,7 \cdot U_c < U_1 < 2,8 \cdot U_c$</p>
2	<p>Estimation of voltage – current characteristics of grading resistors. Connect the gapped surge arrester to the test circuit according to fig. 3b. Fix the value of shunt resistance $R = 1000 \Omega$. Measure the current for a few voltage values less or equal to the $0,8 U_{50\%}$ to avoid sparking. Draw the function $U_2 = f(I)$</p>
3	<p>Estimation of voltage – current characteristics of metal oxide surge arrester. Connect the metal oxide surge arrester to the test circuit according to fig. 3c. First, increase the low voltage to the maximum value of 80 V and measure the voltage on the current shunt. Then, decrease the voltage and measure the voltage on the current shunt at a few points. Draw the function $U_2 = f(I)$ - The maximum continuous operating voltage U_c is unknown. U_c should be about 70% of rated voltage U_r. The value of rated voltage is situated close over the characteristic knee point at voltage – current characteristics. Try to establish the value of U_c for the arrester under study.</p>
4	<p>Connect the oscilloscope to the current shunt. For the 2 values of low voltage $U_1 = 50$ V and $U_1 = 75$ V measure the current amplitude and compare with the result from task 3. Explain the differences.</p> <div style="display: flex; justify-content: space-around;"> <div data-bbox="246 1058 610 1253">  <p style="text-align: center;">$U_1 = 50$ V</p> <p style="text-align: center;">Fig. 4. nearly sinusoidal current shape</p> </div> <div data-bbox="744 1058 1088 1253">  <p style="text-align: center;">$U_1 = 75$ V</p> <p style="text-align: center;">Fig. 5. Non-sinusoidal current shape</p> </div> </div>
<p>Current channel: $R = 1000 \Omega$, 50 mV/unit, 5 ms/cm Voltage channel: voltage divider + probe HC-OP20, attenuation 10:1, 5 V/unit</p>	

9. 5. Additional information

Oscilloscope probe model HC-OP20 manufactured by Hung Chang Products Co., LTD.

It is a passive, low-impedance attenuation probe. The probe has been designed and calibrated for use on instruments having an input impedance of $1 \text{ M}\Omega$ paralleled by 20 pF .

The probe incorporates a 3 - position (1X, REF, 10X) slide switch in the head, compensating network and a cable length of 1,4 meters.

Table 1. Electrical characteristics of the probe HC-OP20

Characteristic	Performance requirements	
Oscilloscope input capacity	15 pF – 40 pF	
Attenuation	1:1	10:1
Input capacity	72 pF ± 10%	17 pF ± 2 pF
Internal resistance	237 Ω ± 10%	9 MΩ ± 1%
Band width	15 MHz (± 3 dB)	60 MHz (± 3 dB)
Max input voltage	500 V (AC p-p or 300 V (DC + AC p-p	

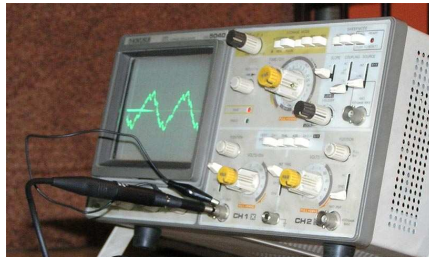


Fig. 6. Connection of probe HC-OP20 to the oscilloscope

9. 6. Control questions

1	What materials are used for manufacturing the varistors used in old gapped surge arresters ?
2	What materials are used for manufacturing the varistors used in new gapless surge arresters ?
3	Why the old surge arresters have air gaps? Why the new arresters can have no gaps ?
4	Must we do the correction of sparking voltage to the normal atmospheric conditions ?
5	The advantage of gapless solution for the value of protection level.
6	Why the porcelain housing of a surge arrester is dangerous ?
7	Explain the term „ <i>thermal run away</i> ”.
8	Call and explain the main parameters of surge arresters U_r and U_c .

9. 7. References

- [1] Haddad A., Warne D.F. (editors), Advances in High Voltage Engineering, The Institution of Electrical Engineers IEE, 2004, Chapter 5, ZnO surge arresters.
- [2] Chrzan K.L., High voltage surge arresters (in Polish), Dolnośląskie Wydawnictwo Edukacyjne, Wrocław 2003.

PRACTICAL 9 : DIAGNOSTICS OF SURGE ARRESTERS

Manual measuring report date

Laboratory team number

1. Reporter
2. Student
3. Student
4. Student
5. Student
6. Student

Tutor's signature

Task 1. Measurement of sparking voltage (gapped arrester GZSc 30/5)

	1	2	3	4	5	6	7	8	9	10	U ₁	U ₂	Standard
											mean	mean	deviation
											V	kV	%
U ₁	V												

Task 2. Estimation of voltage – current characteristics of grading varistors (gapped arrester)

		1	2	3	4	5	6	7
U ₁	V							
U ₂	kV							
U _{shunt}	V							
I	μA							

Task 3. Estimation of voltage – current characteristics of metal oxide arrester POLIM-D

		1	2	3	4	5	6	7
U ₁	V				50		70	80
U ₂	kV							
U _{shunt}	V							
I	μA							
I	μA _{peak}	from oscilloscope for U ₁ = 50 V and for U ₁ = 70 V			-	-

Task 4. Current measurement by means of oscilloscope

PRACTICAL 10

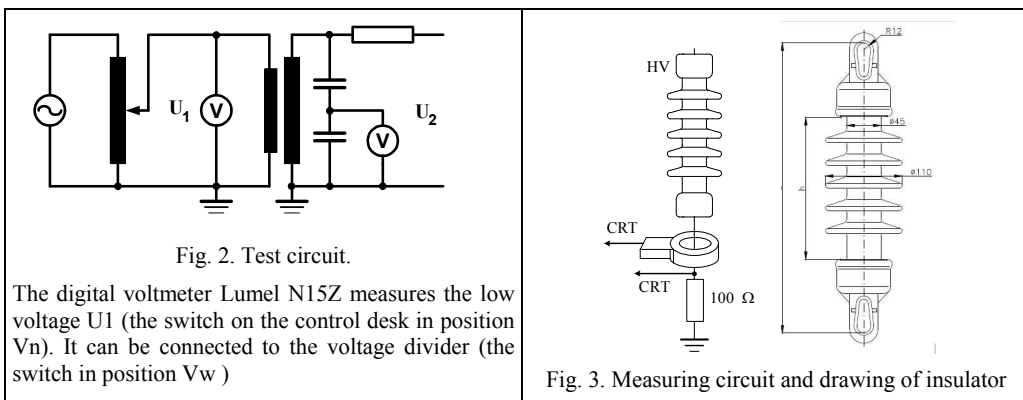
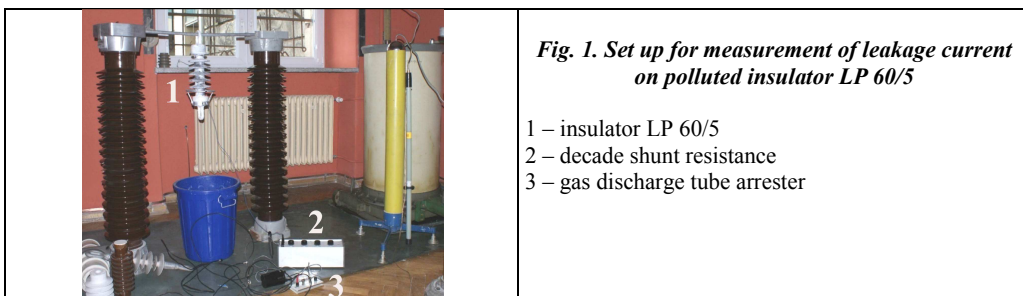
LEAKAGE CURRENT ON POLLUTED OVERHEAD INSULATORS

10. 1. Purpose of the experiment

The purpose of the experiment is to measure the leakage current by means of a current shunt and by a current probe. The fictive flashover voltage will be calculated using the measured highest current amplitude I_h

10. 2. Experimental set up

This experiment is carried out in the box shown in fig. 1.



10. 3. List of measuring devices and test object

- Test transformer TP110, voltage ratio $\eta = 479$
- Damping resistance 500Ω
- Capacitive voltage divider voltage ratio **311** (without short-circuiting gear), **822** (with short-circuiting gear)
- Voltmeter with digital display Lumel N15Z, 300 V, $R > 2 \text{ M}\Omega$, Error $0,5\% \pm 1$ digit
- Electrostatic voltmeter type C50, 75 V, 20 Hz – 10 MHz
- Electrostatic voltmeter type C50, 150 V, 20 Hz – 10 MHz
- Electromagnetic voltmeter
- *Current probe KYROYTSU model 8112 range 200 mA, 1 mA/mV*
- *Current shunt (decade resistance) $R = 100 \Omega$*

- Oscilloscope probe model HC-OP20, attenuation 10:1 (see additional information at the tutorial 9)
- Oscyloskop Kikusui DSS 5040

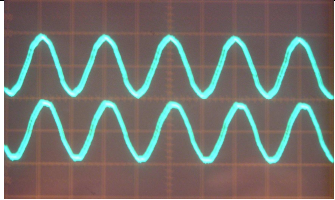
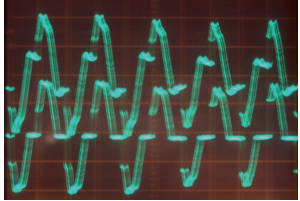
Table 1. Technical data of porcelain insulator LP 60/5

Number of sheds	5	Leakage distance	52 cm
Shed diameter	135 mm	Form factor	2,1
Shank diameter	60 mm	Total surface	1510 cm ²

10. 4. Measuring and calculation tasks

Carry out 3 voltage test of polluted insulator and measure the leakage current by means of current shunt and / or by current probe. The test transformer should be connected to the external 70 kVA autotransformer. At the opened disconnecting switch fix the selected value of voltage and then close promptly the disconnecting switch. Try to avoid the flashover.

The three task with the value of test voltage, voltage settings on oscilloscope, and additional hits are given below.

Task 1. Measurement of leakage current by means of shunt resistance and the current probe on continuous pollution layer (without dry bands)			
	Upper channel of oscilloscope Current probe	20 mV / cm	17 mA _{peak}
	Bottom channel of oscilloscope Current shunt resistance R = 100 Ω	2 V / cm	17 mA _{peak}
		U ₂ = 20 kVrms	
Task 2. Leakage current on insulator with burning arcs			
	Upper channel of oscilloscope Current probe	10 mV / cm	20 mA _{peak}
	Bottom channel of oscilloscope Current probe R = 100 Ω	1 V / cm	20 mA _{peak}
		U = 35 kVrms	
Task 3. Voltage and leakage current with burning arcs. The arc ignition causes the voltage drop			
	Channel 1 Current probe	50 mV / cm	25 mA _{peak}
	Channel 2 Voltage divider, voltage ratio 857 (with short-circuiting gear) + probe HC-OP20, attenuation 10:1	2 V / cm	
		U = 30 kVrms	

Task 4. Calculate the flashover voltage of LP60/5 insulator for the highest value of leakage current I_h measured during the experiment at the voltage U using the formula (3) and then the formula (4), and the parameter value given in bolt letters (see the additional information below).

10. 5. Additional information



Fig. 4. Current probe KYROYTSU model 8112, current ranges up to 200 mA/ 2 A/ 20 A, 40 Hz – 10 kHz, at the range of 200 mA the measuring constant is equal to 1 mA/mV

1. Calculation of surface conductivity κ_s from measurement of leakage current I according to task 1.

$$U = 20 \cdot 1,41 = 28 \text{ kV}_{\text{peak}}$$

$$\kappa_s = f / R = 2,1 \cdot 17 \text{ mA}_{\text{peak}} / 28 \text{ kV}_{\text{peak}} = 1,3 \text{ } \mu\text{S} \quad \text{wher: } f \text{ is the form factor of insulator}$$

2. Calculation of flashover voltage from the leakage current value.

Equivalent diameter of insulator D_e is the diameter of a cylindrical insulator having the same leakage distance L (cm) and the same resistance when polluted with the same surface conductivity as the insulator with sheds.

$$D_e = \frac{L}{\pi \cdot f} \quad (1)$$

f - Form factor of insulator

K - Factor taking into consideration the current concentration in the arc spot

$$K = \frac{R_{pa}}{R_p} = \frac{1}{2 \cdot \pi \cdot \kappa_s} \left(\log \frac{2 \cdot L_U}{\pi \cdot r} - \log \tan \frac{\pi \cdot X_{CU}}{2 \cdot L_U} \right) = 0,46 \quad (2)$$

$$\frac{L_U - X_{CU}}{\pi \cdot D_e \cdot \kappa_s}$$

R_{pa} - pollution layer resistance taking into account the current concentration at the arc spot in $\text{k}\Omega$

R_p - pollution layer resistance between wide electrodes (without arc) in $\text{k}\Omega$

L_U - leakage distance of shed division in cm

X_{CU} - critical arc length on a shed division in cm

r - arc radius in cm, the radius equal to 0,2 cm was assumed

κ_s - surface conductivity in μS

D_s - shed diameter in cm, $D_s = 11 \text{ cm}$

L - leakage distance of whole insulator in cm, $L = 52 \text{ cm}$

X_c - critical arc length of the whole insulator in cm, $X_c = 0,6 \cdot L = 31 \text{ cm}$

The critical flashover voltage U_C divided by the leakage distance L is given by the following formula:

$$E_C = \left(\frac{D_S}{D_e} \right)^{\frac{1}{n-1}} \left[\frac{X_C}{L} \cdot \frac{D_e}{D_S} + K \cdot \frac{L - X_C}{L} \right] \cdot \left(\frac{U}{2L} \right)^{\frac{n}{n+1}} \cdot A^{\frac{1}{n+1}} \cdot I_h^{\frac{-n}{n+1}} \quad (3)$$

$$E_C \text{ (kV}_{peak} / \text{cm)} = \frac{U_C}{L} \quad \Rightarrow \quad U_C = E_C \cdot L \quad (4)$$

U - applied voltage in kV_{peak}

I_h - the highest current measured in A_{peak}

Note, you have measured the voltage in kV_{rms} .

Note, you have measured the current in mA_{peak} .

$A = 400$, $n = 0,33$ - Arc parameters

Calculation of form factor f

The form factor of an insulator is given by:

$$f = \int_0^L \frac{1}{2\pi \cdot r(x)} dx \quad (5)$$

where:

L - leakage distance,

x - position as measured along insulator profile (along shortest leakage current path)

$r(x)$ - radius at position x

The approximate evaluation of the integral in equation (5) can be done by measuring the radius at various positions along the creepage path, typically on an insulator such as shown in figure 6. Then we use this data as inputs to a numeric integration procedure.

Another simplified method for form factor calculation was proposed by Jacobus Holtzhausen for the cap and pin insulators [3]. The procedure can easily be adapted to the long rod insulators. The long rod insulator consists of cylindrical shank and sheds. The form factor f_S of a cylinder having a height h and a radius r :

$$f_S = \frac{h}{2\pi \cdot r} \quad (6)$$

According to Holtzhausen's method the surface of a shed is represented by a model consisting of 2 cones, having an outside radius r_2 , equal to the radius of the modelled shed (fig. 5). The upper cone has a surface length L_1 , equal to the creepage length along the top of the actual shed. Likewise, the lower cone represents the bottom of the actual shed, having a creepage length of L_2 . The radius r_1 is made equal to the radius of the shank.

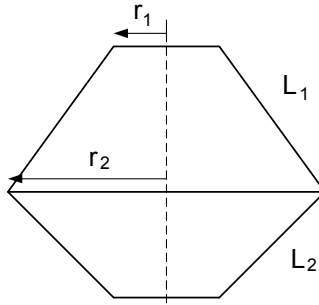


Fig. 5. Model of a shed

It can be shown that the form factor of a cone, such as the upper one, is given by:

$$f_1 = \frac{1}{2\pi(r_2 - r_1)} \cdot \ln \frac{r_2}{r_1} \quad (7)$$

The form factor for the whole shed is given by:

$$f_S = f_1 + f_2 = \frac{L_1 + L_2}{2\pi \cdot (r_2 - r_1)} \cdot \ln \frac{r_2}{r_1} \quad (8)$$

The insulator LP 45/5 has 5 shanks with the same height of 2 cm (with the same form factor f_2), the bottom shank with the height of 4 cm (form factor f_4) and 5 sheds. Finally, the form factor f of the whole insulator LP 45/5 is the sum:

$$f = 5 \cdot f_2 + f_4 + 5 \cdot f_S \quad (9)$$

10. 6. Control questions

1	Pollution class, how it helps to select appropriate overhead insulators to particular environmental conditions.
2	The relation of leakage distance and pollution flashover.
3	The highest value of leakage current I_b , the critical leakage current I_C , the maximum value of leakage current just before flashover I_{max} by Verma..
4	The warning value of leakage current
5	The construction of composite insulators
6	The advantages of composite insulators

10. 7. References

- [1] Chrzan K.L., : Leakage currents on naturally contaminated porcelain and silicone insulators. IEEE Transactions on Power Delivery. 2010, vol. 25, No. 2, pp. 904-910, <http://www.ieeexplore.ieee.org/iel5/61/5437451/05427112.pdf?arnumber=5427112>
- [2] E. Kuffel, W.S. Zaengl, J. Kuffel, High Voltage Engineering Fundamentals, Newnes 2000, Chapter 9
- [3] Holtzhausen J.P., Vosloo W.L., High Voltage Engineering, Practice and Theory, Stellenbosch University, 2008, Chapter 4

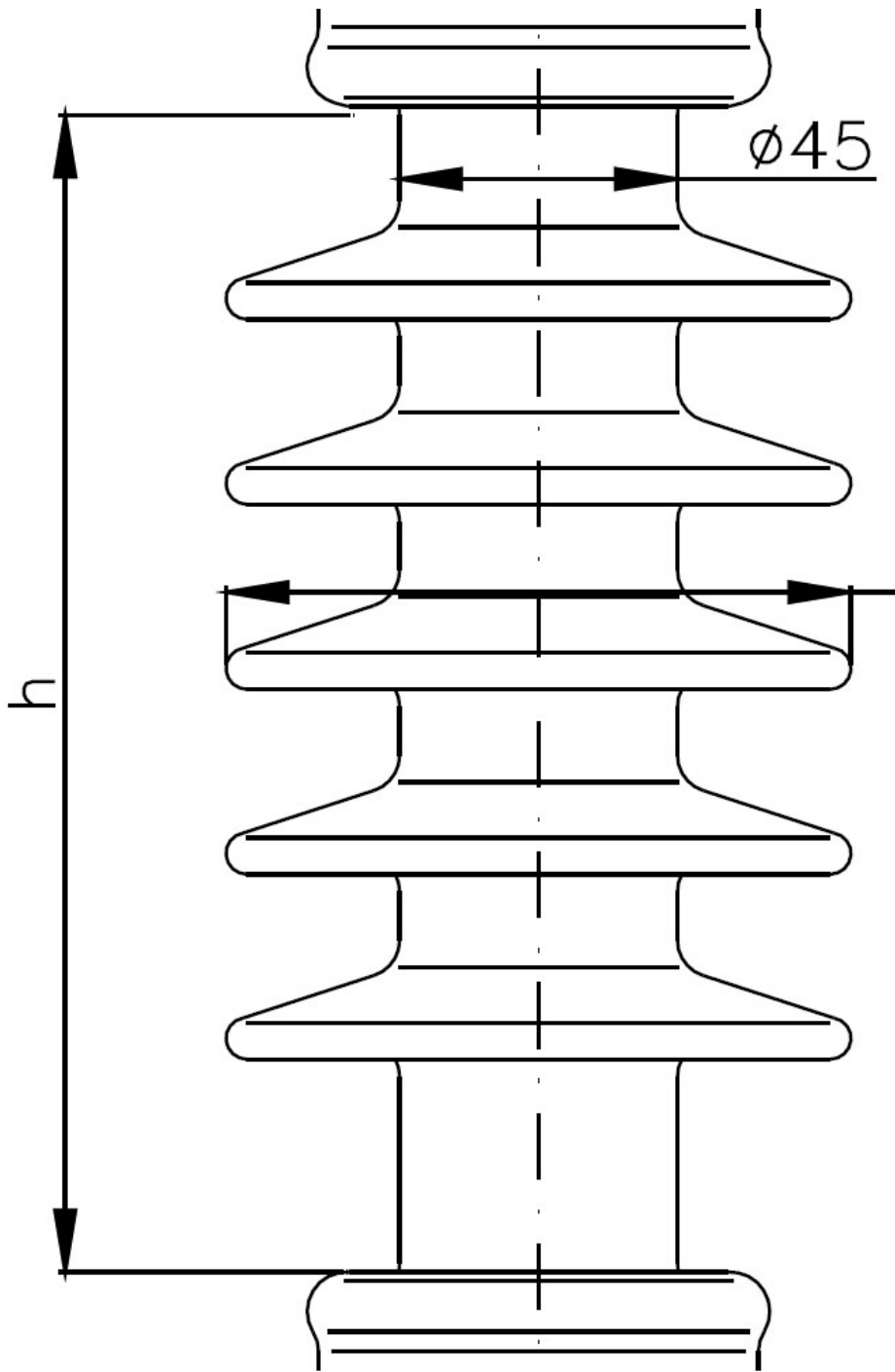


Fig. 6. Drawing of LP 45/5 insulator in scale 1 : 1

PRACTICAL 10 : LEAKAGE CURRENT ON POLLUTED OVERHEAD INSULATORS

Manual measuring report from date

Laboratory team number

1. Reporter
2. Student
3. Student
4. Student
5. Student

Tutor's signature

Task 1. Measurement of leakage current by means of shunt resistance and the current probe on continuous pollution layer (without dry bands)			
	Upper channel of oscilloscope Current probe mV / cm mA _{peak}
	Bottom channel of oscilloscope Current shunt resistance R = Ω V / cm mA _{peak}
			U ₂ = kVrms
Task 2. Leakage current on insulator with burning arcs			
	Upper channel of oscilloscope Current probe mV / cm mA _{peak}
	Bottom channel of oscilloscope Current shunt R = Ω V / cm mA _{peak}
			U = kVrms
Task 3. Voltage and leakage current with burning arcs. The arc ignition causes the voltage drop.			
	Channel 1 Current probe mV / cm mA _{peak}
	Channel 2 Voltage divider, voltage ratio 821 (with short-circuiting gear) + probe HC-OP20, attenuation 10:1 V / cm	
			U = kVrms

Task 4. Calculation of flashover voltage of LP60/5 insulator for the highest value of leakage current (write in the report) - form factor 2,1

Task 5. Calculate the form factor of insulator LP 45/5

PRACTICAL 11

THE REVERSE POLARITY PHENOMENON OF INSULATION ARRANGEMENTS WITH WEAKLY NON-UNIFORM FIELD

11. 1. Purpose of the experiment

The purpose of experiment is the confirmation of the reverse polarity phenomenon between sphere- sphere electrodes under lightning impulses. Additionally, the construction and elements of multi-stage Marx generator will be analysed.

11. 2. Experimental set up

This experiment is carried out in the box shown in fig. 1.

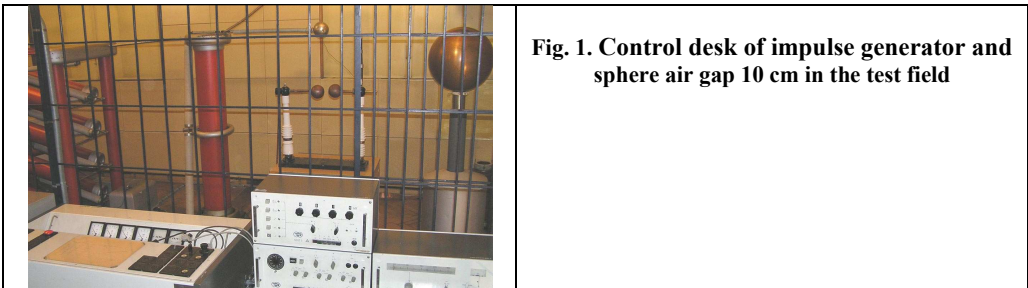
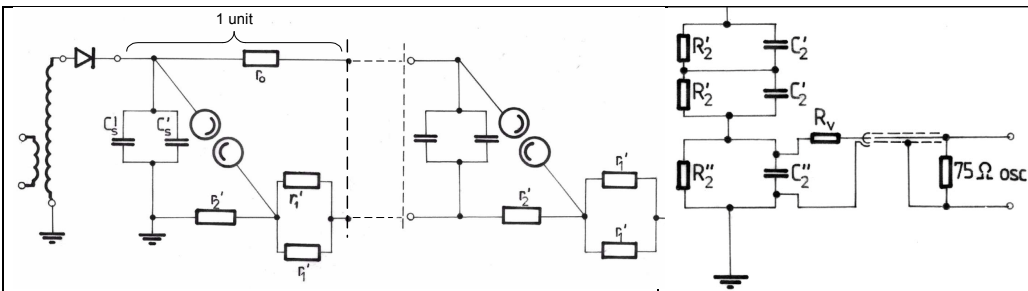


Fig. 1. Control desk of impulse generator and sphere air gap 10 cm in the test field



<p>Fig. 3. Electrical circuit of 4-unit impulse generator GU500</p> $C'_S = 0,035 \mu\text{F} \quad r'_1 = 122 \Omega \quad r_0 = 16,5 \text{ k}\Omega \quad r'_2 = 1360 \Omega$	<p>Fig. 4. RC voltage divider</p> $C'_2 = 2966 \text{ pF} \quad R'_2 = 4026 \Omega$ $C''_2 = 888 \text{ nF} \quad R''_2 = 36,8 \Omega$ $r_v = 94 \Omega$
---	---

11. 3. List of measuring devices and test object

- RC voltage divider type SMCR 1500/500 TUR Dresden, voltage ratio **631** with cable having characteristic impedance of 75 Ω
- Precision impulse peak voltmeter SV642 Haefely, measuring range: low input: 16 V – 160 V, 1 M Ω
high input: 160 V – 1600 V, 2M Ω
- Sphere-sphere air gap with the diameter of **10 cm**

11. 4. Measuring and calculation tasks

1	Estimate the 50% positive impulse breakdown voltage of sphere air gap with the electrode distance of 9 cm. The measurement should be carried out according to series method.
2	Estimate the 50% negative impulse breakdown voltage of sphere air gap with the electrode distance of 9 cm.
3	Correct the results to the normal atmospheric conditions. Draw the figure from the paper [1] and mark there points you have found + $U_{50\%}$ and - $U_{50\%}$.
4	Based on the result of the voltage test and the Gauss grid estimate: <ul style="list-style-type: none"> - 50% flashover voltage – $U_{50\%}$ - standard deviation – s the Gauss grid is attached to the practical 5.

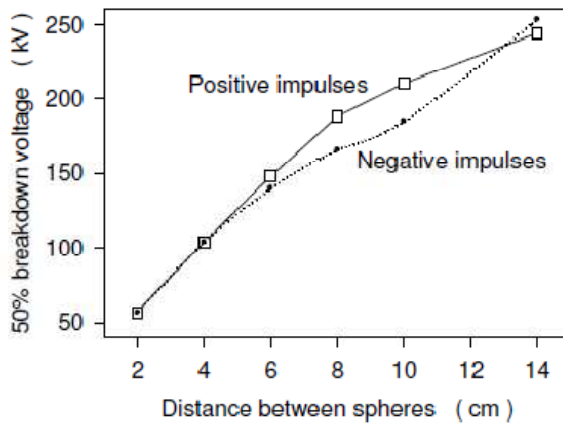


Fig. 5. Breakdown voltage of sphere-sphere air gap with the diameter of 10 cm [3]

11. 5. Additional information

In the uniform field (plate – plate) the breakdown voltage does not depend on the polarity. There is a great polarity effect in strongly non-uniform fields. A very good example is the rod – plate electrode arrangement where the breakdown voltage for small distance depends strongly on the rod shape. The positive breakdown voltage at the sharp rod end is always lower than under negative polarity (fig. 6a).

On the contrary, the positive breakdown voltage is a little higher at the distances smaller than „a” when the rod tip is a hemispherical (fig. 6b). The positive breakdown voltage is smaller if the electrode distance is greater than „a”. The electric field is weakly non-uniform when $S < a$, in this case the onset voltage of ionization is equal to the breakdown voltage $U_O = U_b$ but the onset voltage of positive corona is higher than the onset voltage of negative corona. When $S > a$, the electric field becomes higher and strongly non-uniform and the breakdown voltage at positive polarity of rod is lower than at the negative one.

The shape of the rod end is not important for the value of breakdown voltage at greater electrode distances. The electric strength of rod – plane arrangement depends only on the voltage polarity and distance S .

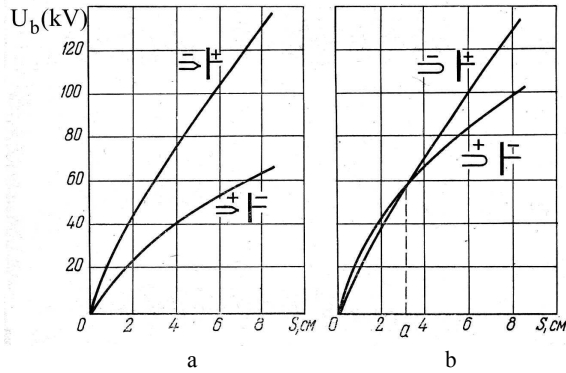


Fig. 6. Breakdown voltages in rod – plate arrangement depending on rod polarity and the shape of rod tip [4]

11. 6. Control questions

1	The insulation arrangements with uniform, weakly uniform or very non-uniform electric field.
2	Definition of the non-uniformity factor β
3	The influence of voltage polarity on the electrical strength of insulation arrangements having the different non-uniformity factor β .
4	Estimation methods of 50% breakdown voltage: series method and up and down method.
5	Measurement of high voltages by means of shere air gap.
6	The correction of breakdown voltage measurement with regard to atmospheric conditions.
7	Peak value voltmeter
8	Marx impulse generators, working prnceple, electrical circuit, voltage efficiency

11. 7. References

[1] E. Kuffel, W.S. Zaengl, J. Kuffel, High Voltage Engineering Fundamentals, Newnes 2000, Chapter 2

[2] J.P. Holtzhausen, W.L. Vosloo, High Voltage Engineering, Practice and Theory, Stellenbosch University, 2008, Chapter 4

[3] Chrzan K.L., H. Schwartz, H. Haeusler, Effect of impulse polarity on the flashover voltage of polluted cap and pin insulators. 16th International Conference on High Voltage Engineering, ISH, Cap Town 2009, paper E-30. Full text: <http://zet10.ipee.pwr.wroc.pl/record/346/files/>

[4] Tiniakov N.A., Stiepanshuk K.F., Technika vysokich napriazhenij. (in Russian) Wyzshaja szkola, Minsk 1971

PRACTICAL 11 : THE REVERSE POLARITY PHENOMENON OF INSULATION ARRANGEMENTS WITH WEAKLY NON-UNIFORM FIELD

Manual measuring report from date

Laboratory team number

- 1. Reporter
- 2. Student
- 3. Student
- 4. Student
- 5. Student
- 6. Student

Tutor's signature

Climatic conditions: T =°C, p = hPa, RH =%

$\delta =$

1. Estimation of positive breakdown voltage of sphere air gap with diameter of 10 cm according to serial method, s = 9 cm

Charging DC voltage of one unit = kV										Distance between spark gaps = mm										
	1	2	3	4	5	6	7	8	9	10	11	12	13	14	15	16	17	18	19	20
U	kV																			
B or W																				
Mean value of peak voltage from withstands U = kV										Breakdown probability =										
Corrected value to normal atmospheric conditions U _N = kV																				

Charging DC voltage of one unit = kV										Distance between spark gaps = mm										
	1	2	3	4	5	6	7	8	9	10	11	12	13	14	15	16	17	18	19	20
U	kV																			
B or W																				
Mean value of peak voltage from withstands U = kV										Breakdown probability =										
Corrected value to normal atmospheric conditions U _N = kV																				

2. Estimation of negative breakdown voltage of sphere air gap with diameter of 10 cm according to serial method, s = 9 cm

Charging DC voltage of one unit = kV										Distance between spark gaps = mm										
	1	2	3	4	5	6	7	8	9	10	11	12	13	14	15	16	17	18	19	20
U	kV																			
B or W																				
Mean value of peak voltage from withstands U = kV										Breakdown probability =										
Corrected value to normal atmospheric conditions $U_N =$ kV																				

Charging DC voltage of one unit = kV										Distance between spark gaps = mm										
	1	2	3	4	5	6	7	8	9	10	11	12	13	14	15	16	17	18	19	20
U	kV																			
B or W																				
Mean value of peak voltage from withstands U = kV										Breakdown probability =										
Corrected value to normal atmospheric conditions $U_N =$ kV																				

Reserve

Charging DC voltage of one unit = kV										Distance between spark gaps = mm										
	1	2	3	4	5	6	7	8	9	10	11	12	13	14	15	16	17	18	19	20
U	kV																			
B or W																				
Mean value of peak voltage from withstands U = kV										Breakdown probability =										
Corrected value to normal atmospheric conditions $U_N =$ kV																				

Charging DC voltage of one unit = kV										Distance between spark gaps = mm										
	1	2	3	4	5	6	7	8	9	10	11	12	13	14	15	16	17	18	19	20
U	kV																			
B or W																				
Mean value of peak voltage from withstands U = kV										Breakdown probability =										
Corrected value to normal atmospheric conditions $U_N =$ kV																				

APPENDIX A

SPECIAL EXPERIMENTS IN HIGH VOLTAGE LABORATORY

In this section, we are going to treat, briefly the following topics.

1. Exploding wire
2. The stroke of high voltage discharge to the water surface
3. Flame in electric field
4. Particles of foamed polystyrene in DC field
5. Glow discharges as illustration of Paschen's law
6. Discharges along the long string of metal pipes
7. Electric wind motor
8. Neon tubes in electrical field

A. 1. Exploding wire

The high lightning current flowing through the metal roof gutter can press it into a structure which resemble to a deformed pipe or wire. The current flowing in the same direction on the opposite gutter sides draws the counterparts causing the distortion. However, the behaviour of thin wire is quite different. The current density in the order of 10^5 A/cm² causes the tensometric elongation, material electroplasticity and stripped disintegration. The current density greater than 10^7 A/cm² results in explosion [1]. The exploding wire phenomenon has been known for over 200 years; it was first reported on by Edward Nairne in 1774. The phenomenon of exploding wires have been widely used by plasma physicists for the generation and confinement of plasmas, to the production of metallic nanoparticles or for generation of shock waves [2].

Experiment 1:

Connect one end of a thin metal wire (thickness in the range of 0,04 mm) with the Marx generator and the second one with a post insulator placed on the grounded plate (see the white element at the write bottom corner in the figure 1). Charge the generator to the voltage of 500 kV at least. The open end of the wire enhance the probability and strength of detonation. There is a rapid current increase after flashover of post insulator at the wire end.



Fig. 1. Exploding wire with the thickness of 0,04 mm and the length of 15 m in HV Laboratory of WUT

A. 2. The stroke of high voltage discharge to the water surface

Lightning stroke to ground leaves sometimes dendritic patterns on the surface. It indicates that the discharges propagate outward from the strike points on the earth surface (fig. 2). This surface phenomenon is similar to the well known discharges developing from the vertical grounding rod inside the ground. The limited value of ground resistivity and the high current amplitude promote the development of these discharges. The surface discharges developed from the striking point are dangerous for people and animals because their dimensions can reach the distance of 10 meters [3].

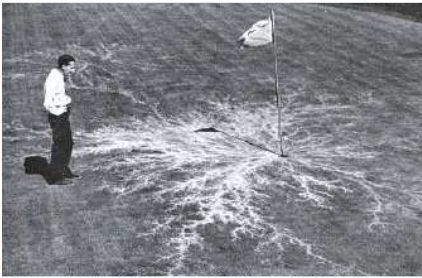


Fig. 2. Traces of discharges resulting from a lightning strike to the flagpole a the center of the dendritic pattern [3].

The dendritic patterns of discharges are observed even on the water surface at the point of lightning stroke [4]. However, the resistivity of water in ponds, lakes, or rivers is hundreds times lower than the soil resistivity. Therefore an additional mechanism was proposed by Moore et.al. [4]. The downward leader having most often the negative polarity, when approaches to the water surface induces the opposite charges on the water surface. The charging constant of water $\tau = \rho \cdot \epsilon_0 \cdot \epsilon_r$, in the range of 10 μs , is so short that the downward leader arriving quickly to the water surface have enough time to polarize it. The discharge can not propagate into the water volume and split on the surface attracted by the surface charges of opposite polarity.

Experiment 2 :

The grounded copper hemisphere with diameter of 1,2 m was filled by tape water (conductivity about 500 $\mu S/cm$). The aluminium rod was hang 0,8 m above the water and connected to the impulse generator. The air breakdown to the water caused the radially sparks along the water surface (fig. 3).

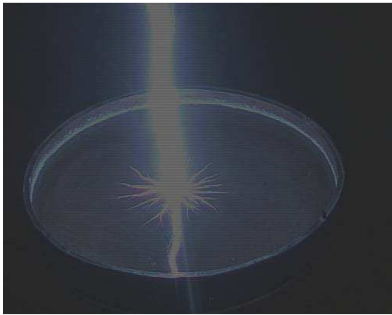


Fig. 3. Impulse lightning discharge to a pool of tape water

A. 3. A Flame in electric field

The outdoor power lines cross often the forest and agricultural areas where fires sometimes occur. The influence of high flames and intense smoke in the line vicinity on the electrical strength of air and the possibility of ground faults were studied in Brazil, Mexico, Canada, USA, South Africa, Australia. In these countries the fire of forest, grass, sugar cane and bushes ravage large areas, often jeopardizing the reliability of the lines. The line outages due to forest fires were observed in Poland too. The basic studies explained the mechanisms responsible for lowering the electrical strength of air in the presence of flame.

The flame is a kind of plasma where air molecules are chemically and thermally ionized. The ion concentration in the propane-air flame is in the range of $10^9 - 10^{12} / \text{cm}^3$. Most of them have the positive charge [5]. The low concentration of negative ions is probably due to the fact that most of the negative charge is transferred by free electrons. The main source of ions and electrons in the flame are the molecules with a low ionization potential, e.g. carbon (the ionization potential of graphite amounts to 4.35 eV). The rate of ionization processes increases with temperature. As it was earlier said, the flame is mostly positive charged, therefore in the dc electrical field it is attracted by the negative electrode (fig. 4b). In the ac field the flame is stretched between electrodes (fig. 4c, 4d). Due to the non-stationary conditions under ac voltage, the flame shift in one direction is lower than under dc voltage (compare fig. 4b and fig. 4c).

The breakdown voltage of plate to plate with 3 cm air gap at normal atmospheric conditions amounts to 61 kVrms. The placement of a candle fire in the middle reduces also the breakdown voltage by 10 times. Additionally, the reduction of breakdown voltage depends on the flame position in the gap and voltage shape. Under dc voltage the smallest reduction is observed when the flame is placed directly at negative electrode. Under the short impulse voltages the reduction of electrical strength is smaller than under the dc or ac voltages.

The air electrical strength decrease, under the influence of flames and smoke, can be explained as a result of 3 factors:

- the high temperature reduces the air density
- the electrical charge is generated in the flame
- the influence of smoke particles.

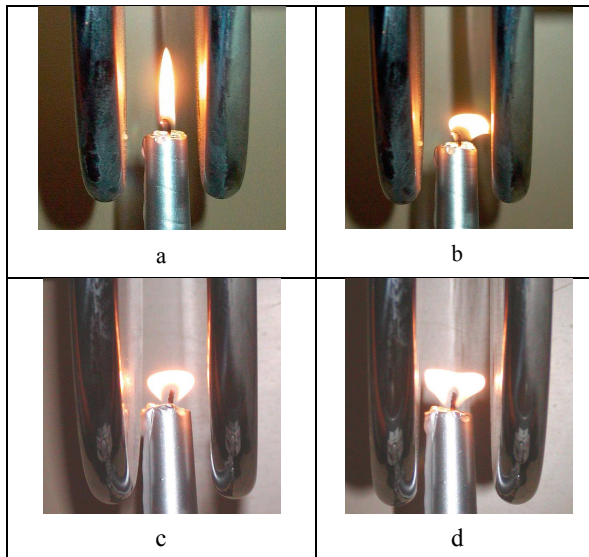


Fig. 4. The flame in an electric field, air gap 3 cm. a – without voltage, b – dc voltage of 3 kV, the right electrode is negative, c – ac voltage of 3 kVrms, d – ac voltage of 6 kVrms [6]

A. 4. Particles of foamed polystyrene in DC field

Sulphur hexafluoride (SF₆), a gas used in high voltage engineering, is generally found to be very sensitive to field perturbations such as those caused by conducting particle contaminants. Particles may be free to move or may be fixed on the surfaces. They may be of conducting material or of insulating material. Particles of insulating materials are not so harmful as they have little effect on the insulating properties of gases. Free conducting particles are most dangerous to Gas Insulated Substations (GIS) operating at high fields. Conducting particles can drastically influence the dielectric strength of SF₆, reducing it as low as 10% of the uncontaminated value.

After acquiring an appropriate charge in the field, the particle lifts and begins to move in the direction of field. The process depends on several parameters e.g. the macroscopic field at the surface of the particle, its weight, Reynold's number and viscosity of the gas [7]. The movement of particles in electric field depends on the voltage shape. The simplest case is DC voltage, with HV electrode at the top and the grounded electrode at the bottom. When the particles approaches to the HV electrode (having the opposite polarity to the polarity of the particle) the small discharge between the particle and the electrode can trigger the full breakdown. When the particle bonds the HV electrode, acquires its charge and is therefore repulsed down.

Experiment 4 :

The electrode arrangement consists of 2 parallel plates separated by a distance of 23 cm. The particles of foamed polystyrene were sprayed by colloidal graphite (GRAPHIT 33 manufactured by Kontakt Chemie) to get a conductive coating. Then, they were put on the grounded bottom electrode. At the voltage of 46 kV ($E = 2 \text{ kV/cm}$), the particles start to lift (fig. 5).

Note that without conductive coating the dielectric particles were not forced to move up even in the field of 20 kV/cm.



Fig. 5. The movement of conductive particles in DC field

A. 5. Glow discharges as illustration of Pashen's law

The simplest form of Paschen's law says that the onset voltage of ionisation U_0 is the function of pressure p and electrode distance s product,

$$U_0 = f(p \cdot s).$$

This function is non-linear and has a characteristic minimum for a given gas. The minimum for atmospheric air breakdown voltage of **360 V** is observed at the product $p \cdot s = 67 \text{ Pa} \cdot \text{cm}$. Under atmospheric pressure the minimum is observed at very small electrode distance of **5 μm** (fig. 6).

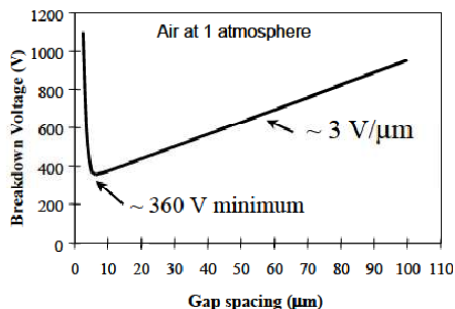


Fig. 6. Paschen curve: Air breakdown voltage versus. gap spacing. Air at a pressure of 1 atmosphere.

The electrode distance in the set of 6 glass cylinders is the same and amounts to 20 cm. However, the gas pressure in every cylinder is different. The smallest $p = 0,13$ hPa is in the left cylinder. The pressures of 0,18; 4; 8; 13; and 53 hPa are in the next following cylinders (from left to right).

Table 1. The pressure, the product of pressure and electrode distance and breakdown voltage

Pressure	hPa	0,13	0,18	4	8	13	53
Pressure * distance	hPa-cm	2,6	3,6	80	160	260	1060
Ionization voltage	V_{peak}			≈ 360			
Breakdown voltage	V_{peak}			2700			

When the AC 50 Hz voltage is applied to all cylinders, the cylinder with the $p \cdot s = 80$ hPa-cm starts to shine at the voltage of $2700 V_{\text{peak}}$ (fig. 7). It means that the experimental's minimum of the product $p \cdot s$ agrees with the value given in the reading books. However, the experimental value of voltage at which this phenomenon is observed is much higher than the theoretical U_0 value of 360 V. However, there is no discrepancy between the theory and the experiment. The Paschen law describes the breakdown voltage in uniform field. In our experiment the electrical field is non-uniform (the electrodes are not plane, their diameter is a few times smaller than the electrode distance). The observed shining is the sign of breakdown or prebreakdown discharges. In nonuniform field the breakdown voltage is considerably greater than the onset voltage of ionization. The partial-discharge onset voltage about $350 V_{\text{peak}}$ is found by means of partial discharge recorder. However, the apparent charge (the ionisation intensity) is too small to be visible even in a very dark room.



Fig. 7. The light emission at the 50 Hz voltage of $2700 V_{\text{peak}}$ in the cylinder with the $p \cdot s$ product of 80 hPa-cm.

When the AC voltage with the higher frequency of 5 kHz is applied and with the amplitude of 1100 V_{peak} (fig.8) the shining glow is observed even in three cylinders (fig. 9). Under so high frequency the plasma is unstable and therefore no sparks are produced in the cylinders with the smaller U₀ value.

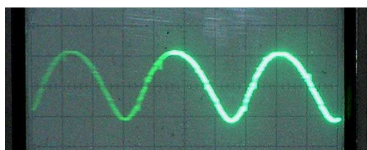


Fig. 8. The voltage generated by vacuum tester PIN-21 (iskrowy próbnik próżni PIN-21) manufactured by ZOPAP Warszawa.



Fig. 9. The gas ionization into three cylinders after application of AC voltage of 1100 V_{peak} with the frequency of 5 kHz.

A. 6. Discharges along the long string of metal pipes

The string consists of 16 metal pipes with the length of 38 cm (fig. 10). The air gap between two pipes has the length of 24 cm which results in the total air gap of 360 cm (tab. 1). The wood borders and 2 fishing lines secure mechanical stability for 10 metres long construction. The metal pipes string is similar to the string of cap and pin insulators with a very small value of capacitance between cap and pin. The capacitance of insulator is in the order of 30 pF. The capacitance of pipe – pipe can be calculated from the following formula [8]:

$$C_0 \cong \frac{4\pi \cdot \varepsilon \cdot l}{\ln \frac{l}{a} + \ln \frac{2h+2l}{2h+l}} = 12,3 \text{ pF}$$

where: l – pipe length, $2h$ – air gap length, $2a$ – pipe diameter

The voltage along a string of 15 cap and pin insulators is non-uniformly distributed (the nonuniformity factor about 3,0). The voltage distribution along the string of metal pipe is more non-uniformly. This is caused by smaller capacitances pipe-pipe than the capacitances of disc insulators and by the fact that the capacitances to ground in the laboratory are higher than the capacitances to ground in the field (smaller dimensions of transmission tower and the greater height of cap and pin insulators).

When the AC voltage is applied to the string of metal pipes, the discharges elongate with the stress amplitude. The gradient along the leader discharges is low, in the range of 1 kV/cm. Therefore, the high potential is moved to the discharge tip what promotes the farther elongation of discharges. This so called

cascade mechanism is responsible for a very long length of discharges. The discharges start to develop from the gap connected to high voltage transformer (in the place of highest electrical field). The breakdown of first gap occurs at the voltage of 330 kV. The breakdown of all series gaps at the voltage of 380 kV is associated with the breakdown of sphere air gap with the distance of 18 cm. When the short discharge connects the sphere gaps, the voltage drops to low value and the discharges along the series gaps extinguish (fig. 12). Note that the distance between spheres (uniform field) is **20** times smaller than the total length of air gaps between metal pipes (non-uniform field). This shows how the air breakdown depends on the type of electrical field.

Length of one metal pipe	38 cm
Diameter of metal pipe	2 cm
Number of air gaps	15
The total length of air gaps	360 cm

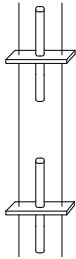
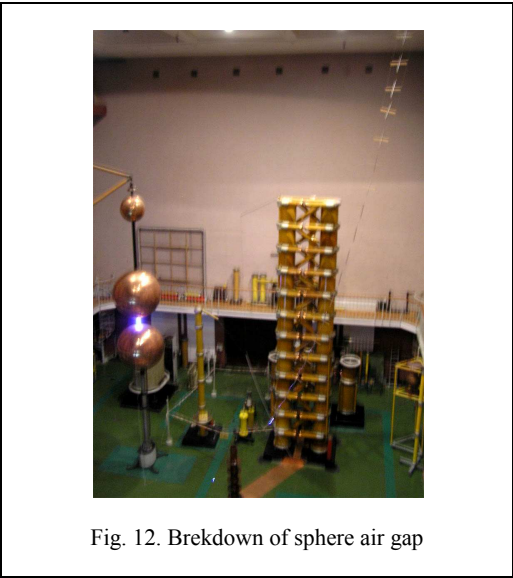
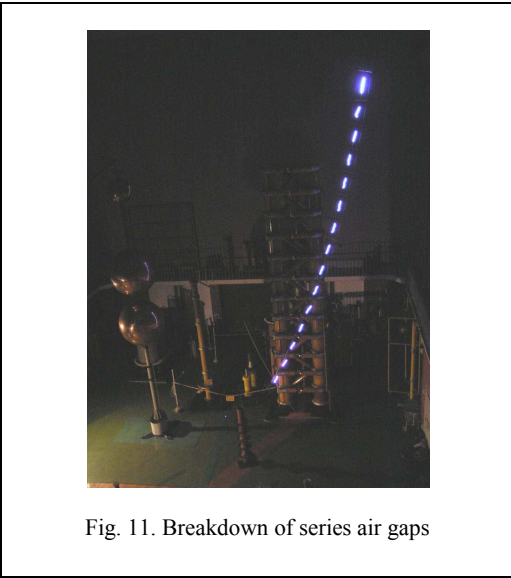


Fig. 10. The string of metal pipes



A. 7. Electric wind motor

In corona discharges in air, the collisions of charged particles with neutral particles induce a gas movement between the point to the plane called electric wind. The electric power applied is essentially transformed into heat ($\approx 90\%$) and only about 1% is used to generate the electric wind. The electric wind velocity outside the gap is proportional to the square root of the discharge current. The wind velocity in a point to plane arrangement can reach the value of 160 m/s when the current get the value of $70 \mu\text{A}$ [9]

Figure 13a shows 4 wire with sharp bended tips mount on the ball-bearing. The construction is mounted on the post insulator with grounded top flange. A metal pipe is hang 30 cm above the wind motor and connected to 110 kV transformer. Under the voltage of 50 kV the wind motor start slowly to rotate due to corona

discharges development at the sharp tips. The rotation speed increases with the height of the voltage (fig. 13b).

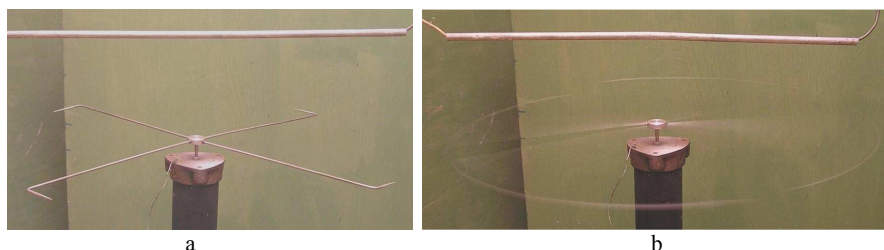


Fig. 13. Electric wind motor in static position without voltage applied to the wire (a) and rotating under the voltage of 100 kV

A. 8. Fluorescent tubes in electrical field

Enough energy is present in electric field to excite the gasses contained in the tube. Usually the fluorescent lamp is under the voltage applied to its electrodes and the internal gasses are excited by the electrodes at either end of the tube to produce light. Under the influence of electromagnetic fields though, those gasses are excited without the need for the electrodes, and produce light without needing to be "plugged in". This principle is used by voltage indicators, neon tubes applied at substations.

Figures 14 and 15 show standard 220 V fluorescent lamps used for lighting purposes. The 120 cm long fluorescent tube was put horizontally on two post insulators in the vicinity of 110 kV transformer (fig. 14a). A weak light is observed at the voltage of 50 kV. The light intensity increases with the voltage and can be documented by a standard digital camera in semi-dark room (fig. 14b).



Fig. 14. 120 cm long fluorescent tube in electric field of 110 kV transformer. a – mounting arrangement, b – light visible in semi-dark room

The round shaped lamp was hang on the damping resistor connected with the 110 kV transformer (fig. 15a). Compared with the straight lamp which had no contact with high potential of transformer, the light intensity is higher in this case (fig. 15b). The round lamp is exposed to a higher electric field than the straight one.

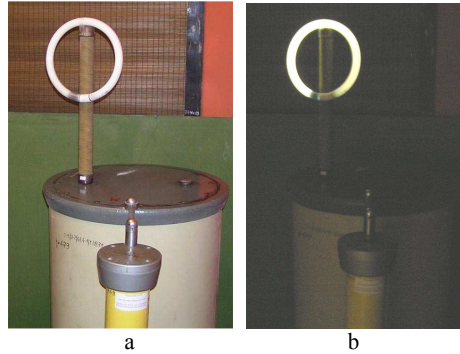


Fig. 15. Round fluorescent tube in electric field of 110 kV transformer.
A – mounting arrangement, b – light visible in a semi-dark room

A. 9. Literature

- [1] Pike-Bieguński M., Rozpad wybuchowy drutu. Przegląd Elektrotechniczny nr 1/1999, pp. 11-15.
- [2] Sen P., Ghosh J. et al. Preparation of Cu, Ag, Fe and Al nanoparticles by exploding wire technique. Proc. Indian Acad. Sci. (Chem. Sci.), Vol. 115, Nos 5 & 6, OctDec. 2003, pp. 449-508.
- [3] Colton, F. B., Lightning in action. National Geographic Magazine, Vol. 97, June 1950, National Geographic Society, Washington, D. C., p. 819.
- [4] Moore C.B., Aulich G.D., Rison W., An examination of lightning-strike-grounding physics. www.lightningsafety.com/nlsi_lhm/Radials.pdf.
- [5] Mousa A.M.: Protecting fireman against fire-induced flashovers. IEEE Trans. on Power Delivery, Jan. 1990, pp. 297-302.
- [6] Chrzan K., Wróblewski Z., The threat caused by fires under high voltage lines. 2nd International Conference on Advances in Processing, Testing and Applications of Dielectric Materials. APTADM, Wrocław 2004, pp. 208-211.
- [7] K. Sakai, S. Tsuru, D. L. Abella and M. Hara, Conducting particle motion and particle-initiated breakdown in DC electric field between diverging conducting plates in atmospheric air. IEEE Trans. on Dielectrics and Electrical Insulation Vol. 6 No. 1, February 1999, pp. 122-130..
- [8] Iossiel J.J., Koczanow E.S., Strunskij M.G., Razczet elektriczeskoj emkosti. Energija, Leningrad 1969.
- [9] Noel F., Batina J., Peyrous R., Held B., Electric wind in point-to-plane corona discharge. Comparison between modelling and experiment. 13 th Conference on Gas Discharges, Glasgow 2000, pp. 957-960.

APPENDIX B

SAFETY IN THE HIGH VOLTAGE LABORATORY

B. 1. Necessety of the safety care

Extreme care is required when working in a high voltage environment because any voltage above 40 V can be lethal. The danger for humans is not only related to the direct contact with a high voltage potential but also to following possible phenomena: insulation breakdown, capacitive and inductive coupling, leakage current along an polluted and wet insulating stick, earth potential rise due to fault current (step and touch potentials).

The effect of electrical currents on the human body is well known. The current disturbs or break the normal function of heart, lunges, muscles and nervous system. The great danger of electricity for the live is ventricular fibrillation of lower chambers of the heart caused by current higher than 60 mA. The high voltage electrocution causes usually severe body damages (internal burns, arc-flash burnings).

The following general safety features are considered for the safety of the operating personnel [1, 2]:

- The actual danger zone of the high voltage circuit must be clearly marked and protected from unintentional entry by walls or metallic fences.
- All doors should be interlocked to remove high voltage automatically when opened.
- Before touching the high voltage elements after testing, visible metallic connection with earth must be established. A suitable earth stick should be provided for this purpose. Special care should be taken with circuits having capacitors, especially with DC voltage.
- All metallic parts of the setup that do not carry potential during normal service must be grounded reliably. Any object in the laboratory should be either well connected to earth potential or at high voltage. "Floating" objects cause problems.
- It is preferred that the region of the high voltage apparatus be mattered by a closely meshed copper grid. The earth terminals of the apparatus are connected to it noninductively using wide copper bands.
- All measuring and control cables and earth connections must be laid avoiding large loops. The measuring signal is transferred to the measuring device via coaxial cables.
- The clearance beween test object and extraneous structure should be at least $1,5 \cdot S$, where S is the flashover distance between electrodes of the test object. In this case the effect of such structures on the test results will be negligibly small.
- A person should never work alone in high voltage laboratory.

B. 2. Safety rules in student high voltage laboratory

1. Students are informed with electrical and fire safety rules in the laboratory during the first lesson. They are getting familiar with elements of test circuits and operating manual of setups (switching-on, switching-off, grounding, measuring).
2. Students have to lern the theory and practical's programm (measuring and calculation tasks) before.
3. First, the set up should be checked, the high voltage connections, insulating clearances, state and continuity of grounding wires.
The student team should be divided in person making particular work: the student who will prepare the report has a leader position, one student reads the indications of reading equipment, the next one switches-on and switches-off the voltage.
4. Students have to get the tutor's permission for the first switching-on the high voltage.
5. The entry to the high voltage field is allowed when the both the switchgear and the disconnecting switch with visible break are open (the green lamp is not sufficient indicator of voltage lack).
6. It is forbidden to work inside the high voltage field without earth stick hang on the output of HV source
7. The door to the high voltage field has to be opened when the persons are within it (open contact of interlock relais).

8. Before you switch-on the high voltage you should check:
 - is anybody in high voltage field ?
 - is the earth stick taken out from the output of the high voltage source ?
 - is the voltage regulator in zero position ?
9. The person responsible for switching operation should be ready to react immediately on unexpected breakdowns or flashover in the test circuit.
10. It is forbidden to “play” with the knobs of switchgear or with the handle of disconnecting switch when some persons are in the high voltage field.
11. Do not use the water in the case of fire, apply the carbon dioxide extinguisher or a dry-chemical extinguisher.
12. The student team consist of a few persons. One person can not carry out the high voltage measurements.
13. A positive result of evaluation (writing test or oral examination) is the condition of admission for the practical.
14. The strange persons are not alligible to entry to the laboratorium during the high voltage measurements.
15. The voltage have to be switched-off, the earth stick put on the output of high voltage source and the door should be open before the team leave the laboratory.

B. 3. References

[1] J.P. Holtzhausen, W.L. Vosloo, High Voltage Engineering, Practice and Theory, Stellenbosch University, 2008, Chapter 6.

[2] Abdel-Salam M., Anis H., El-Morshedy A., Radwan R., High voltage engineering, theory and practice. Marcel Dekker, New York, Basel 2000.

APPENDIX C

THE LABEL DESCRIPTION OF THE FOLDER REPORT

INSTITUTE OF ELECTRICAL ENGINEERING FUNDAMENTALS
OF THE WROCLAW UNIVERSITY OF TECHNOLOGY
High Voltage Laboratory

Academic year

Laboratory group No

First name Surname	I	II	III	IV	V	VI		Mark

APPENDIX D

TEMPLATE OF THE LABORATORY REPORT

WROCLAW UNIVERSITY OF TECHNOLOGY Institute of Electrical Engineering Fundamentals	Jan Kowalski Jakub Sikora	Faculty of Electrical Engineering Year II Term: Thursday, 9:15 Group 1
HIGH VOLTAGE LABORATORY		
Date of training	Measurement of dielectric losses and partial discharges	Evaluation
Number of training		signature

Training aim

List of measuring devices

Measurement circuits

Measuring tables and calculation examples

Figures

Conclusions

APPENDIX E

HISTORY HIGH VOLTAGE LABORATORY

E. 1. Introduction

The electrical energy was applied first for lighting of streets and houses at the end of XIX century. The first trials with electrical arcing lamps in Wrocław were carried out on Powstanców Warszawy Square (present name) in 1882. In the same year, Thomas Edison has built the power station at Pearl street in New York. The first power station in Wrocław was built ten years later at Mennicza and Wierzbowa streets. Similar like in New York, this station used 110 V DC. Due to the increasing need for power, a new power station called “the main station” at Łowiecka street was commissioned in 1901. This plant generated higher voltages of 220V, 580 V DC and 5 kV AC. The installed power in 1914 reached the value of 22 MW and the town in this year was practically fully electrified.

E. 2. Electrotechnical Institute of Wrocław University of Technology

The building construction of the Technical University started in 1906. The German Emperor Kaiser Wilhelm II took part in the ceremony opening in 1910. At the early beginning, the school consisted of the Machinery Division, the General Sciences Division, the Electrotechnical Institute, the Chemical Institute and the Metallurgical Institute. The heat and power station located in A-4 building (present name) delivered the electrical energy and heat for the whole campus. Two damp machines of 300 and 160 hp (horse power), a 80 hp diesel engine and 2 of the 220 V DC generators with a power of 250 kW and 100 kW were installed in one machinery hall.

The former “Elektrotechnisches Institut” was located in building A-5 which houses the Institute of Electrical Machines today. The Institute was composed of a very technical modern equipment of that time: central heating controlled by 5 remote thermometers, an elevator, window veils driven by electrical motors, ventilation with warmed air. The machinery hall (Fig. 1) delivered DC or AC voltages with different amplitude to the tutorial and lecture rooms. From 1909 to 1939, the Electrotechnical Institute was lead by Prof. Georg Hilbert and from 1939 to 1945 by Prof. Paul Boening.



Fig. 1. Machinery hall of Electrotechnical Institute

E. 3. High Voltage laboratories

The first High Voltage Laboratory was located on ground floor of A-5 building. The 20 kVA transformer by Siemens-Schuckert-Werke delivered the voltage of 50, 100 or 200 kV (low side voltage of 160 V). The second 10 kVA transformer (not visible in figure 2) had also 3 voltage ranges of 3,75; 7,5 and 15 kV. The switching and regulation operations were carried out on the control-board hang on the wall (Fig. 2). The metal bath-tub supported by 4 delta insulators collected the water sprayed by the Koerting nozzle. This set up

was used for insulator testing under an artificial rain conditions. A 350 kV Marx generator was built in the laboratory in 1920s.



Fig. 2. The oldest HV laboratory of Wrocław University of Technology in building A-5

Prof. Jerzy Ignacy Skowroński moved this laboratory to the so called gymnastic room located in A-1 building below the Rector office (Fig. 3). The Binder loop visible on the right side in figure 3 was installed along the wall to study the travelling waves. The assistants Anatol Iwanowski, Roman Superat, Jerzy Fekecz and Jerzy Lisiecki worked there.

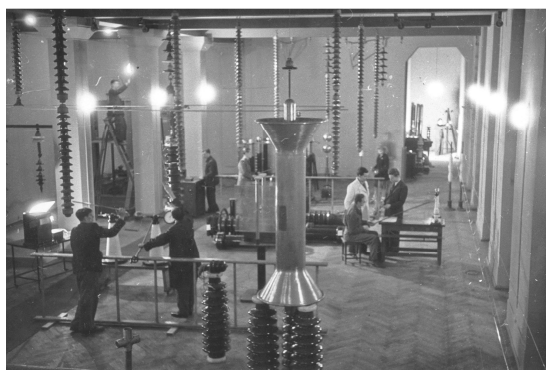


Fig. 3. The second HV laboratory in building A-1

The new D-1 building of Electrical Faculty (commissioned in 1953) houses 3 HV laboratories: the big hall of 26 m length, 16 m width, maximum height of 17 m, the small hall and the so called student laboratory. The Tesla transformer and van der Graaff generator were built in 1950 (Fig. 4). 800 kV transformer and 1,8 MV, 15 kJ impulse generator from ZWAR Warszawa were installed in 1965 (Fig. 5). 2 MV DC source was built in 1971, 160 kV power transformer with the short current in the range of 6 – 20 A in 1974 and the salt fog chamber in 1975. The electromagnetic compatibility simulator was put on the place of DC source in 1991. A steep-front impulse voltage set up for composite insulator testing was mounted in 2001. There are 350 and 110 kV transformers in the small hall (Fig. 6). The student laboratory is composed of a 110 kV transformer, two 60 kV transformers, 120 kV DC source and 500 kV impulse generator manufactured by TUR Dresden.

There are 3 other smaller HV laboratories in Wrocław: in Electrotechnical Institute at Maria Curie-Skłodowska str., in EnergiaPro a local power utility in Mennicza str and in Alstom Power (former Dolmel).



Fig. 4. Van der Graaff's generator (on the left) and Tesla transformer (on the right) in the third HV laboratory (picture from 1960s)



Fig. 5. Big HV hall in D-1 building



Fig. 6. Small HV hall in D-1 building

E. 4. References

- [1] Kalisch P., Die Technische Hochschule Breslau, Elektrotechnische Zeitschrift Heft 50, Dez. 1910, s. 1300-1302.
- [2] Hilpert G., Das Elektrotechnische Institut der Kgl. Technischen Hochschule Breslau. Elektrische Kraftbetriebe und Bahnen, Heft 15 u. 16, 1911, s. 1-12.
- [3] Die Technische Hochschule Breslau. Eigenverlag der Gesellschaft der Freunde der Technischen Hochschule Breslau, Dortmund 1985.
- [4] Lisiecki J., Laboratorium wysokich napięć Instytutu Podstaw Elektrotechniki i Elektrotechnologii. Wiadomości Elektrotechniczne 1981, nr 15-16, s. 366-367
- [5] Chrzan K.L., 100 lat wysokich napięć we Wrocławiu. Wiadomości Elektrotechniczne nr 3/2010, pp. 46-49.

APPENDIX F

ENGLISH – POLISH TERMINOLOGY

AC alternating current	prąd przemienny
accessories, cable accessories	osprzęt, osprzęt kablowy
acquisition, data acquisition	zbieranie, pozyskiwanie, zbieranie danych
ageing, ageing of insulation	starzenie, starzenie (się) izolacji
air bubble	wtrącina powietrzna, pęcherzyk
altitude	wysokość
anti-fog insulator	isolator przeciwmgłowy (do stosowania nad morzem)
apparent, apparent charge	widoczny, pozorny, ładunek pozorny
applied field	pole zastosowań
arc quenching medium	medium gaszące łuk
arcing horns	rożki łukowe, armatura ochronna
arrester, gapless arrester, valve type arrester	ogranicznik, ogranicznik beziskiernikowy, odgromnik zaworowy
attachment coefficient	współczynnik przyłączania
attenuate	osłabiać
auto-recloser	wyłącznik SPZ
auto-reclosing/reclosure	samoczynne ponowne załączenie SPZ
avalanche	lawina
back flashover	przeskok odwrotny
back-up, back-up protection	rezerwowy, zapasowy, zabezpieczenie rezerwowe
bare, bare conductor	goły (nieizolowany), goły przewód
bias	napięcie wstępne, polaryzacja
blackout	wielka awaria systemowa
board, control board	tablica, płyta, tablica sterownicza
breakdown	przebiecie
breaker, circuit breaker	wyłącznik
breaks down	przebija
brittle fracture	kruche pęknięcie
bundled conductors	przewody wiązkowe
busbars	szyny zbiorcze
bushing	izolator przepustowy (przepust)
button	przycisk

<p>cable (underground) cage, Faraday cage cap and pin insulator (disc insulator) cell, solar cell chain channel, inlet channel charge choke, iron-cored choke chopped impulse circuit, tripping circuit circuit breaker clamp, earth clamp clean fog, steam fog clearance, earth-ground clearance coaxial, coaxial cable coil, arc-suppression coil cold switch-on collision conditioning, signal conditioning</p> <p>conduction conductive conductor, cable conductor, lightning conductor contactor, automatic tripping contactor contaminated cord, extension cord core, shank corona coupling, capacitive coupling</p> <p>crack creepage, creepage discharges critical flashover voltage, CFOV cross-arm current transformer cycloaliphatic epoxy resin</p> <p>data logger</p>	<p>kabel (podziemny) klatka, klatka Faradaya izolator kołpakowy ogniwo, ogniwo słoneczne łańcuch kanał, kanał dopływowy (techn.) obciążenie, (elektr.) ładunek dławik, dławik z rdzeniem stalowym impulse ucięty obwód, obwód wyzwalający wyłącznik zacisk, zacisk uziomowy czysta mgła, para wodna odstęp, odległość przewodu od ziemi koncentryczny, kabel koncentryczny cewka, cewka gasząca załączenie na zimno (linii) zderzenie oczyszczanie, uzdatnianie, dopasowanie sygnału przewodnictwo przewodzący przewód, żyła kabla, przewód odgromowy</p> <p>stycznik, stycznik samoczynny zanieczyszczony sznur przyłączeniowy, przedłużacz pień izolatora korona (wyładowanie niezupełne) sprzęgło, połączenie, sprzężenie pojemnościowe pęknięcie pełzanie, wyładowania ślizgowe krytyczne napięcie przeskoku poprzeczka przekładnik prądowy żywica cykloalifatyczna</p> <p>rejestrator danych</p>
--	---

dust deposit density, DDD	gęstość powierzchniowa osadu pyłu
deteriorate	pogorszyć (się)
dew	rosa
dielectric losses	straty dielektryczne
dielectric constant	przenikalność dielektryczna
direct stroke	bezpośrednie uderzenie (np. pioruna)
down conductor	przewód odprowadzający (instalacji piorunochronnej)
down-time	przestój (czas niesprawności)
dry bands	strefy suche (na zabrudzonym izolatorze)
earthing (grounding)	uziemiaenie
electromagnetic interference	zakłócenie elektromagnetyczne
electronegative gases	gazy elektryjemne
environment	środowisko
EPDM rubber (ethylene propylene diene monomer)	kauczuk etylenowo-propylenowy EPDM
erosion	erozja
ESDD equivalent salt deposit density	równoważnik gęstości powierzchniowej osadu soli
failure mechanism	mechanism uszkodzenia
fault clearing	usunięcie uszkodzenia
fibre particles	cząstka włóknista
fibre bridge formation	utworzenie mostka z wtrącin włóknistych
flashover voltage	napiecie przeskoku
floating object	obiekt na wolnym potencjale
fuse	bezpiecznik
gap (air gap)	odstęp, szczelina, (iskiernik)
gapless arrester	ogranicznik beziskiernikowy
gas insulated substation, GIS	rozdzielnia okapturzona (SF ₆)
glass	szkło
glaze	szkliwo
glow corona	wyładowanie jarzeniowe
ground potential rise	wzrost potencjału uziemiaenia
grounding resistance	rezystancja uziemiaenia
high speed autoreclosure	samoczynne ponowne załączanie SPZ
housing	osłona
humidity	wilgotność

<p>ice</p> <p>impulse generator</p> <p>impurities</p> <p>inception voltage</p> <p>indirect stroke</p> <p>insulator (for an overhead line)</p> <p>insulating liquid</p> <p>insulation coordination</p> <p>insulator pollution</p> <p>interface</p> <p>interference</p> <p>inter phase separators</p> <p>interruption of fault current</p> <p>intrinsic strength</p> <p>ion</p> <p>ionisation probability</p> <p>ionisation coefficient</p> <p>isolator (link, disconnect)</p> <p>leader</p> <p>leakage current</p> <p>leakage distance</p> <p>lightning</p> <p>lightning arrester</p> <p>lightning impulses</p> <p>lightning ground flash density</p> <p>lightning protection</p> <p>lightning overvoltage</p> <p>line trap (for power line carrier)</p> <p>long rod insulator</p> <p>loss factor ($\tan \delta$)</p> <p>mean free path</p> <p>metalware</p> <p>mica</p> <p>mold</p> <p>multi stage impulse generator</p>	<p>śnieg</p> <p>generator udarowy (impulsowy)</p> <p>zanieczyszczenia śladowe</p> <p>napięcie początkowe</p> <p>uderzenie (pioruna) obok</p> <p>isolator linii napowietrznej</p> <p>ciecz izolacyjna</p> <p>koordynacja izolacji</p> <p>zanieczyszczenie izolatora</p> <p>interfejs, sprzęg, powierzchnia rozdziału</p> <p>zakłócenie</p> <p>odstępniki międzyfazowe</p> <p>przerwanie prądu zwarcia</p> <p>wytrzymałość samoistna,</p> <p>jon</p> <p>prawdopodobieństwo jonizacji</p> <p>współczynnik jonizacji</p> <p>odłącznik (element izolujący, odcinający)</p> <p>lider (forma wyładowania elektrycznego)</p> <p>prąd upływu</p> <p>droga upływu</p> <p>piorun</p> <p>ogranicznik przepięć (piorunowych)</p> <p>udary (prądu) piorunowego</p> <p>gęstość wyładowań piorunowych doziemnych</p> <p>ochrona odgromowa</p> <p>przepięcie piorunowe</p> <p>filtr liniowy (do elektroenergetycznej telefoni nośnej)</p> <p>izolator długopniowy</p> <p>współczynnik strat dielektrycznych $\text{tg}\delta$</p> <p>średnia droga swobodna</p> <p>okucia (izolatorów)</p> <p>mika</p> <p>forma (do odlewania wyrobów)</p> <p>wielostopniowy generator udarowy</p>
--	--

noise	szum, hałas
non-destructive test methods	próby nieniszczące
non-self-sustaining discharges	niesamodzielne wyładowania
oil impregnated paper	papier nasycany olejem
overhead power line	linia napowietrzna
overvoltage protection devices	urządzenia ochrony przeciwprzepięciowej
overvoltage due to lightning	przepięcia piorunowe
ozone	ozon
partial discharges	wyładowania niepełne
partial discharge detector	miernik wyładowań niepełnych
Paschen's law	prawo Paschena
post, solid core post, pedestal post	izolator wsporczy
power line carrier	elektroenergetyczna telefonia nośna
peak voltmeter	voltomierz wartości szczytowej
photon	foton
photo ionisation	jonizacja świetlna (fotojonizacja)
pollution chamber	komora do prób zabrudzeniowych
pollution characteristics	charakterystyka zabrudzeniowa
pollution layer	warstwa zabrudzeniowa
polymer concrete	beton polimerowy
polythene (or polyethylene)	polietylen
porcelain	porcelana
positive ion	jon dodatni
power frequency overvoltages	przepięcia o częstotliwości sieciowej
probe	sonda
propagated	rozprzestrzeniony, rozchodzący się
protection measure	środki ochrony
protective devices	urządzenia ochronne
protective gaps	iskierniki ochronne
polytetrafluoroethylene (teflon), PTFE	politetrafluoroetylen (teflon)
puncture	przebicie
push-button	przycisk
polyvinylchloride, PVC	polichlorek winylu (PVC)
rain	deszcz
ribs	żebra (na kloszach izolatorów)
rime, hoar-rime	szron
radio influence voltage, RIV	napięcie zakłóceń radiowych

root-mean-square, ~ voltage	średniokwadratowy, napięcie skuteczne
roughness factor	współczynnik tarcia
salinity	koncentracja soli
salt fog method	metoda słonej mgły
Schering bridge	mostek Schoeringa
self-sustained dischaeged	wyładowania samoistne (samo podtrzymujące się)
shed	klosz
shedding (load shedding)	zrzut obciążenia
shielding angle	kąt osłony
silica filler	wypełniacz z krzemionki
silica gel breathers	żel krzemionkowy (absorbujący wilgoć)
silicone carbide arrester (gapped arrester)	ogranicznik iskiernikowy (odgromnik zaworowy)
silicone rubber	kauczuk silikonowy
solid insulating material	dielektryk stały
solid layer method	metoda warstwy stałej
space charge	ładunek przestrzenny
spark	iskra
sphere gap	iskiernik kulowy
standard switching impulse	udar łączeniowy normalny
static contact angle	statyczny kąt zwilżania
step potential	potencjał krokowy
strain insulators, tension insulator	isolator odciągowy
streamer discharge	wyładowanie strimerowe
striking distance	odległość decyzji (pioruna)
sulphur hexafluoride (SF ₆)	sześciofluorek siarki
surface conductivity	konduktywność powierzchniowa
surface discharges	wyładowania powierzchniowe
surge (characteristic) impedance	impedancja falowa
surge diverter lightning arrester)	ogranicznik przepięć
switching	łączenie
switching overvoltage	przepięcie łączeniowe
switch-on, switch-off	włączyć, wyłączyć
synthetic resin bond paper	papier łączony z żywicą
temporary (50 Hz) overvoltage	przepięcie dynamiczne
thermal run away (instability)	rozbieganie (niestabilność) temperaturowe
thermal breakdown	przebicie cieplne

thermal ionization	jonizacja cieplna
touch potential	napięcie dotykowe
toughened glass	szkło hartowane
tracking	śląd pełzny
transient overvoltages	przebiegi o dużej częstotliwości
travelling waves	przebiegi falowe
treeing	drzewienie
Trichel pulses	impulsy Trichela
tripping	wyzwalanie, wyłączanie
ungrounded object	obiekt nieziemiony
up and down method	metoda góra-dół
utility, power utility	użyteczność, zakład elektroenergetyczny
vacuum	próżnia
visual corona	widzialne wyładowania koronowe
void	wtrącina w postaci pustej szczeliny
voltage divider	dzielnik napięcia
voltage gradient	gradient napięcia
water repellent	hydrofobowy
weather proof	odporny na warunki atmosferyczne
winding	uzwojenie
wire, ground wire, wireless	drut, przewód odgromowy, bezprzewodowy
withstand voltage	napięcie wytrzymywane
wye	połączenie gwiazdowe, trójnik
yoke	jarzmo

about the author

Dr. Krystian Leonard Chrzan was born on October 15, 1955 in Odolanow, Poland. From 1978 to 1983 he studied Electrical Engineering at the Wroclaw University of Technology. Since 1983 he is with the Institute of Electrical Engineering Fundamentals of the Wroclaw University of Technology where he received his Dr. – Ing. in 1987. From 1988 to 1989 he was a scholar of the Alexander von Humboldt Fellowship at the high voltage laboratory of the University of Stuttgart (Prof. K. Feser). From 1991 to 1993 he worked at the high voltage laboratory of Technical University of Zittau (Germany, Prof. J. Pilling, Prof. R. Baersch) and for Cardiff University (2004-2005, Prof. R.T. Waters). He spent research stays at the high voltage laboratories in Stuttgart (1985, 1994, 1995, 1996, 1999, 2003), Dresden (1995), Mannheim (FGH, 1996, 1997, 2002), Prague (EGU, 2001), Darmstadt (2002), Cottbus (2007), Lvov, Kiev (2008), Stellenbosch, South Africa (2009, Dr. J.P. Holtzhausen), Tomsk, Beijing and Shenzhen (2010, Prof. Z. Guan), Indian Institute of Science, Bangalore (2011, Prof. Joy Thomas Meledath) and at the Lightning Research Center Camp Blending (2000, Florida, Prof. M. Uman). He is author or co-author of **over 200** scientific papers and a book “Surge arresters for high voltages”.